REPORT DOCUMENTATION PAGE

Form Approved
OMB No. 0704-0188

1. REPORT DATE *(DD-MM-YYYY)*
04-02-2008

2. REPORT TYPE
Final Report

3. DATES COVERED *(From - To)*
May 10, 2007 to February 10, 2008.

4. TITLE AND SUBTITLE
Ocean Wave Energy Harvesting Devices

5a. CONTRACT NUMBER
HR011-06-C-0030

5b. GRANT NUMBER

5c. PROGRAM ELEMENT NUMBER

6. AUTHOR(S)
Cheung, Jeffrey, T; Childress, Earl, F, III

5d. PROJECT NUMBER

5e. TASK NUMBER

5f. WORK UNIT NUMBER

7. PERFORMING ORGANIZATION NAME(S) AND ADDRESS(ES)
Teledyne Scientific & Imaging, LLC
1049 Camino Dos Rios
Thousand Oaks, CA 91260

8. PERFORMING ORGANIZATION REPORT NUMBER
SC71273.HDWE

9. SPONSORING/MONITORING AGENCY NAME(S) AND ADDRESS(ES)
Defense Advanced Research Projects Agency
Advanced Technology Office/ATO
3701 North Fairfax Drive
Arlington, VA 22203-1714

10. SPONSOR/MONITOR'S ACRONYM(S)
DARPA/CMO

11. SPONSOR/MONITOR'S REPORT NUMBER(S)
ARPA Order No. V233/00

12. DISTRIBUTION/AVAILABILITY STATEMENT
Approved for public release: distribution unlimited.

13. SUPPLEMENTARY NOTES
The views and conclusions contained in this document are those of the authors and should not be interpreted as representing the official policies, either expressly or implied, of the Defense Advanced Research Projects Agency or the U.S. Government.

14. ABSTRACT
Development of a mechanically sound buoy design, which generated 10W average power in Beaufort Sea State 1, and showed potential for up to 20W in Sea State 4. Development of a wave energy harvesting buoy capable of generating 2W in Sea State 1, and with proper mechanical alignment able to generate over 4W. Development of two modeling capabilities: a classical mechanical model used for optimizing the electromagnetic design, and a hydrodynamic model to predict device performance given a set of buoy/generator design characteristics and environmental conditions. The latter model allows input of actual wave spectra, winds and currents. It also has the capability to simulate mooring designs and their impact on power production. A literature search to determine available wave energy in the 1-3 second wave period band was sufficient to meet the 20W power requirements in Sea State 1. The result of this study indicated a device with conversion efficiency on order of 10% could generate 20W on average from waves with conversion efficiency on order of 10% could generate 20W on average from waves with periods faster than 3 seconds.

15. SUBJECT TERMS
Wave Energy Harvester, mass spring linear generator, Hydro-dynamic Modeling

16. SECURITY CLASSIFICATION OF: a. REPORT	b. ABSTRACT	c. THIS PAGE	17. LIMITATION OF ABSTRACT	18. NUMBER OF PAGES	19a. NAME OF RESPONSIBLE PERSON / 19b. TELEPHONE NUMBER *(Include area code)*
U	U	U	SAR	97	Childress, Earl, F, III / (858) 842 2652

TELEDYNE
SCIENTIFIC & IMAGING, LLC
A Teledyne Technologies Company

January 2008	SC71273

Ocean Wave Energy Harvesting Devices

Phase 3
Final Report

For 5/10/2007 – 2/10/2008

Contract No. HR0011-06-C-0030

Sponsored by
Defense Advanced Research Projects Agency
Advanced Technology Office/(ATO)
Program: Ocean Wave Energy Harvesting Devices
DARPA Order No. V233/00, Program Code: 5X20
Issued by DARPA/CMO under Contract No. HR0011-06-C-0030

Earl Childress
Program Manager

Ocean Wave Energy Harvesting Phase 3 Final Report

TABLE OF CONTENTS

1.0 BACKGROUND 1

1.1 PHASE 3 OBJECTIVES 1
1.2 TEAM 1
1.3 ACHIEVEMENTS 2

2.0 FUNDAMENTAL DESIGN PRINCIPLES 4

2.1 ENERGY FLOW IN WAVE ENERGY HARVESTING BUOY 4
2.1.1 Wave motion to buoy motion energy transfer 4
2.1.2 Buoy motion to spring-mass inertia of the magnet car 5
2.1.3 Magnet car motion to electrical energy output 6

3.0 AVAILABLE WAVE ENERGY CALCULATIONS 7

4.0 HYDRODYNAMIC MODEL DEVELOPMENT 8

4.1 POTENTIAL ERROR SOURCES 10

5.0 HARDWARE DESIGN AND OPTIMIZATION 10

5.1 LINEAR GENERATOR DESIGN AND OPTIMIZATION 11
5.2 OPTIMIZATION 12
5.2.1 Airgap optimization 12
5.2.2 Spring-mass system optimization 13
5.2.3 Resistive load optimization 13
5.3 BUOY DESIGN AND OPTIMIZATION 15

6.0 RESULTS FOR ENERGY HARVESTING BUOYS 16

6.1 SCALE MODEL 16
6.2 3W BUOY 17
6.3 20 W ENERGY HARVESTING BUOYS AND MONTEREY BAY TEST 18
6.4 OCEANSIDE FIELD TEST NOVEMBER 16, 2007 24

7.0 TECHNOLOGY TRANSITION OPPORTUNITIES AND APPLICATIONS 30

7.1 SPAWAR 30
7.2 TELEDYNE BENTHOS 30
7.3 TELEDYNE GEOPHYSICAL 31

8.0 CONCLUSIONS AND RECOMMENDATIONS 32

9.0 APPENDIX 1 – DARPA PROGRAM COMPLETION REPORT 33

9.1 EXECUTIVE SUMMARY 33
9.2 PROGRAM OBJECTIVE AND TECHNICAL NEED 34
9.3 PROGRAM DESCRIPTION AND MILESTONES 35
9.4 SCIENTIFIC AND TECHNICAL RESULTS AND ACCOMPLISHMENTS 36
9.5 APPLICATIONS AND CONSIDERATIONS FOR THE FUTURE 38
9.6 PROGRAM TRANSITION 38

10.0 APPENDIX 2 – NUMERICAL MODEL TUTORIAL 39

1.0 Background

The ocean is a tremendous source of energy in the form of random waves. Harvesting energy from these motions has been a subject of interest for centuries. However, numerous attempts have been unsuccessful as devices failed to survive the severe and corrosive marine environment. Even today, a reliable and cost effective solution has not yet been developed. In this program, Teledyne Scientific Company (TSC) attempts to develop a unique solution to address these challenges.

This program has been funded by DARPA contract HR0011-06-C-0030 through three phases of development. The concept was first validated in Phase 1 (February 2003 – May 2004), in which we carried out fundamental studies on the near-zero friction ferrofluid bearings, fabricated a low frequency linear generator, and integrated the generator to a floating platform to produce 0.37 Watts of power from light wind waves just off the coastline in La Jolla, California. In Phase 2 (June 2005 – April 2006) we improved the performance by developing a mass-spring type low frequency linear generator, enabled by the same near-zero-friction liquid bearing to improve dynamic sensitivity and robustness. Phase 2 suggested the potential to harvest tens of Watts of energy with a small device in multiple sea states. During Phase 3, the work centered around two areas: 1) designing, developing, and deploying under known conditions devices to generate 3 Watts of power, and 20 Watts of power, respectively; and 2) further development of the numerical model to predict wave energy generator performance for given sea conditions.

1.1 Phase 3 Objectives

The objectives of the **Ocean Wave Energy Harvesting Devices Phase 3** program are:

1. Demonstrate autonomous self-powered buoy capable of generating 20 Watts output in arbitrary conditions encompassing a broad range of sea states (Sea States 1-5). Size and weight not to significantly exceed profile of Mark 46 Torpedo (L ~ 2.6m; D ~ 324 mm; Wt ~ 235 kg).
2. Demonstrate autonomous self-powered buoy capable of generating 3 Watts in calm waters (Sea State 1), with size and weight amenable to manual deployment from a boat by two persons.
3. Demonstrate "rules and tools" for design of self-powered buoys, based on simulations encompassing all significant parameters for ocean behavior and device physics, verified by comprehensive wave tank and ocean testing.

1.2 Team

There are two team members:

1. Teledyne Scientific Company (TSC) – Prime contractor: Linear generator design and fabrication; device design; computer simulation; bench and field test.
2. Oceanscience Group (OS) – Subcontractor: Buoy design/manufacturing and field test.

Government participation in this Phase 3 program was critical to success. Government sponsored participants were:

Mr. Jeff Lloyd - Logistics, field testing, report reviews, technology application for Navy
SPAWAR Systems Center – San Diego
53560 Hull Street
San Diego, CA 92152
jeffrey.m.lloyd@navy.mil
619-553-1699

Mr. Warren Bartel - Hydro-dynamic model development
NAVFAC Engineering Service Center
1100 23rd Ave, Port Hueneme, CA 93043 USA
warren.bartel@navy.mil
(805) 982-1215

1.3 Achievements

The Phase 3 program achieved the following:

- Development of a mechanically sound buoy design, which generated 10W average power in Beaufort Sea State 1, and showed potential for up to 20W in Sea State 4. The device is completely sealed from the environment.
- Development of a wave energy harvesting buoy capable of generating 2W in Sea State 1, and with proper mechanical alignment able to generate over 4W.
- Development of two modeling capabilities: a classical mechanical model used for optimizing the electromagnetic design, and a hydrodynamic model to predict device performance given a set of buoy/generator design characteristics and environmental conditions. The latter model allows input of actual wave spectra, winds and currents. It also has the capability to simulate mooring designs and their impact on power production.
- A literature search to determine available wave energy in the 1-3 second wave period band was sufficient to meet the 20W power requirements in Sea State 1. The result of this study indicated a device with conversion efficiency on order of 10% could generate 20W on average from waves with periods faster than 3 seconds.
- Device response was broadened by employing a hybrid buoy design with a wave following float collar integrated with a long spar instrument well, which housed the linear generator and electronics.

Table 1 below summarizes the Phase 3 program.

Table 1. Key aspects of the Phase 3 program.

Tasks	1. Enhance and validate simulation model for prediction of generator performance 2. Develop generator/buoy design approaches for broadband response 3. Perform trade study to optimize design based on enhanced simulation results 4. Build and ruggedize optimized generator/buoy assemblies 5. Conduct extended field testing at Monterey test site 6. Improve simulation model and design as necessary based on ocean testing to provide final "rules and tools" for generator/buoy design 7. Identify appropriate DOD transition path and key applications 8. Write final report 9. Verify simulation-predicted behavior of optimized buoys via field testing in wave tank and sea tests with documented wave conditions
Technical Problems	1. Serious mechanical issues were encountered during the course of each generator design, as a result of very stringent tolerances on non-metallic parts to maintain air gap dimensions and optimize generator power output. These issues created significant cost and schedule impacts which prevented addressing broadband response as planned in task 2. 2. Mass spring linear generator current state of the art makes devices for higher power (> than 100W) sufficiently large and impractical.
General Methodology	1. Laboratory experiments, numerical and physical model simulations, prototype fabrication, wave tank testing, and field trials.
Technical Results	1. Enhanced numerical model capability developed and validated. 2. Hybrid (spar-discus) buoys can provide a broader wave frequency response, increasing wave-buoy energy transfer efficiency. 3. Buoy/generator designs were produced to generate 2-4W and 10-20W in Beaufort Sea States 1-3. 4. Magnet/coil and magnet/buoy mass ratios should be maximized while maintaining stability and dominant heave motion. 5. Available wave energy in the 1-3 s band is sufficient to produce 20W of power.
Important Findings and Conclusions	1. Reproducible robust system design producing a. 10W average over five hours in Beaufort Sea State 1 b. >20W intermittently in Beaufort Sea State 4 2. Numerical modeling tool able to predict system performance for a buoy design operating in a given set of environmental conditions.
Significant Hardware Development	1. Designed, built and tested four wave energy harvesting buoys with data loggers and integrated accelerometer packages a. One scale model buoy producing 300mW b. One 3W buoy c. Two 20W buoys
Special Comments	1. Presented technical paper at Ocean Energy Conference, August, 2007 2. Presented technical paper at ADCP User Conference in November 2007 3. Teledyne is internally funding development of a prototype wave energy powered "gateway" subsurface-to-RF communications buoy. This program will be completed in 2008.
Implications for Future Research and Development	1. Long-term device testing should be undertaken to characterize performance over a broader range of ocean conditions. 2. Development of battery charging electronics to achieve charging efficiency greater than 80% for energy produced by wave harvesting buoy. 3. Current designs are costly to build. Further development should be undertaken to reduce cost of manufacturing. 4. Available spring technology currently drives the size and frequency of the generator. Other spring types should be investigated, including air and compression springs.

2.0 Fundamental Design Principles

2.1 Energy flow in wave energy harvesting buoy

The net energy conversion efficiency of a wave energy harvesting buoy is a product of the efficiencies of three sequential energy transfer processes:

$$\eta_{net} = \eta_1 \times \eta_2 \times \eta_3$$

where η_1 = Wave to buoy motion transfer efficiency

η_2 = Buoy to magnet motion transfer efficiency

η_3 = Electrical generator efficiency

The device design must take all into consideration and optimize the efficiency of each energy transfer process. The following paragraph gives a brief description of the underlying physics of these processes and the basis of the numerical modeling. In the actual devices, there is significant feedback among the three transfer processes, and they are not separable from one another.

2.1.1 Wave motion to buoy motion energy transfer

The response of a buoy to waves is one of the most intensely studied subjects in the field of hydrodynamics. The frequency dependence of wave height $A_w(f)$ and buoy heave motion $A_b(f)$, which is most relevant for driving a linear generator, can be expressed as:

$$A_b(f) = RAO(f) \times A_w(f)$$

where $RAO(f)$ is the Response Amplitude Operator defined as the ratio of the buoy heave height to the water surface elevation. This operator is characteristic for each buoy depending on its shape, drag characteristic and mass distribution. The two extreme cases of a cylindrical shaped buoy with draft L and cross section of the water plane "A" are Spar buoy (L>>A) and Discus buoy (L<<A). Their RAO are very different as shown in Fig. 1.

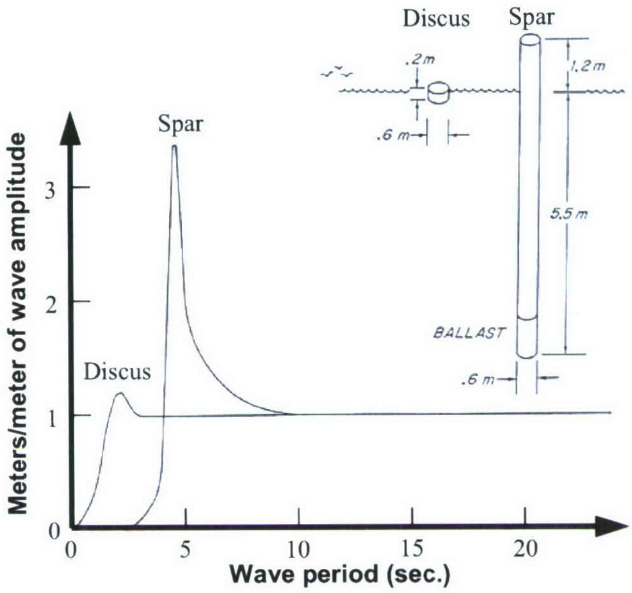

Fig. 1. The Response Amplitude Operator of a Discus buoy and a Spar buoy.

The spar buoy acts a tuned oscillator with a natural heave frequency $f = \frac{1}{2\pi}\sqrt{g/L}$, where g is the gravitation constant. It resonates with wave motion and produces large heave displacement in a narrow band at the resonant frequency. Although the enhanced heave motion is beneficial to a linear generator, the lack of response to a wide range of sea states limits its use as the platform for a wave energy harvesting buoy. The other extreme case, a discus buoy, acts as a wave follower with RAO of unity though out the wave band. However, it does not have any enhanced heave motion and its size is too large to be practical for our uses. An alternative approach is the hybrid buoy design by attaching a short cylindrical float collar to the top of a spar buoy. This design exhibits some tuned heave enhancement and the response is much broader.

2.1.2 Buoy motion to spring-mass inertia of the magnet car

The second process is the energy transfer between the buoy and the spring-mass linear generator with a natural frequency $f_g = \frac{1}{2\pi}\sqrt{\frac{k}{m}}$, where k is the spring constant and m is the mass. In a simplified view, the buoy and the generator can be treated as coupled oscillators each with a different damping term. The damping of the buoy is caused by its drag. The damping of the magnet car (the moving assembly that carries the magnets) corresponds to its interaction with the counter EM force at it passes through the coils. The classical mechanical formulation of this problem involves solving a pair of differential equations of motion.

$$k_1(\Delta h - y_1) - k_2(y_1 - y_2) - \gamma\left(\frac{dy_1}{dt} - \frac{dy_2}{dt}\right) - \gamma_1\left(\frac{dy_1}{dt} - \frac{d\Delta h}{dt}\right) = m_1 \frac{d^2 y_1}{dt^2} \qquad (1)$$

$$k_2(y_1 - y_2) + \gamma_{EM}\left(\frac{dy_1}{dt} - \frac{dy_2}{dt}\right) = m_2 \frac{d^2 y_2}{dt^2} \qquad (2)$$

Where y_1 and y_2 refer to the reference coordinates of the buoy and the magnet car, respectively. Other parameters in the equations are:

m_1: Mass of the buoy only

Δh: Amplitude of a monochromatic, sinusoidal wave $\Delta h = A\sin(2\pi t / T)$ where A is the wave peak amplitude and T is the wave period.

γ_1: The damping coefficients between water and the buoy.

m_2: Mass of the magnet car

k_2 : Spring constant of the spring(s) connected to the magnet car

γ_{EM}: The damping coefficient due to the counter EM force between the magnet car and the coils

This formulation gives accurate prediction of system performance under ideal conditions. It serves as a design tool to select parameters of key components such as spring constant, magnet car mass and resistive load for optimal performance.

2.1.3 Magnet car motion to electrical energy output

This is the generator efficiency and can be measured by bench test under controlled conditions. Energy output can be calculated by solving equations (1) and (2) in the previous section to obtain the oscillatory displacement between the magnet car and coil. From that, the velocity of magnet car with respect to the coils, V_{mag}, can be determined and output energy, E_{out}, can be obtained by the simple relationship $E_{out}=V^2_{mag}\gamma_{EM}$. This approach is used both in the classical mechanical model as well as the more elaborate Orcaflex hydrodynamic model. It is valid if damping is caused only by the counter EM force. In our device, this is a good assumption since the parasitic frictional loss is reduced by using the ferrofluid lubricant.

The above formulations define the underlying physical principle of the wave energy harvesting device operation. Their model calculation results provide design guidelines in mass distribution, device layout and the selection criteria of critical hardware components. Some of these selection criteria are:

- Springs
    - Spring constant (natural frequency of the linear generator)
    - Initial tension (determines the device length)
    - Maximum load (determines the mass of the magnet car)
    - Mass (1/20 or less than the mass of magnet car in order to sustain resonant oscillation)
    - Maximum deflection length (Dynamic range and lifetime issues): the devices are designed so the range of the spring extension is less than 60% of the maximum deflection.
- Magnets
    - High strength magnets (NdFeB magnet Grade 42 and higher)
- Coils
    - Number of turns (optimize energy capture)
    - Wire gauge size (optimize system output voltage range)

3.0 Available Wave Energy Calculations

A literature search was conducted to determine the calculations required to estimate available wave energy for a given set of wave conditions. Our work focused on energy available between 1-3 second wave periods to determine if we could reach our power production goals by optimizing for this band only. The United States Minerals Management Service (MMS) has published a white paper on harnessing wave energy entitled "Wave Energy Potential on the Outer U.S. Continental Shelf". From this paper the common measure of wave power, P, is $P = \rho g^2 T H^2 / 32 pi$ watt per meter (W/m) of crest length (distance along an individual crest), where:

ρ = the density of seawater = 1,025 kg/m3,
g = acceleration due to gravity = 9.8 m/s/s,
T = period of wave (s), and
H = wave height (m).

Further MMS states, "typical wave energy in U.S. offshore regions (at a depth of 60M) ranges from 2 to 6 kW/m in the mid-Atlantic, 12 to 22 kW/m in regions such as Hawaii with trade winds, and 36 to 72 kW/m in northwestern U.S. coastal areas near Washington and Oregon."

Applying this equation to the wave data collected at Scripps Pier during testing in July leads to the results presented in Table 2 below.

Table 2. Available Wave Energy from data collected by a TRDI ADCP on July 20, 2007

LaJolla, CA July 20, 2007 - Scripps Pier ADCP Data

Total Available Power	9:17am	9:37am	1:00pm	1:21pm	1:42pm	
1-3.0 second	**129**	**205**	**244**	**280**	**253**	**W/m**
2.5-5.0 second	544	626	564	526	586	W/m
5-8 second	1904	1774	1565	1702	2070	W/m
8-21 second	248	345	666	315	1761	W/m

The power in the 1-3 second band has on average more than 220 watts/m available. To equate this available power number to a specific device harvesting capability, it is important to determine device type. There are three classes of wave energy device types: a terminator, an attenuator or a point absorber.

According to MMS, terminator devices extend perpendicular to the direction of wave travel and capture or reflect the power of the wave (OWC), attenuators are long multi-segment floating structures oriented parallel to the direction of the wave travel (Pelamis), and point absorbers have a small horizontal dimension compared with the vertical dimension, and utilize the rise and fall of the wave height at a single point for wave energy capture (OPT and Teledyne).

Studies indicate the point absorber harvests data from a significantly larger area and therefore the available power number should be a factor of 3-5 times greater than its linear cross section would indicate. Assuming a very conservative factor of 1 for a "point absorber" wave harvester the required efficiency for the system needs to be 10% to meet the 20W power generation goal given an average available power in the 1-3 second wave periods of 251 W/m for Monterey Bay during October 2006 (NDBC M1 Wave Buoy Data Review). These calculations are open to interpretation due to the nature of point absorbers and the disagreement among the industry on best practices. We will track these numbers for each new deployment and calculate system efficiency for future modeling and reference. We are not assuming these numbers are conclusive at this point, but we can use them as indicators and baseline for future tests.

4.0 Hydrodynamic Model Development

Warren Bartel of the Naval Facilities Engineering Command, Engineering Service Center, was identified as the leading expert in buoy hydrodynamic modeling, and was contracted through SPAWAR to develop the power performance model for the wave energy harvesting buoy. The model was developed using Orcaflex (www.orcina.com) ocean structural software. The NFESC hydrodynamic model implementation for the energy harvesting buoy uses the following approach:

- Models buoy and magnet stack assemblies as rigid bodies
- Employs ocean fluid hydrostatics and hydrodynamic modeling capability for currents, wind and waves
- Assumes Relative Motion Morison equation theory for wave loading
- Has mooring system modeling capability with extra buoys, cables and anchor
- Accepts as Input:
    - Buoy Geometry, Mass, Spring constant Inertia, Magnet Mechanical Properties, Ocean Wave and Current information
- Produces Output:
    - Time series and Frequency Spectra of Motions of Buoy, Motions of Magnet Assembly, Mooring Cable Tensions

The process for running a simulation is:

- Buoy properties are first built and calculated using Solidworks software. The size, weight and moment of inertia are used for input into the Orcaflex model
- The EMF damping for the magnet sliding through the coils is translated in to an equivalent mechanical damping in the model. The EMF damping is measured using an Oscilloscope after the buoy is built to confirm the model estimate.
- The buoy added-mass and viscous damping are first estimated based on reference material and then updated using field pluck test measurements to fine tune the values
- Drag coefficients for the buoy are based on Reynolds number and shape of the buoy
- The mooring line properties are calculated for material chosen and allows elasticity and fluid drag and inertia effects
- The relative velocity of the magnet stack assembly inside the buoy is used to calculate the electrical power, $P=V^2/R$

Fig. 2 shows the model output for buoy heave and magnet stack velocity. Fig. 3 shows the power output over a 3 minute simulation.

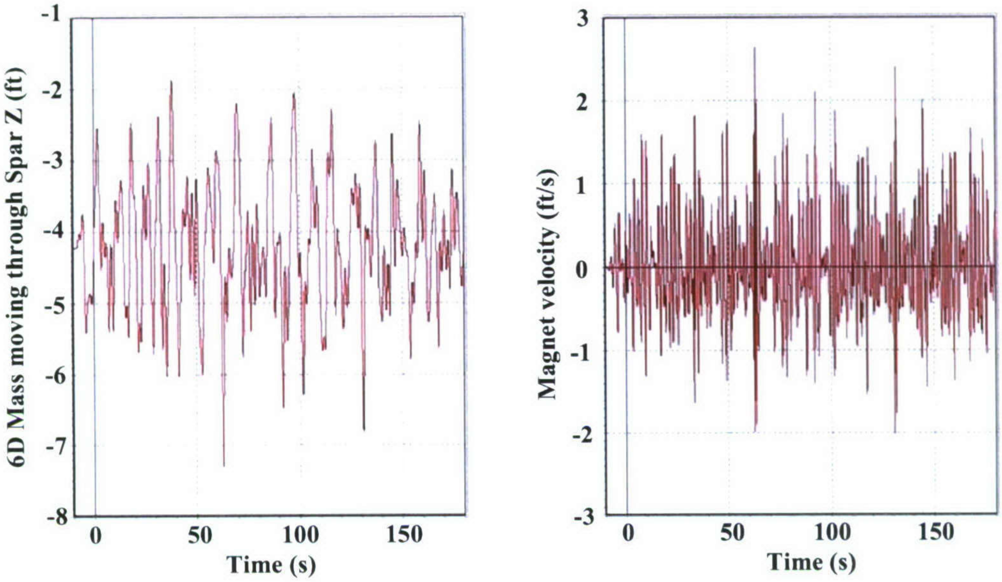

Fig. 2. Buoy heave motion and magnet stack velocity from a 2 minute simulation.

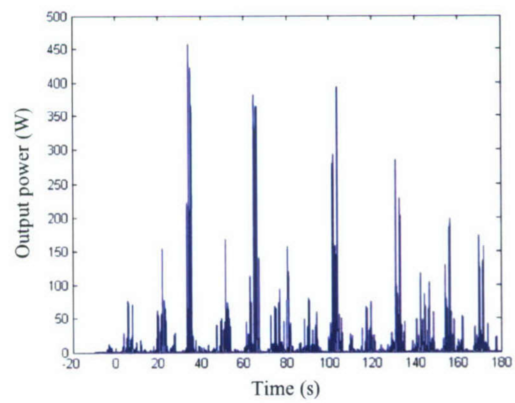

Fig. 3. Power output from 3 minute model simulation.

Overall model performance (accuracy) is still being evaluated. However, the hindcasts of the Monterey and Oceanside tests, shown below in Table 3, depict generally good agreement with field measurements. Wave data input for the model below 0.58 hz had to be extrapolated due to the cut-off frequency of the measured wave data from the NDBC buoys in Monterey and Oceanside.

Table 3. Comparison of measured and calculated power from deployments in Monterey Bay, CA on October 25th and 26th, 2007 and Oceanside, CA on November 16th, 2007

Date/Time	Measured power (W)	Model prediction (W)	% Difference
10/25/2007 / 1430	15.1 W	25.9 W	+71%
10/26/2007/ 1030	11.6 W	12.3 W	+6%
11/16/2007 / 0930	8.9 W	9.0 W	+1.1%
11/16/2007 / 1330	9.0 W	8. 1 W	-10%

4.1 Potential Error Sources

- Measured wave input data not accurately measured for waves below 3 second periods requiring extrapolation for the model input.
- Orcaflex uses a non-directionally spread wave, so it may be that more energy is created by a combined surge, sway, heave, roll, pitch and yaw response as wave energy is approaching from multiple directions. Orcina may add this feature in future software releases.
- The model equivalent EMF damping assumes a linear relationship and may not accurately reflect the actual damping under all conditions. This is currently the best implementation unless a mathematical model of this can be derived. Orcaflex can interface with external software for the coupling.

The model has been invaluable in three areas to date:

1. Buoy design – the model has been used to optimize the buoy shape and collar size for maximum power generation.
2. Resistive load determination – The model has been used to simulate "pluck tests" for maximum power under a given set of environmental conditions, and to provide output wave forms which can then be used in the lab to choose the best resistive load.
3. Mooring design – The model has allowed to us simulate several moorings designs and their impact on power generation.

5.0 Hardware Design and Optimization

In order to achieve the program goals, we used a basic design that consists of a spring-mass type linear generator mounted inside a hermetically sealed buoy to couple energy from wave motion via resonant oscillation. The enabling technology is the use of lubricant to significantly reduce the friction between the moving parts of the generator and increase its dynamic sensitivity to capture energy from the slightest external motion.

We developed the buoy and the generator in a parallel effort and combined the two to build the wave energy harvesting devices. Devices were tested under controlled wave tank condition as well as in the ocean with different sea states. In order to achieve the 20W device program goal, we took an incremental approach by first making a small Scale Model (<1 W), then a 3 Watt device and eventually the 20W device in conjunction with extensive hydrodynamic and numeric modeling. In addition to using the Orcaflex hydrodynamic model described in the previous section, we developed a numerical tool that solves the equations of motion for coupled oscillators subjected to sinusoidal, monochromatic forcing. Results were used to predict the general device performance trends and to determine the optimal load resistance for extracting electrical energy from the generator.

Operation of the wave energy harvester may be viewed as two discrete steps. First, wave energy produces buoy motion. Then this motion is transferred to the linear generator to produce electrical energy. The induction coils (i.e. stator) are fixed to the buoy and the magnet assembly (i.e. magnet car) is suspended from springs. The oscillatory motion causes the coils to cut the magnetic flux and produce electrical energy. Unlike the common rotary generator, the linear generator uses heavy magnets and a heavy yoke plate network to provide very high magnetic flux density in a narrow air gap.

5.1 Linear generator design and optimization

Our generator design, shown in Fig. 4, consists of disc-shaped induction coils of alternating polarity that are fitted into a cartridge of insulating material. The coil cartridge is placed in the space (airgap) between two rows of permanent magnets mounted on high permeability yoke plates to form a "magnet car". Magnets are arranged such that adjacent magnets have the opposite polarity and opposing magnet faces have the opposite polarity, thus completing a magnetic flux loop through the airgap with flux lines perpendicular to the coils. Heavy NdFeB magnets were used to produce a magnetic flux density exceeding 6000 Gauss in the airgap. Voltages are induced across the individual coils as the magnet car slides through the coil cartridge. Power can be extracted by connecting the output to a resistive load. Transversal linear generator has two major advantages that are relevant to the development of 20W device. They are:

1. Scalability: A generator module consists of a pair of magnets, a yoke plate, and a coil. Multiple units can be stacked to a form a 3D array for maximum packing density. For example, the 20W device used in the Monterey Bay test has 40 generator units arranged in five layers. Each layer has two columns and each column has four units.
2. Favorable weight distribution: Since the magnet car is the moving part of the oscillator, its mass is directly related to the amount of power that can be captured and stored. Therefore, the majority part of the generator mass should be distributed in the magnet car. In our current design, the magnet car to coil mass ratio exceeds 20:1.

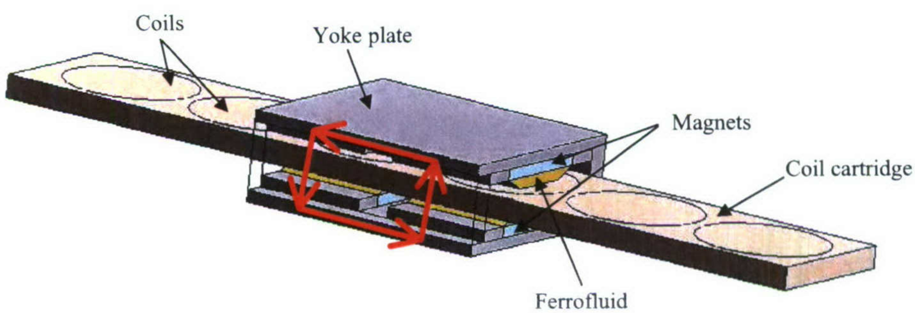

Fig. 4. Teledyne linear generator design. The red arrow lines are the magnetic flux loop. Multiple modular units can be stacked to form a 3-dimensional array.

5.2 Optimization

In order to optimize the generator performance, the three important design issues are: (1) Airgap dimension, (2) Spring-mass characteristics, and (3) Load impedance or load resistance. We will discuss them in the following:

5.2.1 Airgap optimization

As the coils cut the magnetic flux in the airgap, voltage is induced across all coils. Electrical energy can be extracted by connecting the output to a load with an impedance R_L. The induced voltage V and extracted energy E can be expressed as:

$$E = V^2 / R_L$$

where

$$V = A_{total} \, {dB_g}/{dt}$$

A_{total} is the total area enclosed by all turns of the coil. B_g is the density of magnetic flux, perpendicular to the coil, in the airgap. For energy harvesting, we maximize magnetic flux density in the airgap, the total area enclosed by the coil, and the relative magnet-coil velocity. Magnetic flux density in the airgap B_g can be determined from the following relation:

$$B_g = B_r \left[\frac{t_m}{t + \mu_r g} \right]$$

where	t_m	= thickness of the magnet
	B_g	= magnetic flux density in airgap
	B_r	= remnant flux density in magnet (strength of the magnet)
	μ_r	= relative permeability
	μ	= airgap size

Equation (2) shows that the airgap dimension should be as small as possible in order to achieve high magnetic flux density. Yet at the same time, according to equation (1), large A_{total}, or the total area enclosed by all turns of the coil, is needed. This will require a large airgap. Therefore, there is an optimum airgap dimension. Based on magnetic flux distribution analysis and empirical measurement, we determined the optimum airgap for the 20W device to be 11.4 mm. Table 4 lists the design parameters for the 20W device.

Table 4. 20W Device Design Parameters

Magnet thickness	6.35 mm x 38 mm square
Magnetic flux density in the airgap	6,500 –7,500 Gauss (measured)
Remnant flux density in magnet	11,300 Gauss (Grade 42, NdFeB magnets)
Relative permeability	1.05
Airgap size	11.4 mm

5.2.2 Spring-mass system optimization

The magnet car is suspended from a set of springs to form an oscillating system. It serves as a part of the linear generator as well as an energy storage reservoir. Energy is constantly transferred to the coils to generate electricity as it is replenished by coupling with the wave motion. For best performance, the natural frequency of the generator must be matched to an appropriately energetic band of the wave power spectrum. The size of the spring-mass system can be estimated by solving the equation of a coupled oscillator. Fig. 5 shows the power vs. period dependence of a linear generator with different magnet masses. The spring constant scales up accordingly so the natural oscillating periods remain constant at 1.6 sec. This calculation gives us guideline in choosing the spring mass characteristics in order to deliver the desired power. The magnet masses for various devices tested in this program are: 1 kg (Scale Model), 9 kg (3W device), and 29.5 kg (20W device). As the magnet mass increases, multiple springs were used in parallel to deliver the required performance.

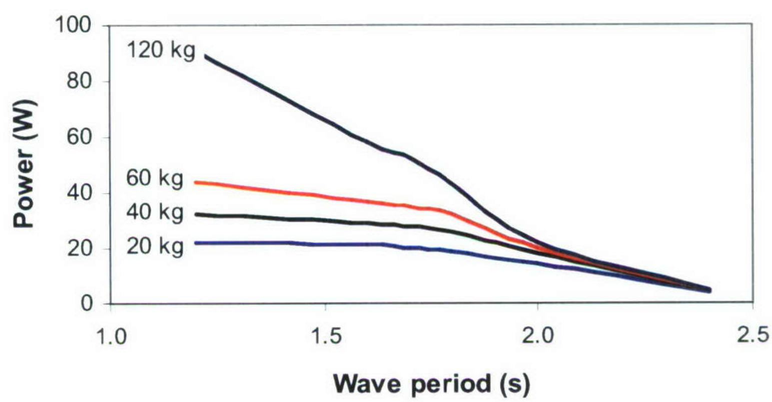

Fig. 5. Model calculation on the output power vs. wave period dependence for linear generators with different magnet mass.

5.2.3 Resistive load optimization

The load resistor plays a significant role in linear generator performance. Fig. 6 shows power vs. period dependence with different load resistors. Calculations were made for the 20W device tested at Monterey Bay. The resistor load is expressed as a damping coefficient Γ that determines the EM coupling between the coil and the magnet car. If the load is too small (i.e. large resistor), such as Γ=10 in the calculation, the system is under-damped. The power dependence shows a sharp peak at the resonant period of the oscillator. Under this condition, oscillating amplitude of the magnet car can exceed the mechanical limit of the springs. This not only affects the spring lifetime (and device lifetime) but also causes large shift of the center of gravity (CG) and makes the device unstable. As the load resistance increases (i.e. large damping coefficient such as Γ=100), the device is over-damped. In this case, the motion of the magnet car is restricted by a large cogging force leading to low output in the low frequency wave band. Based on this calculation, we chose Γ=40 as the best load. Under this condition, the maximum spring extension is 38 cm, much lower than the mechanical limit.

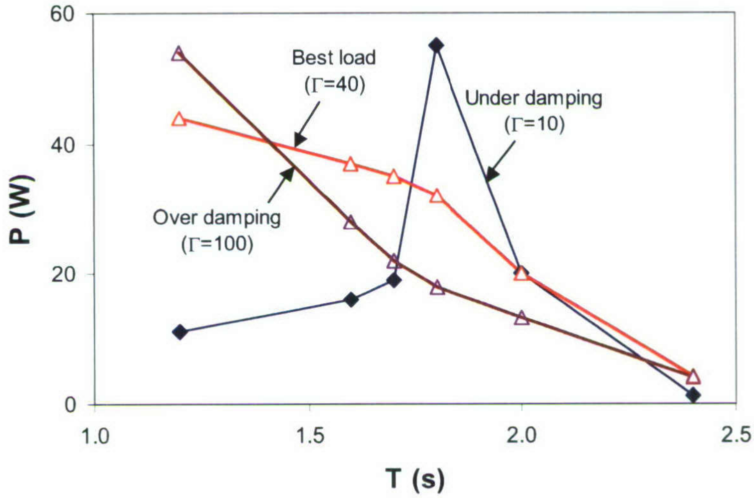

Fig. 6. Model calculation for power vs. wave period dependence for three different EM damping conditions.

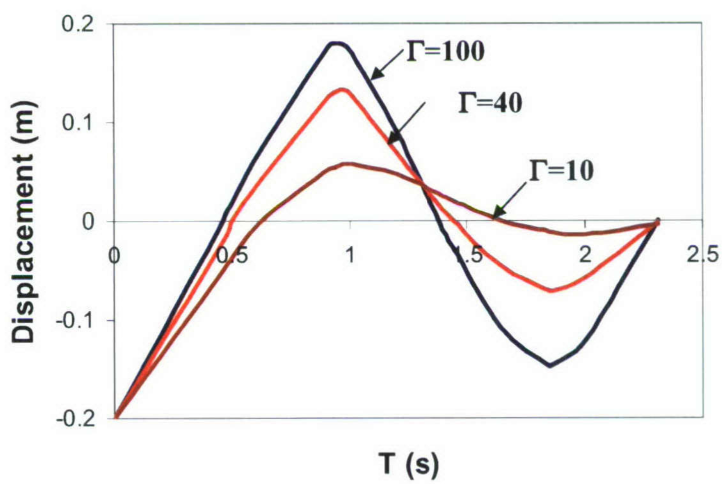

Fig. 7. Calculated magnet car displacement oscillation decay in "Pluck" experiment under three different EM damping conditions (i.e. load resistance).

The relationship between the damping coefficient Γ and the load resistance is difficult to calculate without the precise knowledge of magnetic field distribution in the airgap. But it can be determined semi-empirically by a "Pluck Test" to measure the magnet car oscillation decay after a known initial excitation. The best load resistance can be determined by matching the measured damping data with model calculation. Fig. 8 shows the calculated magnet oscillation decay under the best damping coefficient $\Gamma=40$. Two initial extension values were used at 20 cm and 15 cm. The height of the first oscillation peak L_1 should be 13.6 cm and 8.3 cm, respectively. We then select a load resistor to match this performance. For the 20W device, an excellent match was achieved in both cases by using a 50 Ohm load resistor. This load was used for the Monterey Bay test. After the deployment, we removed the generator from the buoy and repeated the pluck tests. Results remained unchanged, indicating no mechanical degradation.

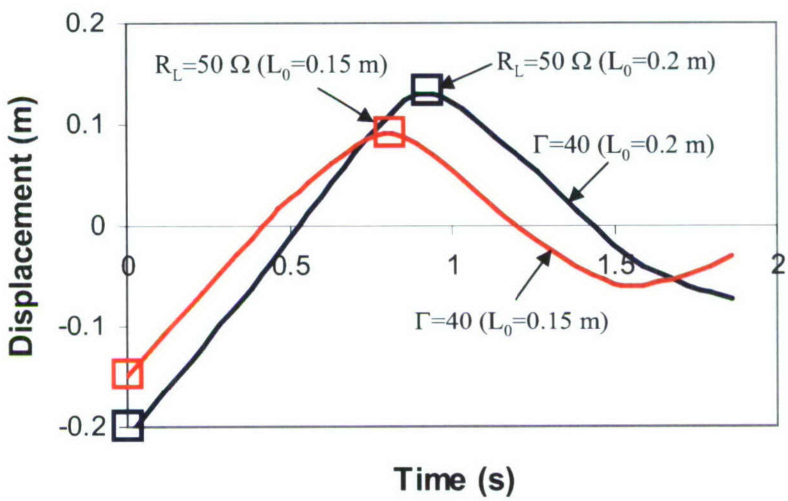

Fig. 8. Pluck experiments to determine the "Best Load" for the 20W device tested at Monterey Bay. The Blue and Red solid curves are calculated oscillation amplitude decay for initial displacement of 0.2 m and 0.15 m, respectively. The Red and Blue squares are measurement data for a 50 Ohm load.

This systematic approach to determine the best load has taken out the guesswork and proved to be effective. Furthermore, the load calculation also accurately predicts spring extension during generator operation. This allows design of the spring so that spring life will not become an issue.

5.3 Buoy design and optimization

The buoy is designed to achieve maximum wave energy to heave coupling over a broad range of wave conditions. It must also be stable under all conditions. The challenge is further complicated by the presence of the oscillating magnet with its considerable mass. We combined the results from hydrodynamic modeling and wave tank tests to design the buoy.

The initial approach was a plain spar buoy. But the idea was quickly found to be unsuitable because of the narrow frequency response. A pure spar buoy heaves in a very narrow band of wave spectrum with a natural period $T = 1/2\pi\ (g/L)^{1/2}$, where L is the draft and g is the gravitational constant. Outside of this narrow band, the spar buoy has little motion. A small spar is also more difficult to stabilize due to the constant change of the center of gravity with magnet car oscillation.

In order to address this issue, we added a float collar near the top of the spar to make a hybrid spar-discus buoy. The collar adds stability and broadens the heave response of the buoy. For the 20W device, after extensive test at OTRC, we chose a 600 mm diameter collar. The natural period of this device is under 1 second and it is responsive to a much broader range of wave periods. The collar is sufficiently small to not appreciably perturb an oceanic wave field. The OTRC test also indicated that adding a conical float section just below the cylindrical collar can reduce the drag and increase the degree of heave. This design was used at Monterey.

6.0 Results for Energy Harvesting Buoys

Prior to the 20W device, two smaller energy harvesting buoys were built and tested. A brief summary of their performance follows.

6.1 Scale model

The Scale Model had a 1 kg magnet stack suspended from a single spring. This produced a generator natural period of 1.5 seconds. There were six induction coils whose outputs were connected to a rectifier bridge network to form a single output. The device was placed inside a 150 mm diameter tube with a 250 mm diameter float collar. Extensive bench tests, wave tank tests (SIO) and ocean tests (Imperial Beach and Oceanside) were carried out. Key findings were:

- Monochromatic wave tank test results are in excellent agreement with “dry” bench test. (Fig. 9)
- Ferrofluid liquid bearing plays a key role and allows the device to perform in positions deviating from vertical resulting a 3- to 7- fold performance improvement
- In choppy waves off the coast of Oceanside, the unit produced close to 300 mW of power. A Fourier analysis of the power spectrum shows similar results as measured at the SIO wave tank under discrete monochromatic waves.

The Scale Model study led us to the float collar design for later buoys and increased our understanding of the significance of buoy motion on device performance. Results were used to validate and calibrate hydrodynamic simulation using the Orcaflex software.

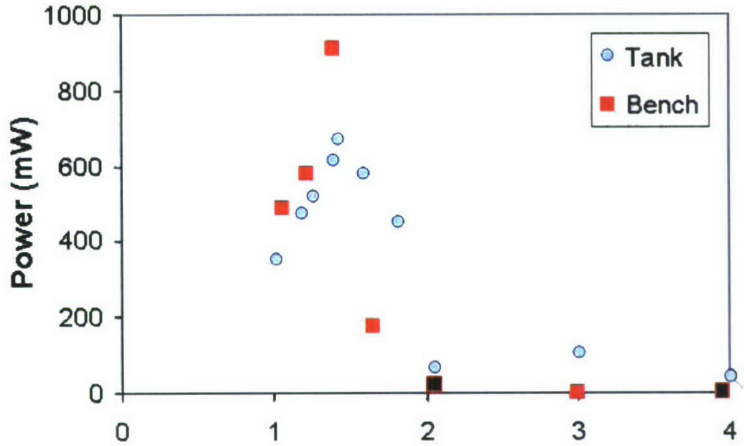

Fig. 9. Scale model comparison of wave tank test with laboratory bench test.

6.2 3W Buoy

The 3W was similar to the scale model. Brass ballast was attached to the bottom of the magnet stack to achieve the required 10 kg mass as shown in Fig.10. The device was field tested off Scripps Pier under two sea states. We used real time wave data from a bottom-mounted ADCP. The results allowed us to refine the hydrodynamic model. The maximum power was 1.88 W when the sea was choppy. The 3W device had excessive friction associated with long excursion and lack of stiffness of construction materials.

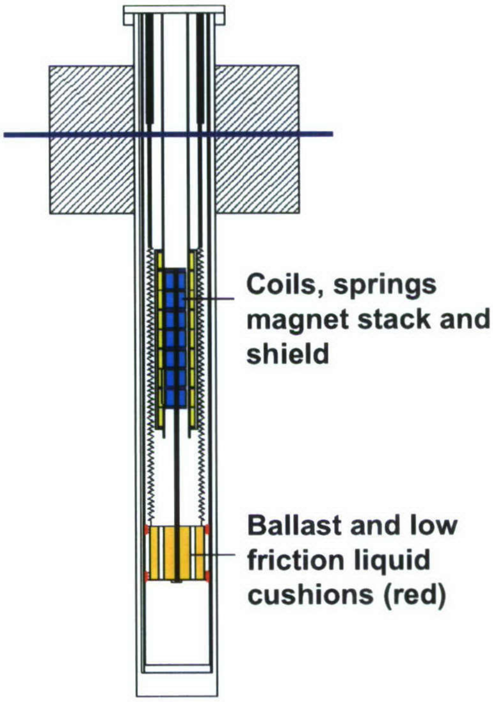

Fig. 10. Scale model. Comparison of wave tank test with laboratory bench test.

6.3 20W Energy Harvesting Buoys and Monterey Bay Test

We designed and manufactured two 20W buoys. The first one was used for the OTRC test and the second device was used for the Monterey Bay test.

<u>20W OTRC Buoy:</u>
This device design is shown in Fig. 11. It has 42 pairs of 40 mm diameter magnets. The magnets are arranged radially in eight groups and slide over eight coil cartridges with coils at matching center-to-center spacing. Because of the mechanical complexity, the spring-mass oscillator suffered from mechanical friction that had a significant impact on the wave tank test results.

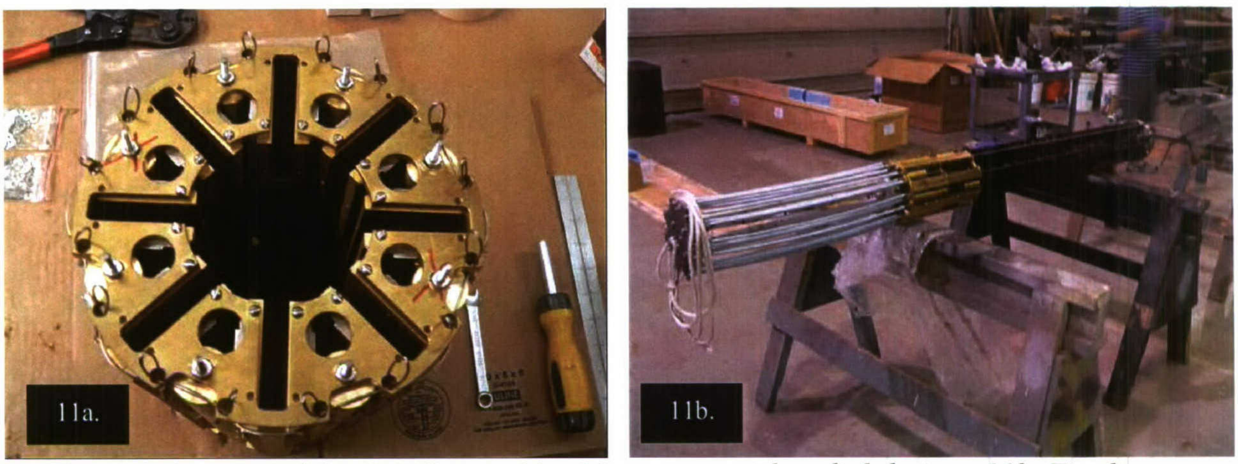

Fig. 11. 20W device used for OTRC test. 11a. Magnet car with radial design. 11b. Final generator assembly with multiple springs, magnet car and matching coil cartridge.

During the OTRC test, we carried out a total of 48 experiments under different wave conditions, both monochromatic as well as simulated sea states. We also studied the effect of different float collars. Key findings of these experiments are:

- A 600 mm diameter float collar gave the best performance both in terms of broadband response and stability.
- The constant oscillatory of the heavy magnet stack (29 kg) changed the buoy CG and induced abnormal buoy movements, which were successfully predicted by hydrodynamic model, thus giving further validation to the model.
- The design of this scale requires very high precision mechanical tolerances that are difficult to achieve in plastic. Design modifications are needed to rectify this limitation.

<u>20W Monterey Bay device:</u>
Fig. 12a shows the 20W device used in Monterey Bay test. It is similar to the unit used in OTRC test with a moving magnet car and fixed induced coils, except the magnet pair generator units are arranged in a 3D Cartesian coordinate as shown in Fig. 12b. The array consists of two rows of air gaps columns. There are 5 columns in each row and 4 magnet pairs in each column. Induction coils are embedded inside polycarbonate blades shown in fig. 12c. The spaces between coils are matched to that of the magnet pairs. This design is more rigid than the device used in OTRC test and the magnet stack can oscillate freely without mechanical damping. The 32 kg magnet car

was suspended from 36 springs with a combined spring constant of 508 Newton/meter, giving the spring-mass system a natural period of 1.58 seconds. We determined the "best load" with the scheme described in previous section to be 50 Ohms. A pluck test measuring the damping characteristics of the magnet movement was recorded and used in a hydrodynamic model simulation. The same pluck test was repeated after the sea test to assure that the device had no mechanical degradation. A 600 mm diameter collar with a low drag conical section was used. The device is 2.0-m tall including ballast and weighs 86 kg. The device also has an onboard data logger with 100-m range Bluetooth transmission for remote data download. An IMU unit records 6 DOF in real time. Two tests were made in Monterey Bay off M1 and M2 buoy in different sea states.

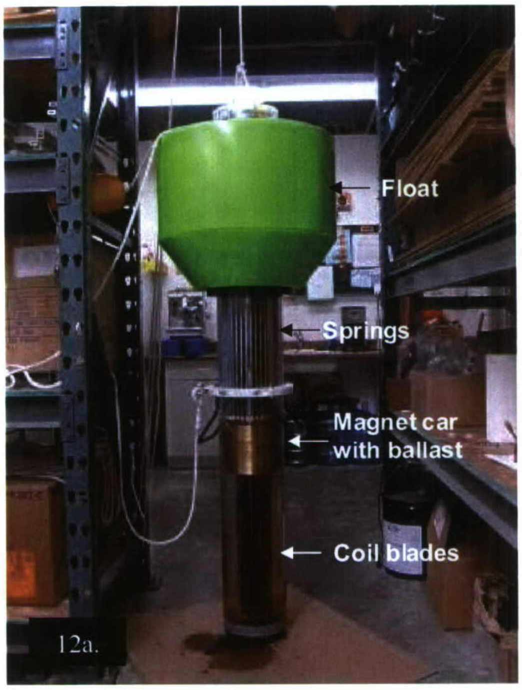

Fig. 12.
12a. 20W device with buoy and float collar used in Monterey Bay test.

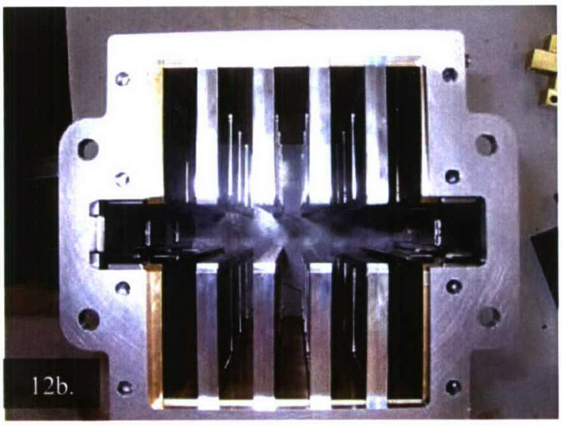

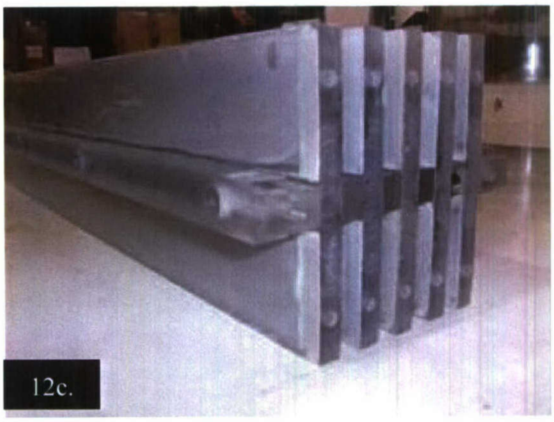

12b. Top view of the magnet car showing 10 air gap columns. 12c. Polycarbonate induction coil blades.

Monterey Bay Test Summary – October 25-26, 2007

A team from Teledyne Scientific, Ocean Science and SPAWAR traveled to Monterey during the week of October 22, 2007 for testing of the wave energy buoy. The field tests were organized and supported by DARPA personnel as well as MBARI and the research vessel Zephyr. Fig. 13 below shows the test locations for each day.

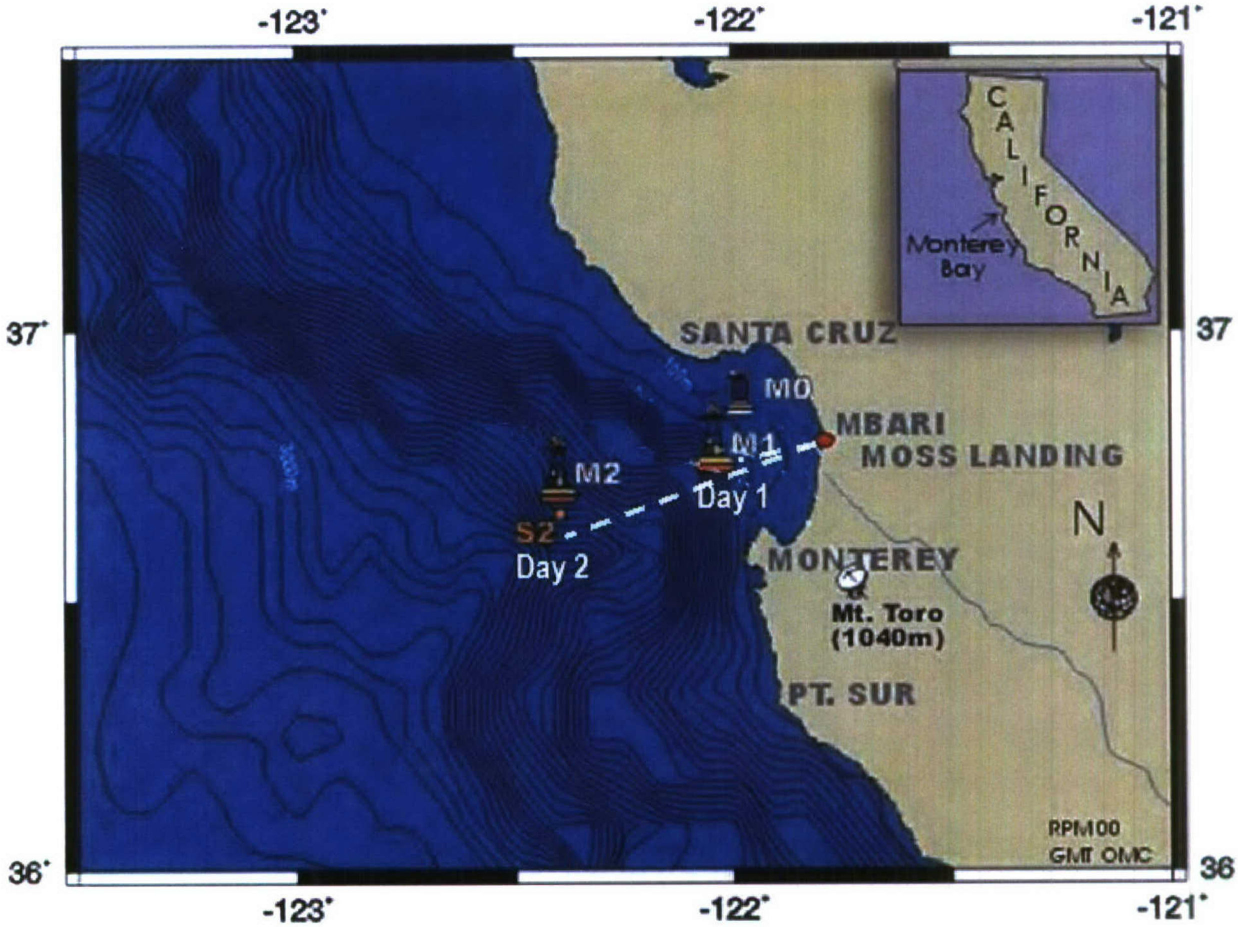

Fig. 13. Monterey Bay Test locations (Day 1 and Day 2)

Day 1 – October 25th

The Zephyr transited to the M1 buoy location and the wave energy buoy was deployed at 10:00 am and recovered at 3:24 pm. Hourly communications checks were conducted and indicated all electronics were functioning correctly. Winds were blustery, and increasing throughout the day. At 3pm, the wind speeds were measured at 20 kts. Significant wave height was 2.7M and peak wave period was 11 seconds. The available wave energy is shown in Fig. 14.

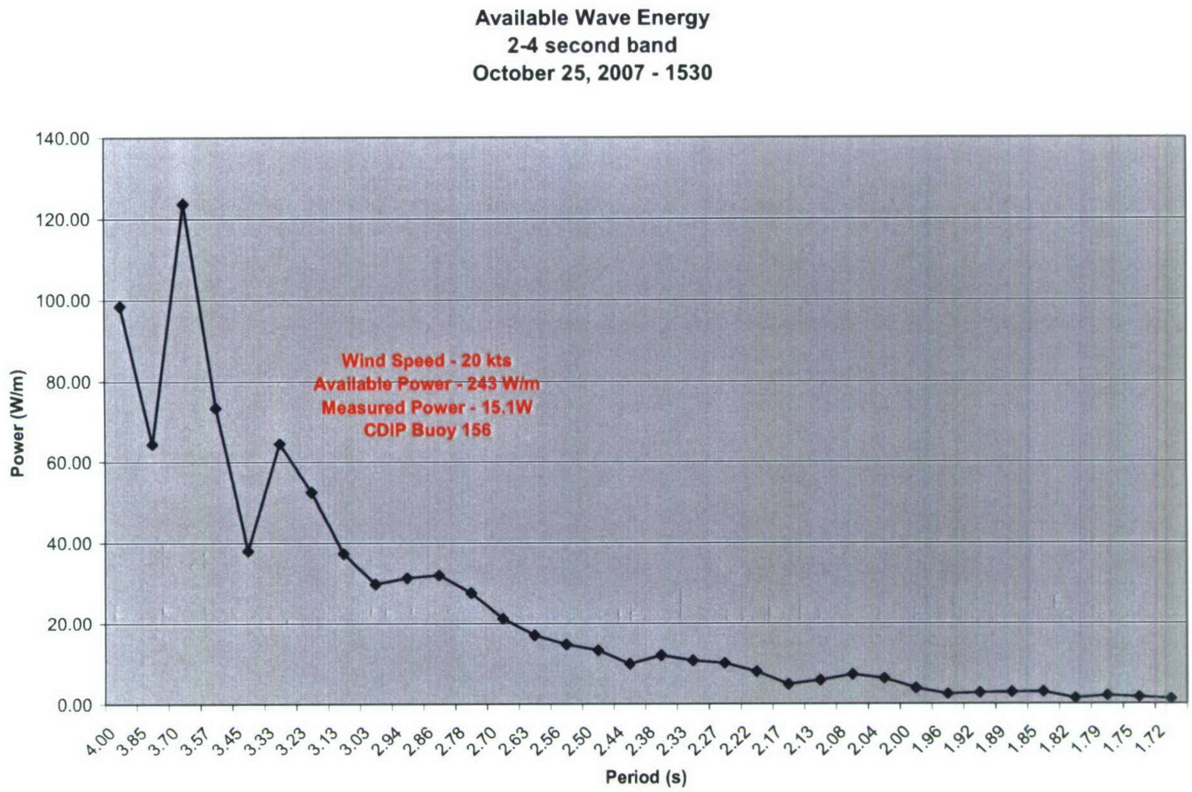

Fig. 14. Available wave energy in the 2-4 second band in Watts/m on October 25th at 1530

However, when the power data was downloaded from the logger, a programming error was discovered which resulted in the logger overwriting all data aside from a 3-minute section just prior to recovery. This data is shown below in Fig. 15 along with a photograph from the same time frame.

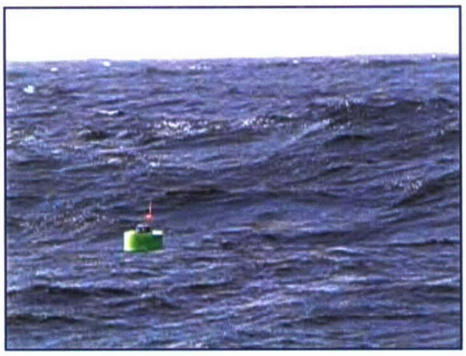

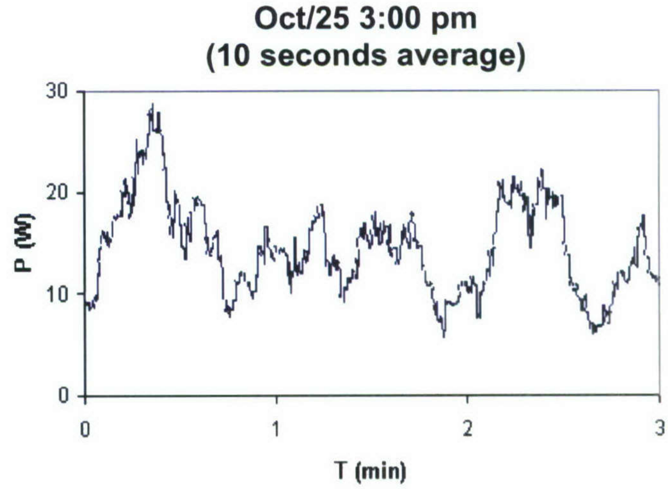

Fig. 15. Test data on Day 1 (Oct. 25 15:00) and photograph from the same time frame.

Day 2 – October 26, 2007

The Zephyr transited out to the M2 buoy location on the 2nd day. The wave energy buoy was deployed at 10 am and recovered just after 3 pm. A 5 hour continuous record of power and 6 DOF motion was recorded. Winds at the start of the deployment were 4 kts and subsided to 1-2 kts for the majority of the day. Significant wave heights were 2.8 M with a peak wave period of 13 seconds for the entire day. Little or no surface wind chop was evident. Fig. 16 below shows the available wave energy calculated from the NDBC buoy located near M2. Significantly less high frequency energy was available as compared to the conditions on the 25th.

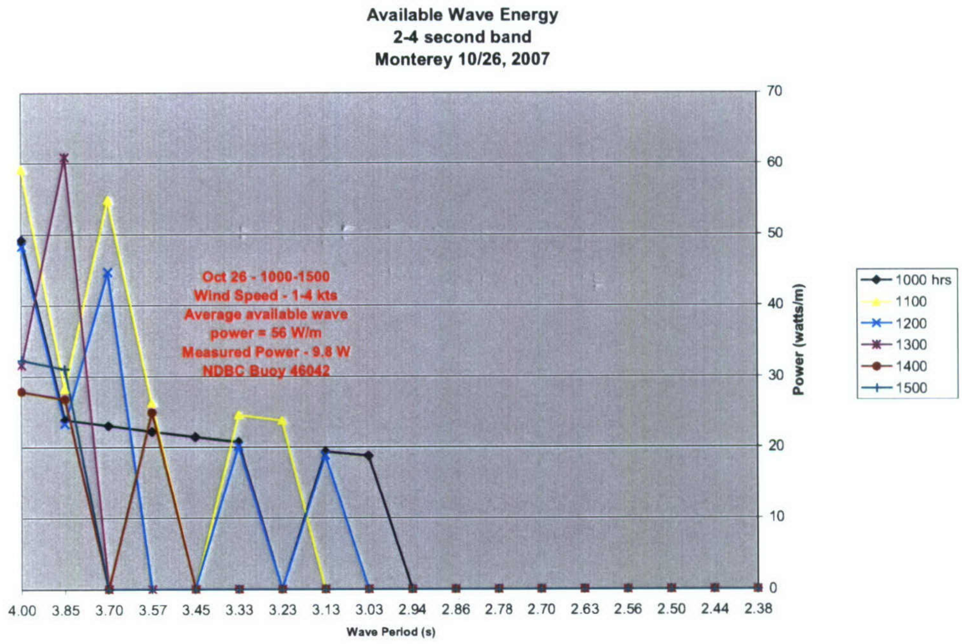

Fig. 16. Available wave energy calculated from the NDBC buoy collocated with the M2 buoy in Watts/m for the 2-4 second band.

Fig. 17 shows the 1 minute running average power from 1000-1100 hrs. Average power during this hour was 11.9W. For the five hour period on October 26th the average power was 9.9W. Fig. 18 is a photograph of the wave energy buoy at 1007 on October 26th.

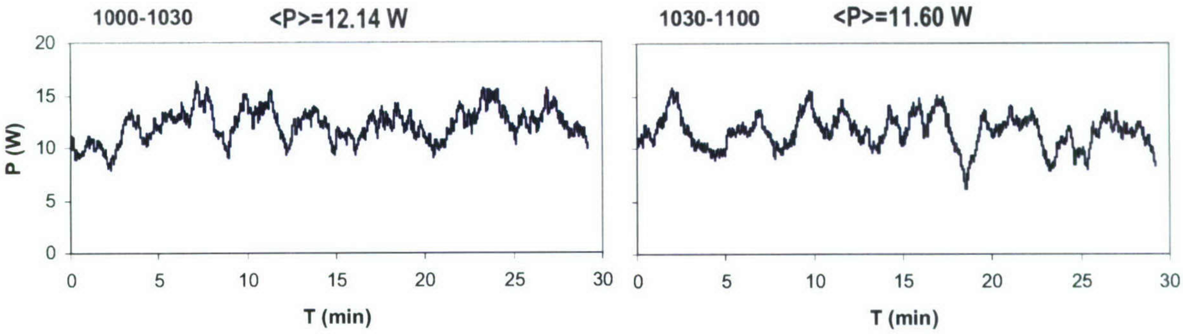

Fig. 17. 1 minute running average power calculations for the time periods of 1000-1100 on October 26, 2007. Average power for this 1 hour dataset was 11.8W. Wind speed was measured at 3-4 kts during this time.

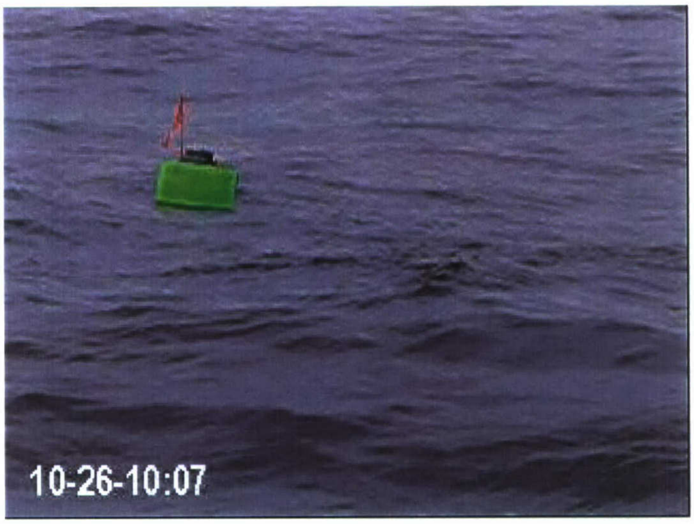

Fig. 18. The wave energy buoy deployed in Monterey Bay on October 26, 2007 at approximately 10 am.

Table 5 shows the total 2 Day summary of results along with calculated efficiency for the available energy in the 2-4 second band as well as the total energy available for all wave bands.

Table 5. 2 day Monterey Bay results summary table. Conversion efficiency is calculated for two scenarios, one from 2-4 seconds only, and another for all measured wave energy.

Date	Time	Duration	Energy bandwidth	NDBC - 46092 Available Wave Energy	watts Measured Power	kts Wind Spd	Beaufort Scale	2-4 second Conversion Efficiency	watts/m All Periods Total Energy	All Periods Conversion Efficiency
25-Oct	3:00 PM	2 min	1.7 - 4 sec	573	15.1	20	5	2.64%	25,851	0.058%
26-Oct	10:00 AM	1 hr	2-4 sec	198	11.87	4	2	5.99%	30,628	0.039%
26-Oct	11:00 AM	1 hr	2-4 sec	217	11.35	2	1	5.23%	37,154	0.031%
26-Oct	12:00 PM	1 hr	2-4 sec	155	10.065	2	1	6.49%	35,189	0.029%
26-Oct	1:00 PM	1 hr	2-4 sec	93	8.5	2	1	9.14%	39,135	0.022%
26-Oct	2:00 PM	1 hr	2-4 sec	79	6.95	2	1	8.80%	38,936	0.018%

Monterey Test Conclusions:

- Mechanical design performed well – No mechanical damping issues
- No mechanical degradation of device after 2 days of in water use. Post deployment generator "pluck test" identical to pre-deployment measurement
- Current design unable to generate 20W average power in Beaufort sea state 1
- Potential for about 20W in sea state 4 was evidenced in brief data collected on October 25th
- Average power of 10W for 5 hours achieved in Beaufort sea state 1
- Device efficiency calculated from available wave energy in 1.7-4 second band varied from 2.6-9.1%.
- Device efficiency calculated from all available wave energy (all frequencies) varied from 0.02-0.06%.

6.4 Oceanside Field Test November 16, 2007

The original design of the 20W device to be tested at Monterey Bay had two magnet cars joined by a semi-rigid link. Each magnet car had 40 generator units arranged in a 2 x 4 x 5 linear array. A single unit consisted of a pair of disk magnets separated by a 0.45" wide air gap in which a row of induction coils embedded in a polycarbonate blade moved through reciprocally during the oscillatory movement of the magnet car. The spacing of the coils matched to the magnet pairs such that the voltage output were in phase and combined to a single load. The total mass of the two magnet cars was 32 kg. They were suspended from 36 extensions springs with a combined spring constant of 508 Newton/meter to give the system a resonance period of 1.58 sec. However, after the first assembly, a slight mechanical misalignment between the magnet cars hindered the movement. The problem was rectified just prior to Monterey Bay test by removing the trailing magnet car and replacing it with equal mass ballast plates attached to the first magnet car.

After Monterey Bay test, we reattached the second magnet car and improved the linkage mechanism to ensure smooth oscillation without any hindrance. The device was tested for six hours in Oceanside Harbor just south of the pier on November 16, 2007 in a 11M RHIB with supporting personnel provided by SPAWAR. The buoy was deployed with a soft tether mooring in about 10M water depth shown in Fig. 19. An anchor was deployed along with several surface floats. The buoy was then tied off to the surface floats. This mooring technique proved very successful and appeared to have little impact on power generation.

Fig. 19. Energy harvesting buoy with surface floats during Oceanside test. The background is the Oceanside Pier.

Conditions for the Oceanside test were far from optimal, small (< 1M), long period (13.5 seconds) waves, and little or no wind for the majority of the day. Fig. 20 below shows the power output averaged over one minute interval at the beginning and the end of the test. There was very little variation throughout the test with power output in a range between 8-10W.

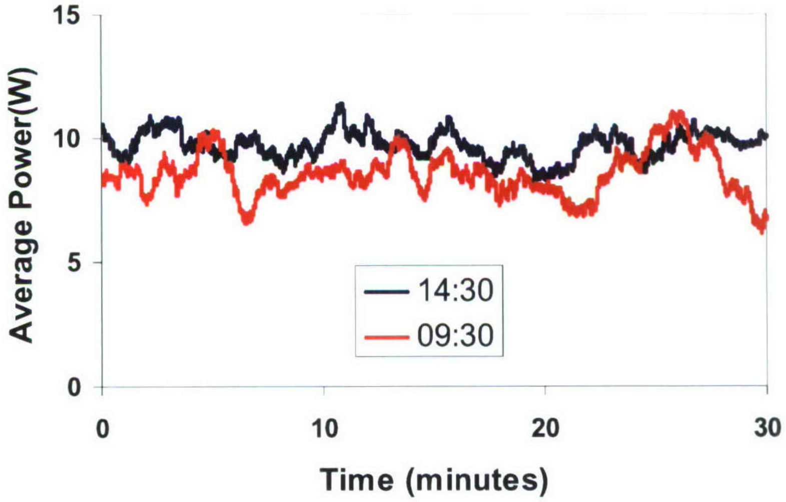

Fig. 20. Power output during the beginning and the end of the test.

Fig. 21 shows the hourly wave spectra for the day. Local winds increased slightly during the day from less than 1 kts to 2.4 kts in the afternoon. Detailed results from the testing are depicted in Table 6 below. On average the wave energy harvester generated slightly more the 9 watts of power, with conversion efficiency in the 2-4 second wave band of 13%. Average conversion efficiency with a single magnet car (Monterey test) was 7%.

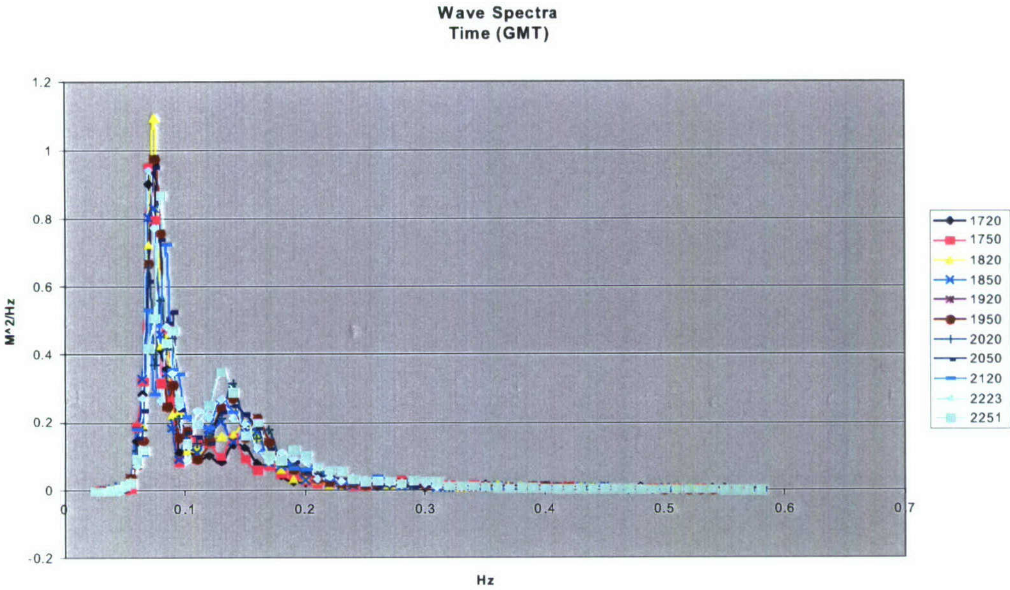

Fig. 21. Hourly wave spectra at Oceanside during Nov. 16 test

Table 6. Oceanside Test Results – November 16, 2007

Summary from CDIP Buoy #045 Wave Data = NDBC Reference - 46224 - Water Depth 223M
November 16, 2007 - Oceanside, CA

Date	Time Local (PST)	watts/m Total Power	watts/m 2-4 sec Power	Measured Power	Total Efficiency	2-4 sec Efficiency	kts Wind Speed	Beaufort Scale	Wave Height and Period M Hsig	Seconds Tp
16-Nov	9:50 AM	2529	83.2	8.53	0.337%	10.25%	1.3	1	0.7	13.3
16-Nov	10:20 AM	2645	82.9	9.05	0.342%	10.92%	1.3	1	0.72	14.3
16-Nov	10:50 AM	2571	60.9	8.91	0.347%	14.63%	1.3	1	0.75	13.3
16-Nov	11:20 AM	2486	69.6	8.88	0.357%	12.76%		1	0.73	13.3
16-Nov	11:50 AM	2748	67.5	8.95	0.326%	13.25%		1	0.75	14.3
16-Nov	12:20 AM	2557	59.0	9.01	0.352%	15.27%	1.8	1	0.77	13.3
16-Nov	12:50 AM	3079	57.4	9.03	0.293%	15.74%		1	0.76	14.3
16-Nov	1:20 PM	2410	61.5	9.2	0.382%	14.95%	2.7	1	0.81	13.3
16-Nov	1:50 PM	2646	76.6	9.22	0.348%	12.04%		1	0.73	13.3
16-Nov	2:23 PM	2858	71.1	9.68	0.339%	13.61%	4.5	2	0.77	11.8
16-Nov	2:51 PM	2882	80.4	9.68	0.336%	12.04%	2.4	1	0.79	14.3
Average		2674	70.0	9.10	0.34%	13.2%			0.75	13.53

The main attribute of the two-fold difference in efficiency is the addition of the second magnet car. An EM "pluck" test was conducted prior to deployment to select the optimum resistive load. In the pluck experiment, the magnet car assembly was extended 8 inches from its equilibrium position and released. The output voltage across a 50 Ohm load was recorded and the amount of captured energy was calculated at one second intervals after the initial release. Results are shown in Fig. 22. It is clear that the two-magnet car device had a much stronger EM coupling.

Consequently, the energy capturing process was faster and more efficient. During the first second, the generator with two magnet cars captured more than 70% of the total energy while the generator with one magnet car only captured less than 50% of the total energy. For the devices under test, the Fast Fourier Transform (FFT) analysis of the output voltage waveform showed a broad peak at 1.6 seconds. In order to maximize the power generation, most of the available energy must be captured in duration shorter that 1.6 seconds before the onset of next oscillation. Therefore, it is essential to have the second magnet cars in a generator to ensure strong EM coupling.

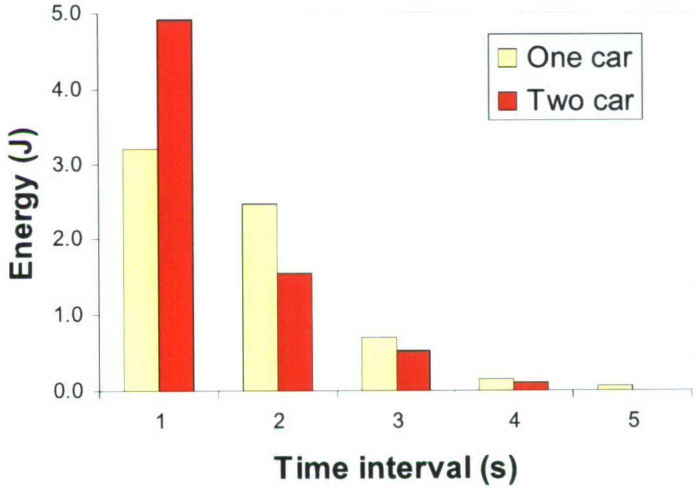

Fig. 22. Pluck experiment results of linear generator with one and two magnet cars.

Buoy movement analysis (comparison)

A 3-axis accelerometer and micro-gyro were installed inside the buoy at the level of the float collar. Data stream was recorded at 10 Hz rate. Raw data were analyzed by Fast Fourier Transform (FFT) averaged over a 30 minutes period for heave, pitch, roll movements and the power output from the coils. These results provide an understanding of wave/buoy interaction and buoy/generator interaction that will validate the hydrodynamic model and offer insight for device design improvement.

Fig. 23 compares the spectral density of the heave movement of the device tested at Monterey Bay and Oceanside. Both cases show two peaks near 1.0 Hz and 0.5 Hz, in agreement with the prediction by the hydrodynamic model. Since the linear generator was tuned to 1.58 sec. or 0.63 Hz, its spring mass system acted as a low pass mechanical filter when it was subjected to random wave forcing. We used a classical mechanical model to calculate the response curve assuming a 50 Ohm load and a constant forcing amplitude of 0.1 meter. The response curve is superimposed on the FFT spectrum for comparison. It has an onset threshold at 0.43 Hz or 2.3 seconds and increases slowly with the wave frequency. The result indicates that the generator harvested directly most of its energy from the high frequency peak. The low frequency heave movement could only contribute to the energy harvested indirectly via more complex hydrodynamic interactions.

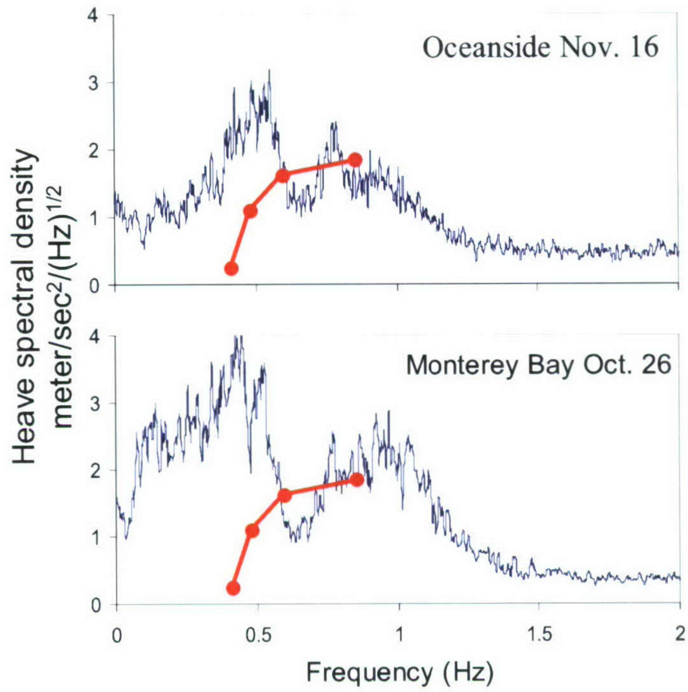

Fig. 23. Buoy heave spectra during Oceanside and Monterey tests. The red curve is the calculated response curve of the generator.

Another interesting buoy movement is its pitch and roll (P/R). Accurate P/R movements were deduced from the onboard accelerometer mounted in the sway and surge directions by FFT. Fig. 24 shows the results for the scale model sea test on June 11. Fig. 25 shows the results and the 20 W model during the MB and OS tests.

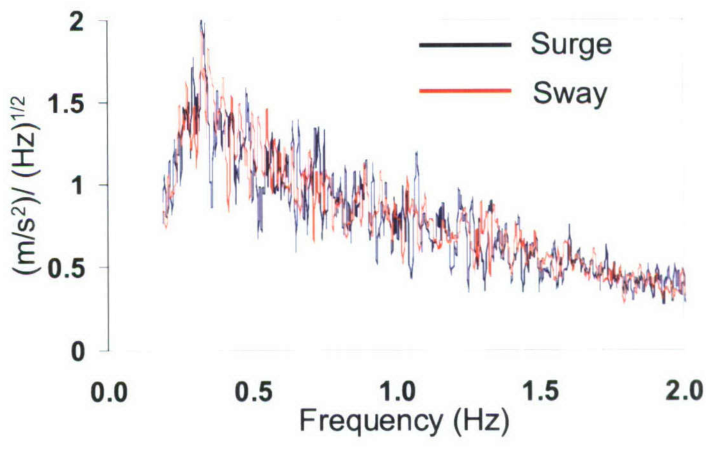

Fig. 24. Surge and sway acceleration of the scale model during June 11 sea test.

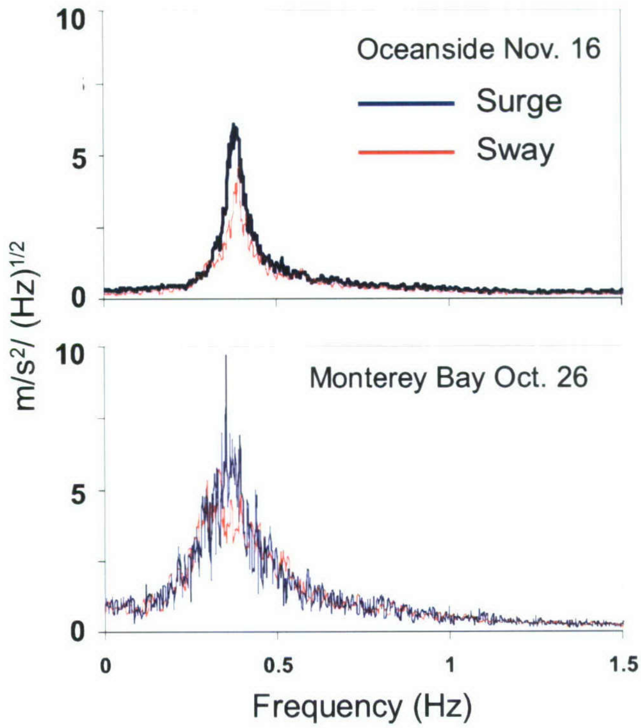

Fig. 25. Surge and sway acceleration FFT of the 20W buoy in Oceanside and Monterey Bay tests.

These results show several interesting features:

1. The scale model is azimuthally symmetric with cylindrical magnet stack oscillating inside induction coils. Therefore, the pitch and roll spectra were identical. However, for the 20W device tested at MB and OS, the linear generator does not have a cylindrical symmetry, therefore, the surge and sway movements differed slightly. Results showed that the surge movement (defined as the movement in the direction perpendicular to the magnet field of the generator) to have a higher peak value. The difference is an indication that the generator movement and the buoy movement were closely coupled.

2. The P/R FFT spectrum of the 20W device had a well defined peak at 0.41 Hz. or 2.41 sec period in both MB and OS tests. Under a very calm sea state 1 condition at OS, the full width at half maximum (FWHM) was only 0.1 Hz. During the MB tests, the peak was broadened random waves in much higher sea states.

3. The acceleration in the sway and surge directions during P/R motion were about 5 meter/sec^2, more than double heave acceleration. Therefore, these well defined P/R movements have the potential to be a reliable and predictable source of motion energy for wave energy harvesting.

7.0 Technology Transition Opportunities and Applications

7.1 SPAWAR

SPAWAR's Deployable Surveillance Group at SSC working with PMS 485 has a need for a self-powered radio transmit buoy. This buoy will take acoustic sensor data from the seafloor, process the data and transmit the data to a receiving craft. This buoy may be operating autonomously in contested waters. It must have low visibility attributes and high anti-tamper attributes. The present power requirement for this Buoy is 100 watts processing and 50 watts of radio transmit power. The anticipated future power requirements are 50 watts total. In addition, this buoy must be tethered to the sea floor with strength and data cable, provide continuous radio transmission, have an above sea level height of 1-2 meters and an above sea level diameter of less than 8 inches. The Power system must be quiet enough not to be heard by a human ear at 50 feet, the buoy/generator must be able to survive sea state 5 and by using energy storage devices be able to sustain continuous power draw of 50 watts from the sea state schedule shown below. Assume a processor and radio payload of 10 pounds dry and 2 cu Ft in volume. Assume an antenna at the top of the buoy that is 10" high, 2" in diameter and weighs 4 pounds. The production cost of this buoy without payload should not exceed $400K each. The buoy must be able to provide continuous power through sequential operation with the following sea states, starting and ending in a fully charged state.

- Sea State 0 - 16 hours
- Sea State 1 - 8 hours
- Sea State 2 - 24 hours
- Sea State 1 - 8 hours
- Sea State 0 - 16 hours
- Sea State 3 - 6 days

7.2 Teledyne Benthos

Teledyne is internally funding a project to build a prototype communications buoy using wave energy. This buoy provides an RF radio link to an underwater network of sensors, which are communicating via acoustic modems. Each sensor transmits its data acoustically to the Gateway Buoy, which in turn relays the data via an RF link to a shore-based computer for display and analysis. This buoy currently uses standard "D" cell batteries and has lifetime limit of 14 days. The buoy requires 1-3 Watts of continuous power. A description of the existing buoy is shown in Fig. 26.

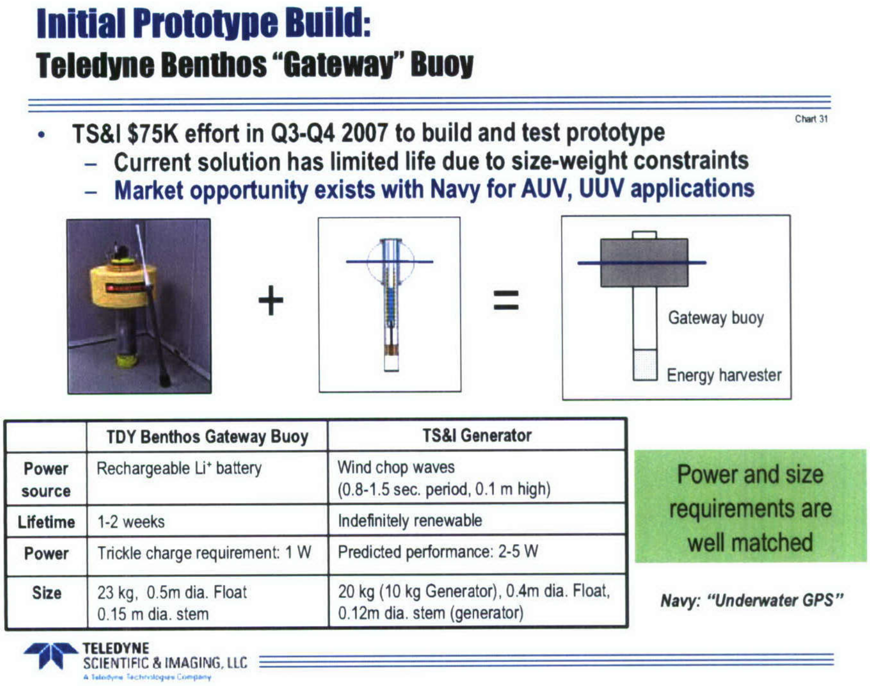

Fig. 26. Teledyne Benthos Gateway with wave energy harvester integration.

7.3 Teledyne Geophysical

Teledyne Geophysical is the leading manufacturer of hydrophone streamer arrays used in offshore oil and gas exploration. These hydrophone arrays require precise position information in order to process the sound returns during seismic exploration and determine where oil and natural gas reserves are located. As offshore exploration continues in deeper water the position accuracy of each array during a survey is becoming more critical. Customers are requesting a self-powered tail buoy which would have electronics to accurately measure position and motion of the streamer array cable. The buoy would be towed behind the survey vessel on the end of each array at a speed of 10-12 kts. Total power requirements is 50 Watts.

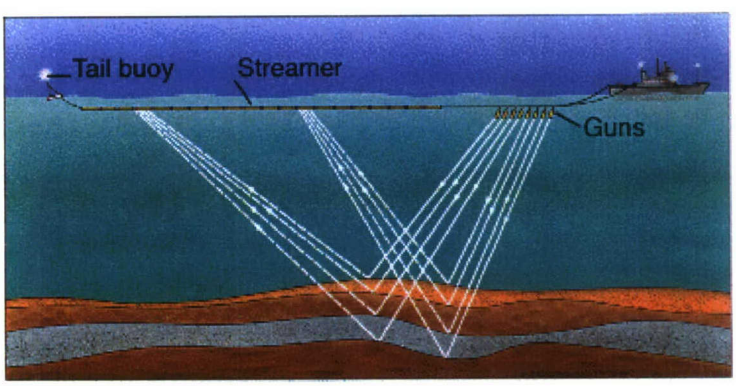

Fig. 27. Teledyne Geophysical tail buoy.

8.0 Conclusions and Recommendations

Program conclusions:

1. The wave energy harvesting technology developed by TSC during this program has proven the ability to create small, self-powered instrumentation buoys requiring from 1-20W of power.
2. The program has created a set of design "rules and tools" by which to guide further development and commercialization.
3. The program has created a numerical modeling capability to predict design performance for a given set of environmental conditions.
4. The ferrofluid liquid bearing is an enabling technology in the linear generator design, allowing the mass-spring generator to perform efficiently at tilt angles of up to 20 degrees which are often encountered in wave and wind environments.

Recommendations for further development:

1. A weak link of this system is the current state of spring technology. The characteristics, reliability and lifetime of the springs in the current design make scaling up the power to above 50W very difficult. Additional spring research should be conducted to explore using air, magnetic and compression springs.
2. A power conversion electronic sub-system should be developed. COTS charging electronics do not have the necessary bandwidth to handle the highly variable power signal generated by the wave energy generator efficiently. Customer electronics for this purpose must be designed.
3. Long term testing under various sea states to test device ruggedness and further validate the performance model should be conducted.

9.0 Appendix 1 – DARPA Program Completion Report

Program Title

Ocean Wave Energy Harvesting – DARPA Contract No. HR0011-06-C-0030

9.1 Executive Summary

The objective of this program was to demonstrate two wave energy harvesting buoys based on the Teledyne high-efficiency linear generator design. The large unit was approximately the same size as the Mark 46 Torpedo, and was designed to generate 20 Watts in a broad range of Sea States (1-5). The small unit had size and weight amenable to manual deployment from a boat by two persons to generate 3 Watts in calm water (Sea State 1). Buoy design and development was performed in parallel with the development of a hydrodynamic/classical mechanical model to simulate the device operation in a given ocean wave spectrum. This modeling predicted device performance and also gave guidance critical to buoy design. Wave tank and sea test data, consisting of power output as well as the six degrees of freedom (DOF) of the buoy movement were used to cross check and refine the model. The purpose of the model was to serve as "rules and tools" for the design of wave energy harvesting buoys in increasing generality, to enable future efforts.

The program was scheduled around major sea and wave tank tests. The key milestones were the 20W unit sea test at Monterey Bay in late October and a wave tank test at the Texas A&M University's Offshore Technology Research Center (OTRC) in mid-September. The tests were preceded by work on the scale model and 3W units, including wave tank tests at Scripps Institute of Oceanography and field tests just offshore at San Diego. During the program, a total of three wave tank tests and six sea tests were conducted. Results were simulated and validated by the hydrodynamic model.

Key accomplishments include the development of modeling capabilities to optimize electromagnetic design by a classical mechanical model and predict device performance by a hydrodynamic model. The device designed for 3 Watts actually generated 1.88 W in a sea test, with the shortfall attributed to a mechanical flaw that reduced the device dynamic sensitivity. That finding and the need to scale up steered us to use a transversal linear generator in the 20W unit because of its more desirable mass distribution. After discovering and resolving several mechanical design issues a sound device designed for 20 Watts was produced and tested in Monterey and Oceanside, CA. This device generated 10W average power in Beaufort Sea State 1 while deployed with a surface mooring, and showed potential for up to 20W in Sea State 4. In all cases, the device showed no sign of mechanical degradation.

The program has shown the feasibility and effectiveness of a completely sealed, corrosion resistant wave energy harvesting device.

9.2 Program Objective and Technical Need

Problem/requirement addressed

The goal for the Wave Energy Harvesting Program was to develop renewable energy sources for buoy-based ocean surveillance applications. These applications include: autonomous target recognition and classification algorithms for asymmetric littoral threats; persistent and ubiquitous sensor systems; tracking and identification of maritime vessels; mobile, distributed, autonomous systems for undersea environments; unmanned underwater gliding surveillance vehicles; and miniature, low power underwater sensor networks. These devices will eliminate the need for batteries, thus enabling more functionality, higher data rate and a longer operational lifetime.

The specific objectives for Phase 3 of the program are:

1. Demonstrate autonomous self-powered buoy capable of generating 20 Watts output in arbitrary conditions encompassing a broad range of sea states (Sea States 1-5). Size and weight not to significantly exceed profile of Mark 46 Torpedo (L ~ 2.6 m; D ~ 324 mm; Wt ~ 235 kg).
2. Demonstrate autonomous self-powered buoy capable of generating 3 Watts in calm waters (Sea State 1), with size and weight amenable to manual deployment from a boat by two persons.
3. Demonstrate "rules and tools" for design of self-powered buoys, based on simulations encompassing all significant parameters for ocean behavior and device physics, verified by comprehensive wave tank and ocean testing.

State of the art at time of program inception

Most Ocean Wave Energy Conversion (OWEC) devices in current operation are designed to produce power in the kilowatt to megawatt range. These state-of-the-art devices are large in size and use elaborate mechanisms to convert random wave motion into a useful form of energy. Due to their mechanical complexity, it is difficult to reduce the size to be integrated to small buoy-based marine surveillance systems without significant performance sacrifice.

A significant amount of the state-of-the-art developments in smaller scale energy harvesting arose from Phase 1 and Phase 2 of the current DARPA effort (thus serving as the basis for our Phase 3 development). These accomplishments include:

1. Demonstrated the performance of a mass-spring system linear generator.
2. Developed a classical mechanical model to accurately predict the device performance under monochromatic, sinusoidal forcing. The model can be used to determine the magnet stack mass and spring constant in device design and the "best" load for power extraction.
3. Obtained limited test data in monochromatic waves but no data in random waves.

Specific technological problem addressed

In this Phase 3 program, we addressed the following specific problems:

1. Development of modeling and simulation tools to predict performance and guide development for specific generator and buoy designs in given sea conditions. The model also helps select best electrical load required to optimize energy generation.
2. Effective power generation in a large variety of wave conditions.

3. Quantitative determination of the effect of a novel bearing on buoy performance when buoy pitch and roll are present (Demonstrated in controlled wave tank test).
4. Increased power generation of the linear generator by increasing the magnet stack mass ten-fold. (e.g., 1 kg for the scale model and 33 kg for the 20W model). Technical issues included the high packing density of the linear generator and spring selection and design.
5. Understanding the effect of a mooring on buoy/generator performance.
6. Ruggedization and survivability of the buoy/generator for sea testing.

9.3 Program Description and Milestones

The following chart shows the progress and milestones.

ID		Task Name	Duration	Start	Finish
1		**Enhance and Validate Simu**	**60 days**	**Mon 5/7/07**	**Fri 7/27/07**
2		Determine Available Mod	5 days	Mon 5/7/07	Fri 5/11/07
3		Collect Reference Ocean	5 days	Mon 5/14/07	Fri 5/18/07
4		Build Two Test Units	10 days	Mon 5/21/07	Fri 6/1/07
5		Sea Tests	5 days	Mon 6/4/07	Fri 6/8/07
6		Develop Enhanced Mode	35 days	Mon 6/11/07	Fri 7/27/07
7		**Develop Generator/Buoy D**	**60 days**	**Mon 5/7/07**	**Fri 7/27/07**
8		Buoy w/Discrete Freque	30 days	Mon 5/7/07	Fri 6/15/07
9		Buoy w/Tunable Frequer	30 days	Mon 6/18/07	Fri 7/27/07
10		**Trade Study to Optimize D**	**60 days**	**Mon 7/30/07**	**Fri 10/19/07**
11		3 watt buoy in Sea State	30 days	Mon 7/30/07	Fri 9/7/07
12		20 watt Buoy in Sea Sta	30 days	Mon 9/10/07	Fri 10/19/07
13		**Build and Ruggedize Gene**	**60 days**	**Wed 8/1/07**	**Tue 10/23/07**
14		3 watt Buoy	30 days	Wed 8/1/07	Tue 9/11/07
15		20 Watt Buoy	30 days	Wed 9/12/07	Tue 10/23/07
16		Monterey Test Plan	5 days	Mon 9/3/07	Fri 9/7/07
17		**Monterey Field Test**	**30 days**	**Mon 10/1/07**	**Fri 11/9/07**
18		Build Test Buoy (s)	10 days	Mon 10/1/07	Fri 10/12/07
19		Pre-liminary Field Test - (	5 days	Mon 10/15/07	Fri 10/19/07
20		Preparation for Monterre	15 days	Mon 10/22/07	Fri 11/9/07
21		Improve Model and Develop "F	60 days	Thu 11/1/07	Wed 1/23/08
22		Identify DoD Transition Path	270 days	Mon 5/7/07	Fri 5/16/08
23		**Monthly Report**	**222 days**	**Mon 5/7/07**	**Tue 3/11/08**
35		Final Report, including Techno	30 days	Fri 1/4/08	Thu 2/14/08

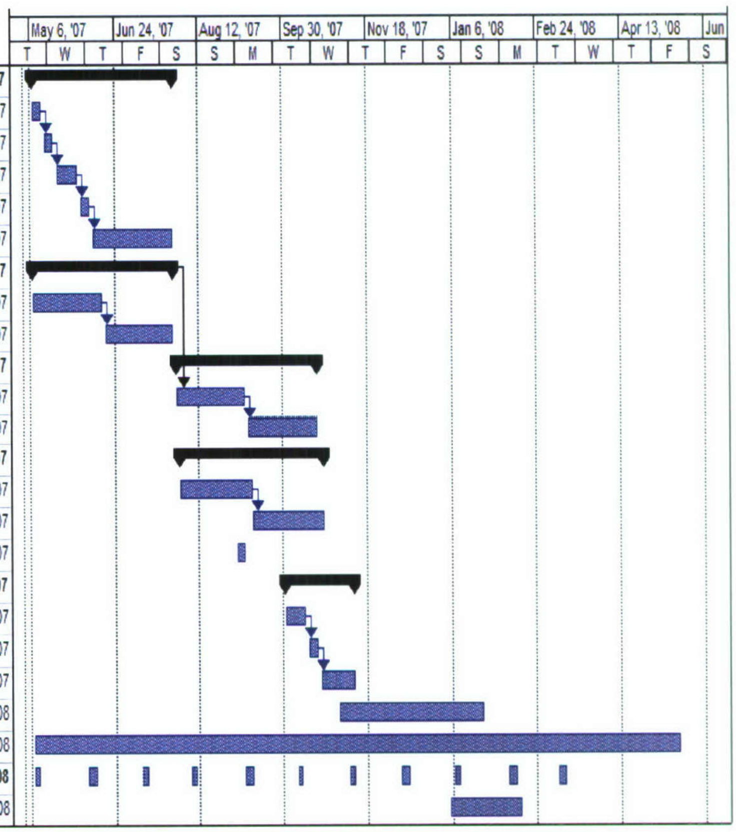

Program structure and plan

The program had two major development efforts, carried out in parallel.

1. Device development: design, fabrication, bench/wave tank/sea testing, data analysis, and reliability.
   - Scale model (<1 W)
   - 3W device
   - 20W device
2. Numerical model development
   - Design guidelines
   - Predict performance
   - Hindcast

In addition, the program included technology transition efforts which were carried out with the Navy throughout the program.

Major technical problems and approaches made during the life of the program

1. Mechanical complication with both the 3W and 20W buoy led to additional costs and program design delays
    - Change from an axial design (3W device) to transversal design (20W device) for scaling up to larger units with higher power production
    - Change from polar array coil plates (20W device used in ORTC tank test) to 2D-array coil plates (20W device for sea tests) for higher mechanical rigidity and better alignment
    - One magnet car (20W device for Monterey Bay test) for better alignment.
    - Second magnet car was later placed back but with improved alignment (for 20W Oceanside test)
2. Due to device size limit, all linear generators were tuned to high frequency waves with wave period between 1.5-1.8 sec. Wave measurements in the high frequency band have proven not reliable for accurate model analysis therefore extrapolation of wave data to high frequency has been required.
3. Due to the mechanical design issues noted above we were unable to consider additional techniques for broadening the response of the wave energy harvester, such as adaptive loads and multiple generators. Instead we focused on high frequency wave energy, which is expected to be present most often in coastal environments, and on use of a hybrid buoy design.

Reason for program completion

The Phase 3 program established "proof of concept" for small, relatively low power, renewable energy systems using waves, and development of the modeling and manufacturing and design techniques required to successfully build these systems. These encompassed the key overall goals of the Phase 3 program.

Further work is required in the cost and manufacturability of the systems and the power system electronics. It is anticipated that this further development will be funded through other DOD entities with specific end uses, and through Teledyne internal development efforts targeted at defense and commercial markets.

9.4 Scientific and Technical Results and Accomplishments

Results of the effort in relation to program objectives

1. A device designed to generate 20 Watts was designed, fabricated, and sea tested. Results from two sea tests (Objective 1):
    - Monterey Bay, CA (Oct. 25, 2007) – Up to 20W in Beaufort Sea State 4 (3 minutes of data)
    - Monterey Bay, CA (Oct. 26, 2007) – Average 10W in Beaufort Sea State 1 (6 hours of data)
    - Oceanside, CA (Nov. 16, 2007) – Average 8-10W in Beaufort Sea State 1 or less
2. A device designed to generate 3 Watts was designed, fabricated, and sea tested.

Results from one sea test (Objective 2):

- La Jolla, CA near Scripps pier (July 20, 2007) – Average 1.88W in Beaufort Sea State 2-3, 0.2-0.5 in Beaufort Sea State 0-1

3. Extensive simulation development to model device performance based on input wave spectrum and device specifications enabled optimized design in parallel with device fabrication (Objective 3).

Technical aspects of the effort that were successful and aspects of the effort that did not materialize as originally envisioned

1. Successful efforts
    - Device development
        - Device designed for 3 Watts – 1.9 Watts measured output in first sea test
        - Device designed for 20 Watts –
            - ORTC wave tank test (partial success with useful buoy movement data for modeling validation)
            - Monterey Bay sea test free drift
            - Oceanside sea test with surface mooring.
    - Enhanced performance model development
2. Did not materialize as originally envisioned
    - Broadband performance either by multiple generator integration or frequency tuning was originally envisioned. However, the mechanical design difficulties encountered throughout the program did not allow consideration of load tuning or multiple generators as methods to broaden the response of the systems and increase the efficacy in a wider range of sea conditions. On the positive side, our "hybrid" buoy design and wind wave energy target has shown promise for small buoy power systems with 5-20W requirements.

Comprehensive list of performers

Jeffrey Cheung – Senior Scientist
Teledyne Scientific
Thousand Oaks, CA
jcheung@teledyne.com

Earl Childress – Program Manager
Teledyne Instruments
Poway, CA
echildress@teledyne.com

Ron George – Buoy Designer
Oceanscience Group
Oceanside, CA
rgeorge@oceanscience.com

Warren Bartel – Hydro-dynamic Modeler
Naval Facilities Engineering Command (NAVFAC)
warren.bartel@navy.mil

Jeff Lloyd – Logistics and Testing
SPAWAR Systems Center, San Diego
Jeffrey.m.lloyd@navy.mil

9.5 Applications and Considerations for the Future

Conclusions of technical feasibility

We have demonstrated the performance of a wave energy harvesting buoy in sea state up to Beaufort scale 4 with power output from 8W to nearly 20W. The device is completely sealed and corrosion resistant in the marine environment. It did not show any degradation after more than 20 hours sea operation. The device can be scaled for high power operation and can be used as a renewable energy source for marine instrumentation.

Recommendations on additional R&D requirements and opportunities

1. Develop 50-100W design to meet Navy requirements for self-powered radio transmit buoy.
2. Investigate and/or develop other spring types and designs in order to control device size as larger power levels are required and to increase the spring lifetime to 3 years or longer.
3. Perform long term testing under various sea states in order to further characterize device performance and reliability. This testing will also improve the numerical model performance.
4. Develop power electronics with conversion efficiency of at least 80%. The electronics must be able to handle large power spikes of a few hundred watts seen in typical device output.
5. Develop Aid to Navigation (AtoN) self-powered buoy system for U.S. Coast Guard, to provide 10-20W of power continuously for 2+ years.

9.6 Program Transition

- Spin-offs internal to DoD outside of major transition
  - Potential opportunity for SPAWAR Systems Center, San Diego. During Q1 2008 a proposal will be developed to address need for self-powered, radio transmit buoys. The total power requirement is 50W.
- Spin-offs to commercial development
  - Teledyne Benthos is developing a low power surface "Gateway" communications buoy for use in underwater acoustic to satellite and/or RF communications link. It is expected that this buoy will be designed and tested during 2008 and sold commercially in 2009. Potential end-users include the Office of Naval Research, Coast Guard, NOAA's National Data Buoy Center, and offshore oil and gas companies.
  - Teledyne has a number of other business units including Teledyne RDI and Teledyne Geophysical that are actively engaged in ocean instrumentation, and may provide additional commercial outlets for the technology.
  - We continue discussions with a range of outside companies and government customers to develop an initial application with sufficient "user pull" to progress the technology into the DOD user space.

10.0 Appendix 2 – Numerical model tutorial

Naval Facilities Engineering Command
ENGINEERING SERVICE CENTER

Preparation of 20 Watt Buoy Model in Orcaflex

Warren Bartel
NAVFAC Engineering Service Center
Ocean Engineering Division
1100 23rd Ave
Port Hueneme, CA 93043
(805) 982-1215
warren.bartel@navy.mil

21 January 2008

Outline

- Information Gathering on Buoy and Magnet Physical Properties
- Build Buoy with Magnets in Orcaflex
- Natural Period Tests
- Random Wave Tests
- Appendix

Final 20W Buoy as Tested

36 Springs = 504 N/M
40 magnet pairs
30 kg with ballast
60 coils
Total Buoy = 113 kgs
50 ohm resistive load
Total Length = 1.8 M
Collar Diameter = 0.6M

20W Buoy Dimensions

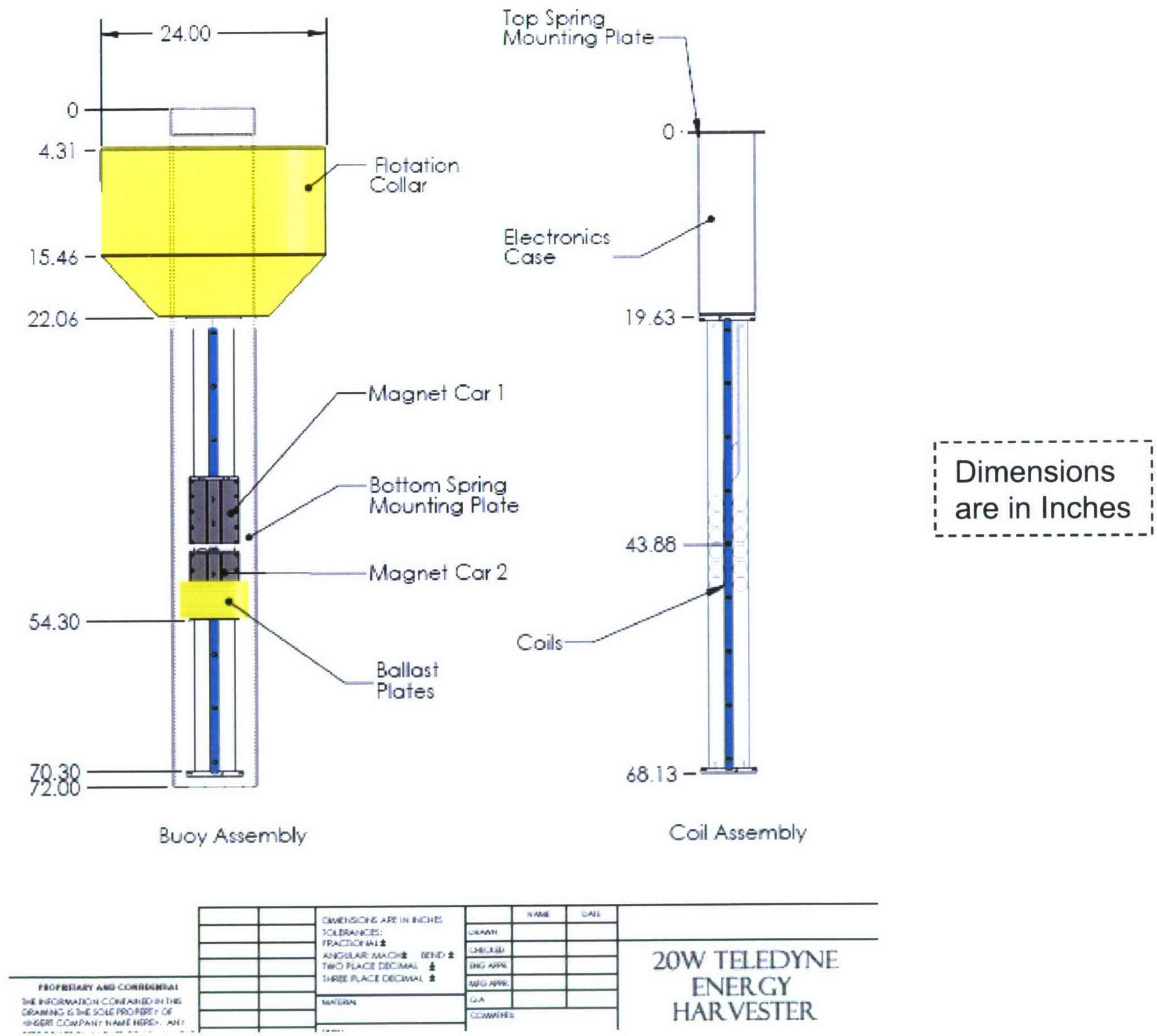

20W Buoy Details

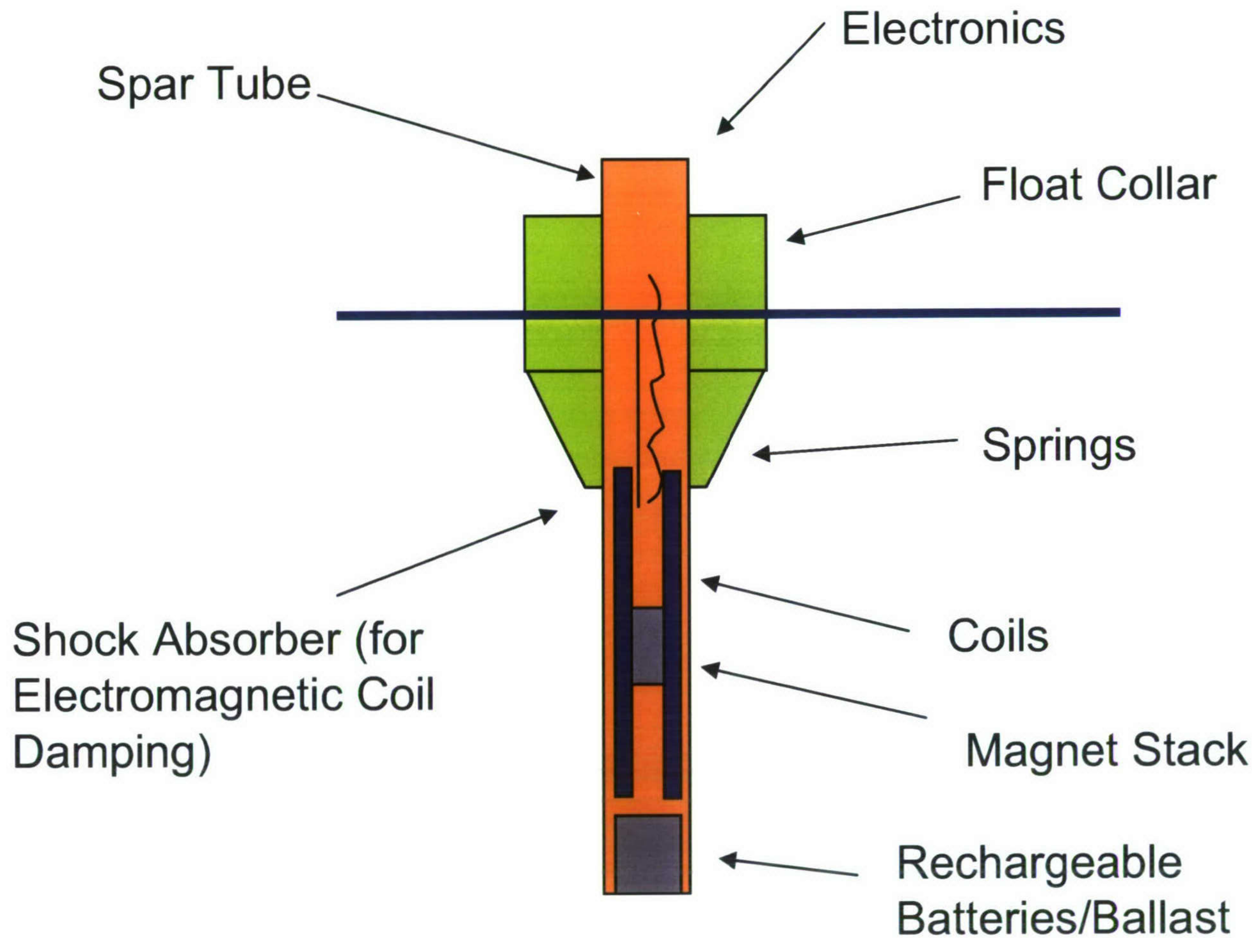

Mechanical Properties for Dual Magnet Car 20W Buoy

- Buoy:
  - Height: 6 ft (1.8 m)
  - Tube Dia: 9 in (22.86 cm)
  - Collar: 24 in (61 cm) wide x 12 in (30.5 cm) tall with Taper
  - Weight with Ballast (no magnet cars): 188 lbs (85.3 kg)
  - Center of Mass: 27.2 in from keel (69 cm)
  - Inertia: X and Y: 530 lb-ft^2 and Z: 12 lb-ft^2
    - X and Y: 21 kg-m^2 and Z: .2 kg-m^2
  - Draft: 5.1 ft (1.55 m)
- Magnet Cars
  - Two Sets
  - Total Weight: 72 lbs (32.66 kg)
  - Springs: EA = 26.649 lbs (K = 34.53 lb/ft) (K=504 N/m)
  - Magnet Stack Center for Stretched Springs = 26 in (66 cm)

Gather Buoy and Magnet Physical Dimensions and Weights and Spring Properties

- Buoy Dimensions for the Hull
- Buoy Mass and Magnet Mass Values
- Magnet Spring Stiffness and Length Values
- Buoy Center of Mass, Moments of Inertia from Solid works
- Decide how to break up the buoy into a section of stacked disks in Orcaflex
- Use MS Excel to Calculate Projected Areas for each disk

Buoy Cylinder Heights, Diameters and Areas from MS Excel Spreadsheet

We need to pre-calculate the sizes of the cylinders to represent the spar buoy with collar. This is done in MS Excel, mainly for odd shapes such as a tapered collar. If the buoy and collar are simple cylinders, hand calculations could be done

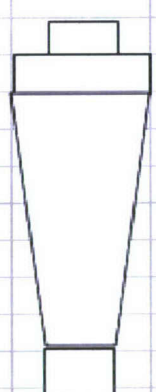

Disk No.	Height (ft)	Dia (ft)	Area X (ft2)	Area Z (ft2)	Orcaflex Az (ft2)
1	0.359167	0.75	0.27	0.442	0.442
2	0.929167	2	1.86	3.142	2.700
3	0.078571	2	0.16	3.142	0.679
4	0.078571	1.770833	0.14	2.463	0.516
5	0.078571	1.574405	0.12	1.947	0.455
6	0.078571	1.377976	0.11	1.491	0.395
7	0.078571	1.181548	0.09	1.096	0.334
8	0.078571	0.985119	0.08	0.762	0.274
9	0.078571	0.78869	0.06	0.489	0.047
10	4.161667	0.75	3.12	0.442	0.442

Launch Orcaflex Ocean Structural Modeling Tool

Units and Water Depth

Launch Model Browser

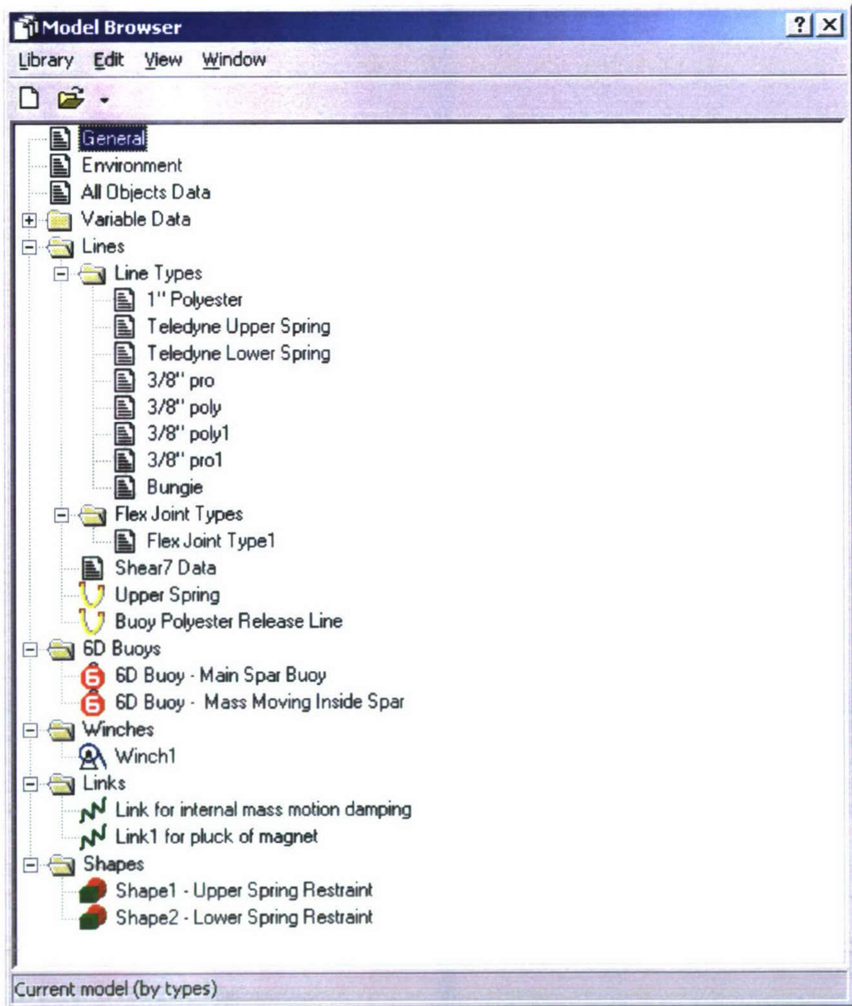

General Tab, Select User Units

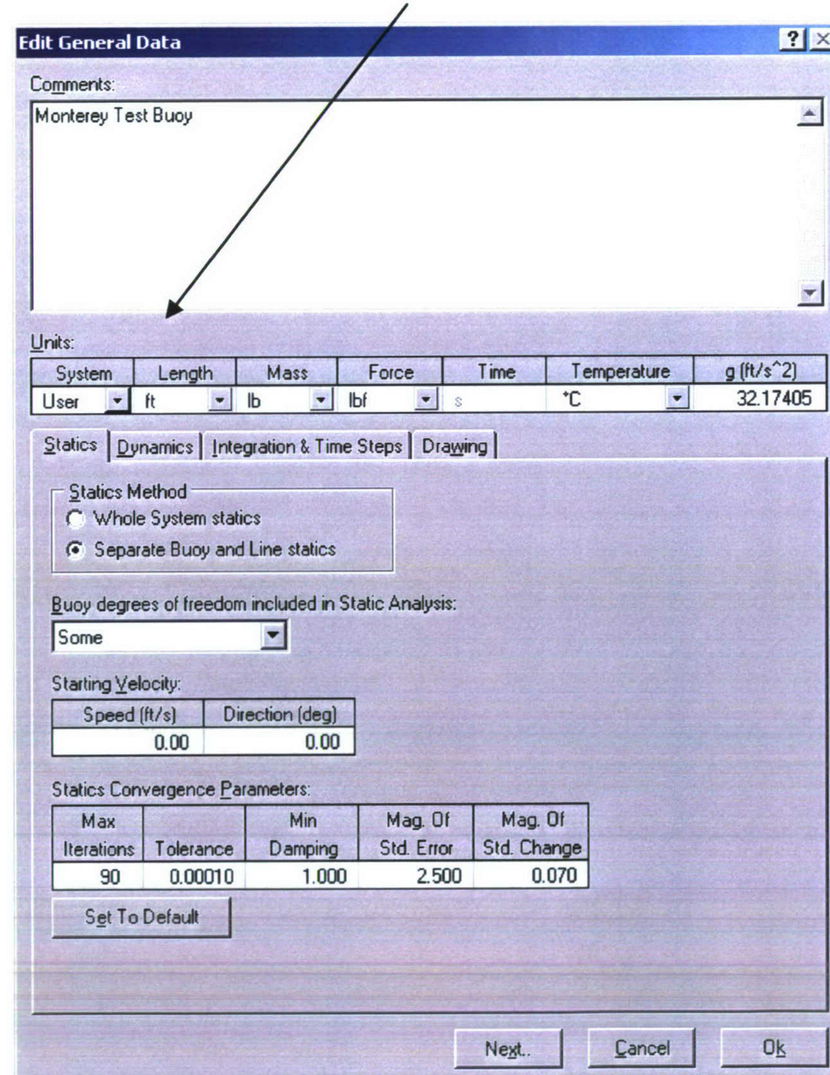

Units and Water Depth

Go Back to Model Browser

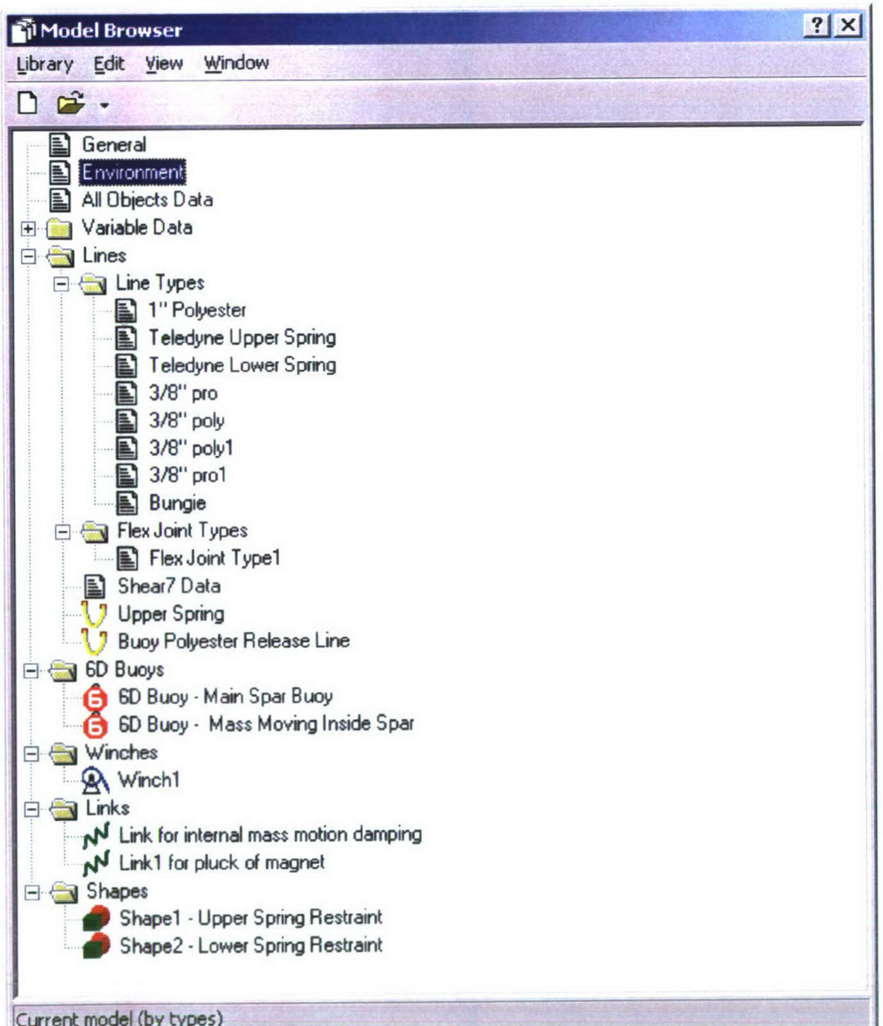

Environment Tab, Select Seabed, and Set Water Depth

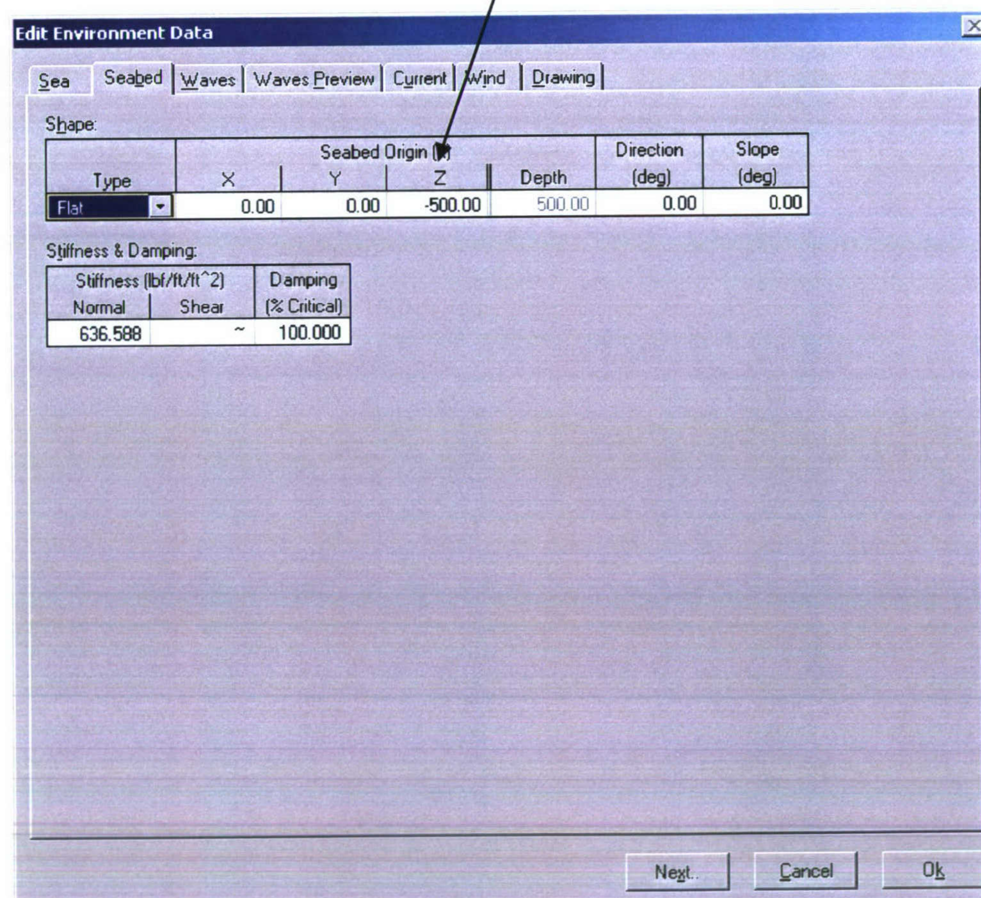

Turn Off Waves

Go Back to Environment Tab

Select Waves and Set Height to Zero

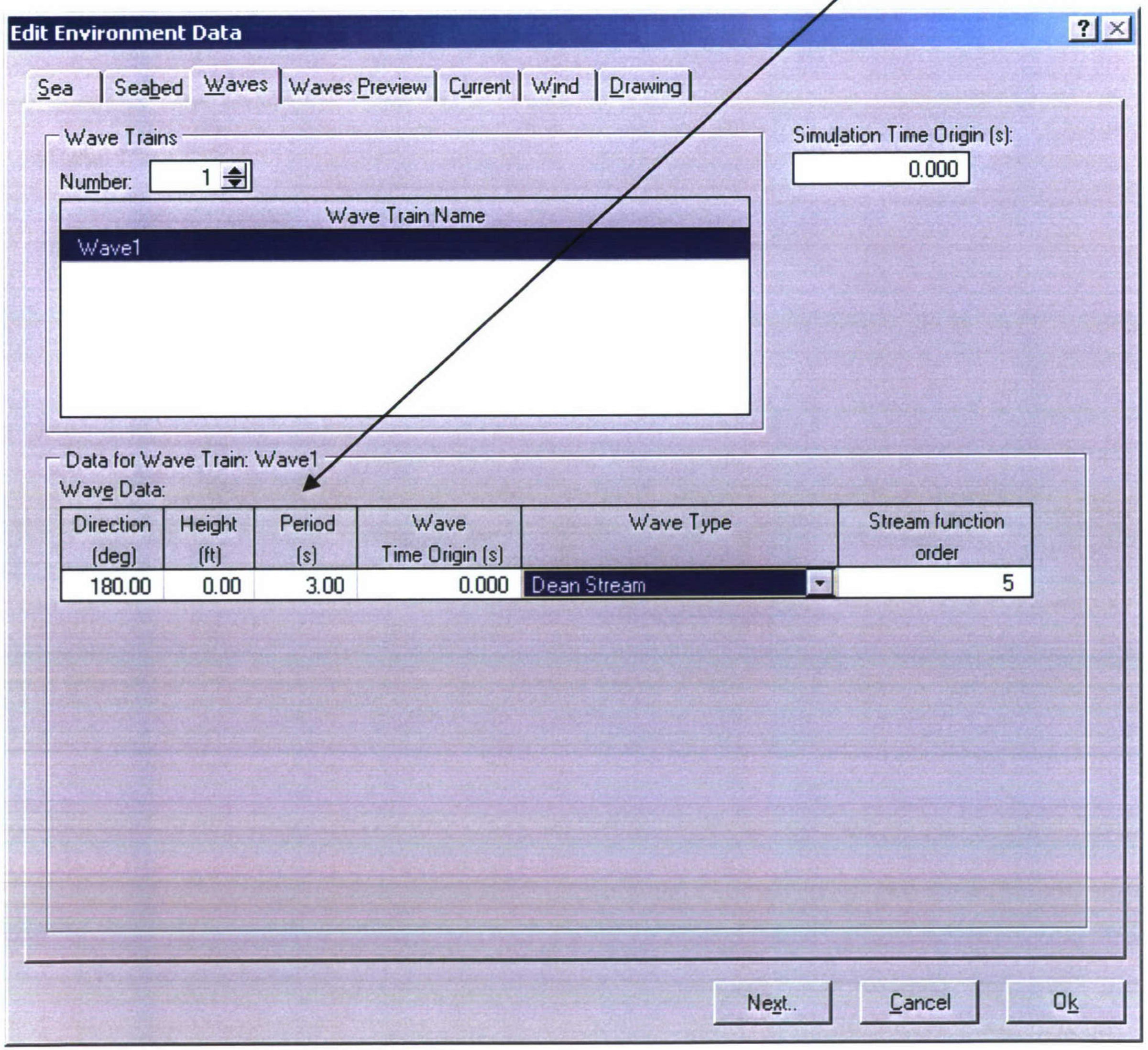

Note, we need to do this for the pluck tests. Waves will be turned back on later.

Turn Off Line Material Damping

Go General Settings Tab

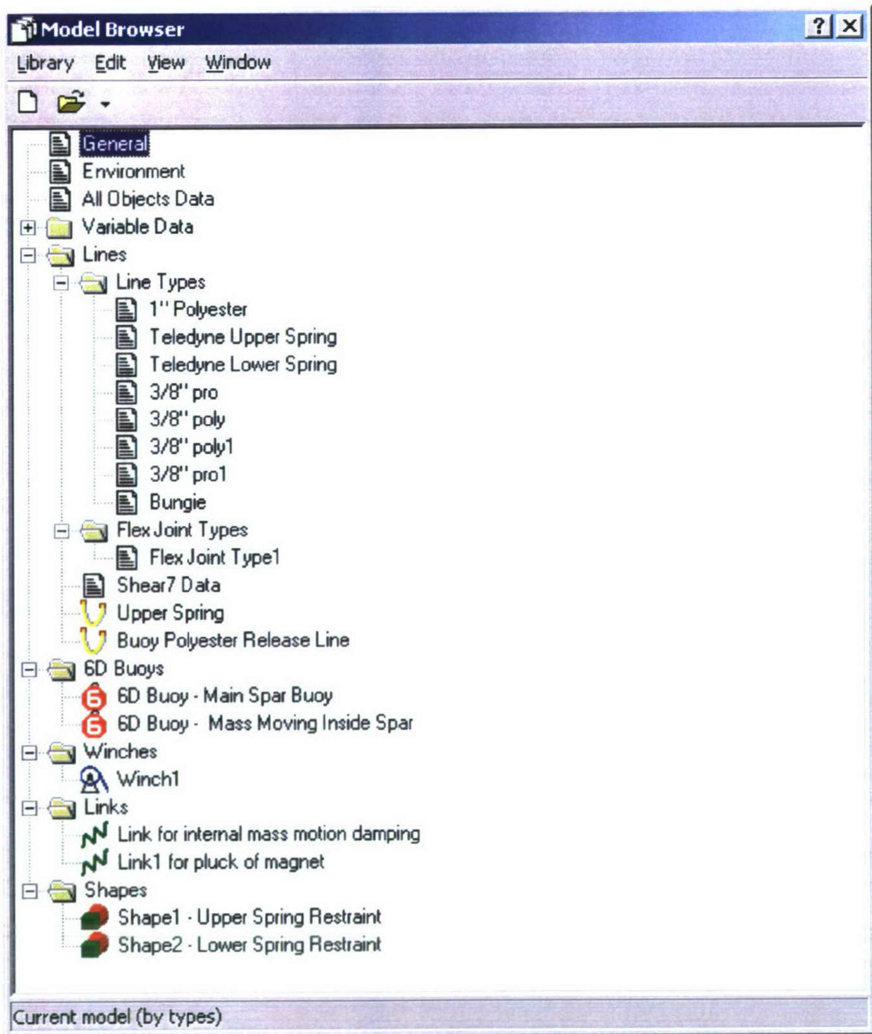

Set Line Damping to zero only for purposes of verifying undamped natural period of magnet stack assembly. Otherwise, this is left alone.

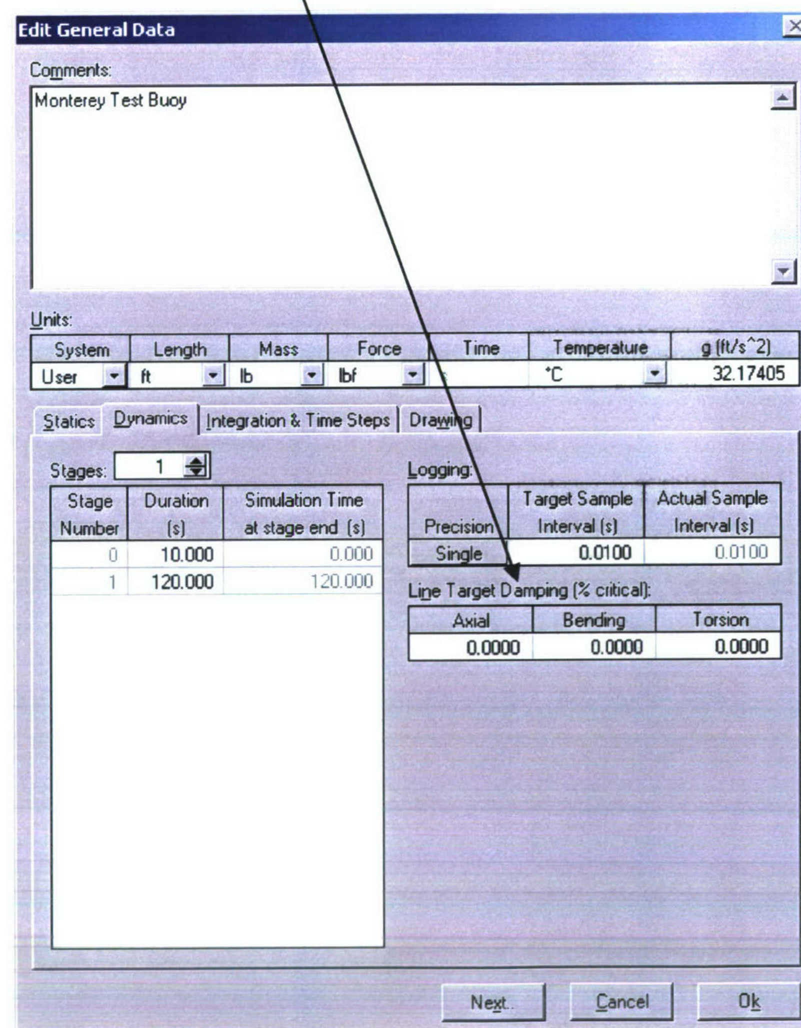

Setup Main Buoy

Select 6DOF Buoy Icon

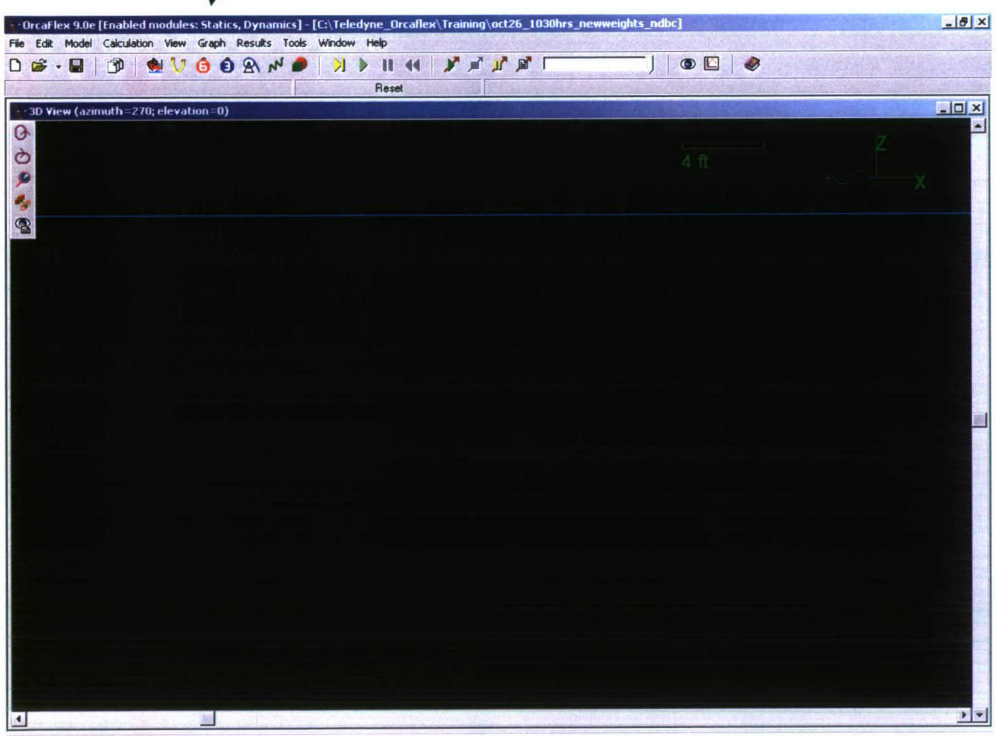

Select Spar Buoy Type

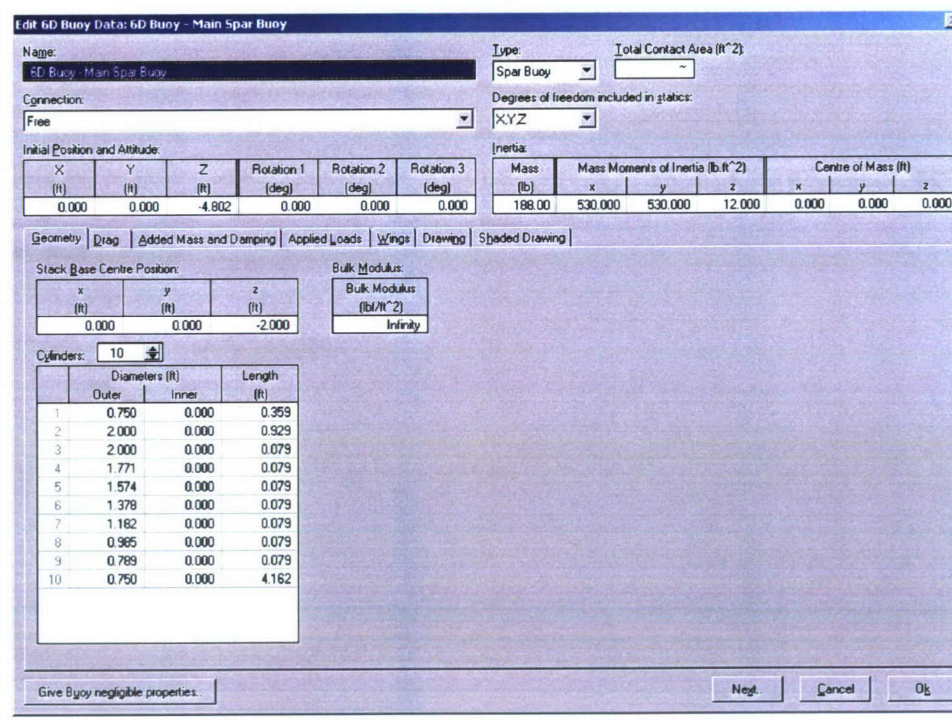

Setup Main Buoy (Cont)

Select Geometry Tab

Set Buoy Properties Throughout

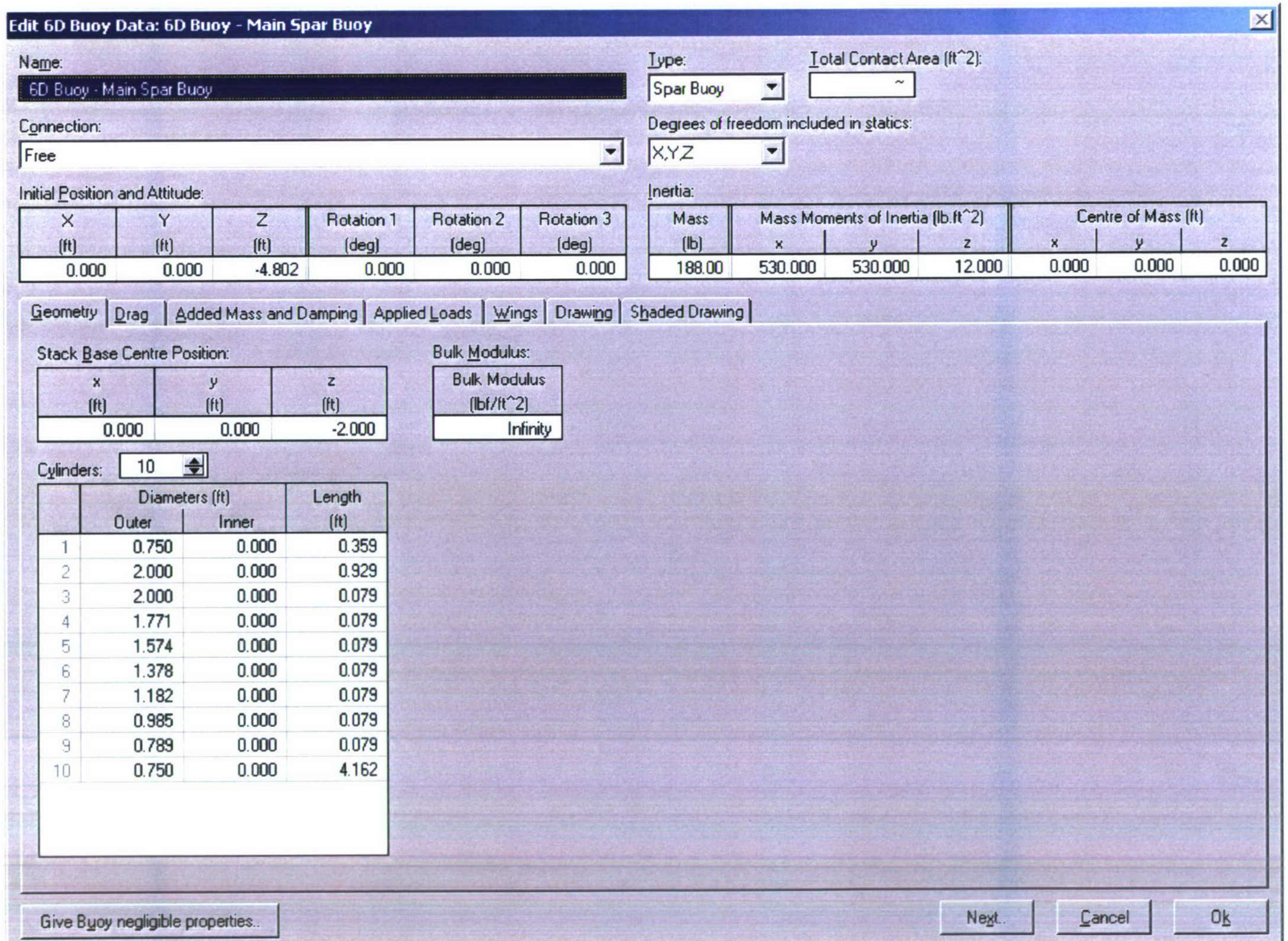

Cut/Paste
from Excel
to Here

Setup Main Buoy (Cont)

Select Drag Tab

Input Drag Areas from Excel

Cut/Paste from Excel to Here

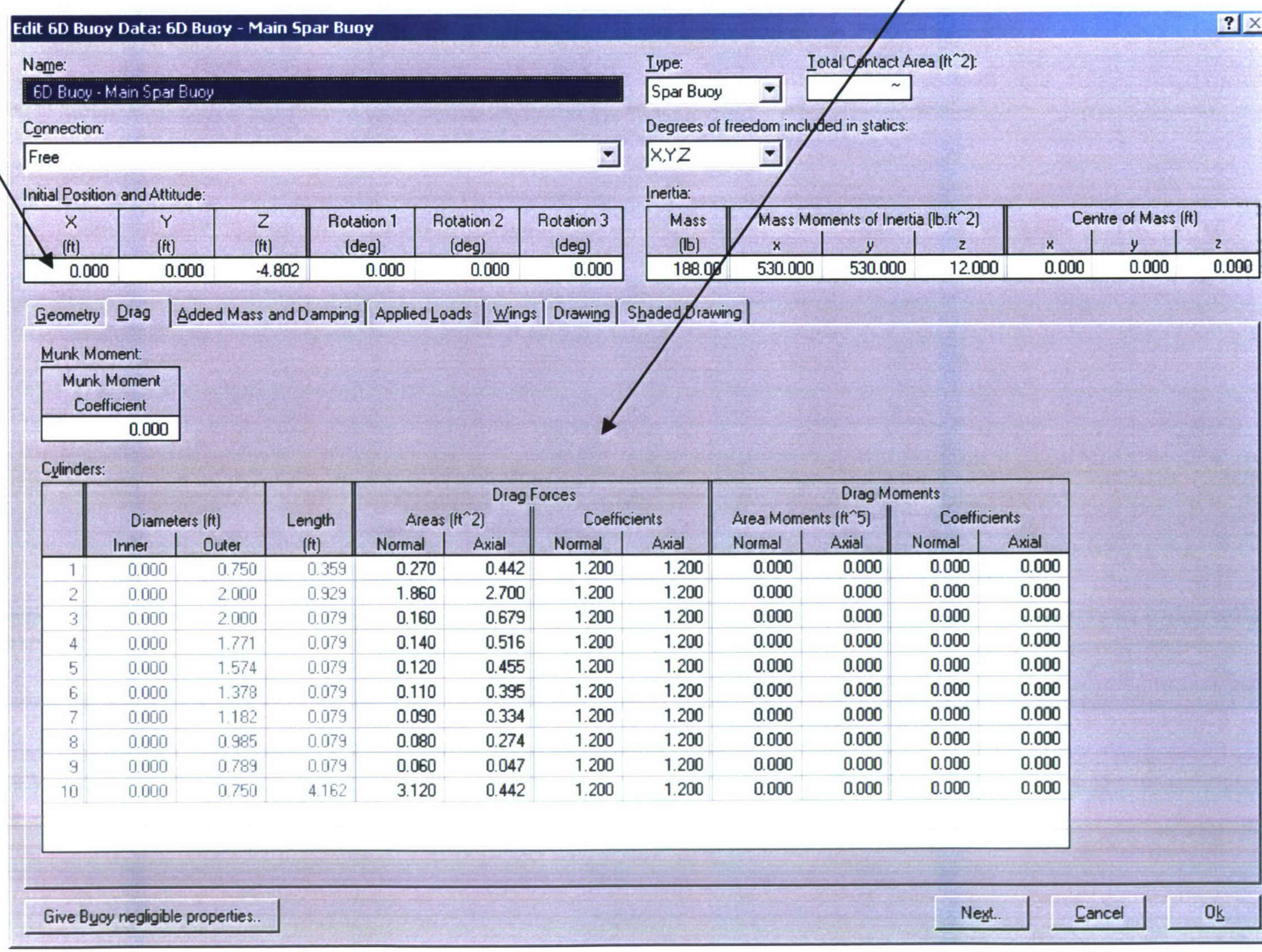

	Diameters (ft) Inner	Diameters (ft) Outer	Length (ft)	Drag Forces Areas (ft^2) Normal	Drag Forces Areas (ft^2) Axial	Drag Forces Coefficients Normal	Drag Forces Coefficients Axial	Drag Moments Area Moments (ft^5) Normal	Drag Moments Area Moments (ft^5) Axial	Drag Moments Coefficients Normal	Drag Moments Coefficients Axial
1	0.000	0.750	0.359	0.270	0.442	1.200	1.200	0.000	0.000	0.000	0.000
2	0.000	2.000	0.929	1.860	2.700	1.200	1.200	0.000	0.000	0.000	0.000
3	0.000	2.000	0.079	0.160	0.679	1.200	1.200	0.000	0.000	0.000	0.000
4	0.000	1.771	0.079	0.140	0.516	1.200	1.200	0.000	0.000	0.000	0.000
5	0.000	1.574	0.079	0.120	0.455	1.200	1.200	0.000	0.000	0.000	0.000
6	0.000	1.378	0.079	0.110	0.395	1.200	1.200	0.000	0.000	0.000	0.000
7	0.000	1.182	0.079	0.090	0.334	1.200	1.200	0.000	0.000	0.000	0.000
8	0.000	0.985	0.079	0.080	0.274	1.200	1.200	0.000	0.000	0.000	0.000
9	0.000	0.789	0.079	0.060	0.047	1.200	1.200	0.000	0.000	0.000	0.000
10	0.000	0.750	4.162	3.120	0.442	1.200	1.200	0.000	0.000	0.000	0.000

Setup Main Buoy (Cont)

Select Added Mass and Damping Tab

Input Values

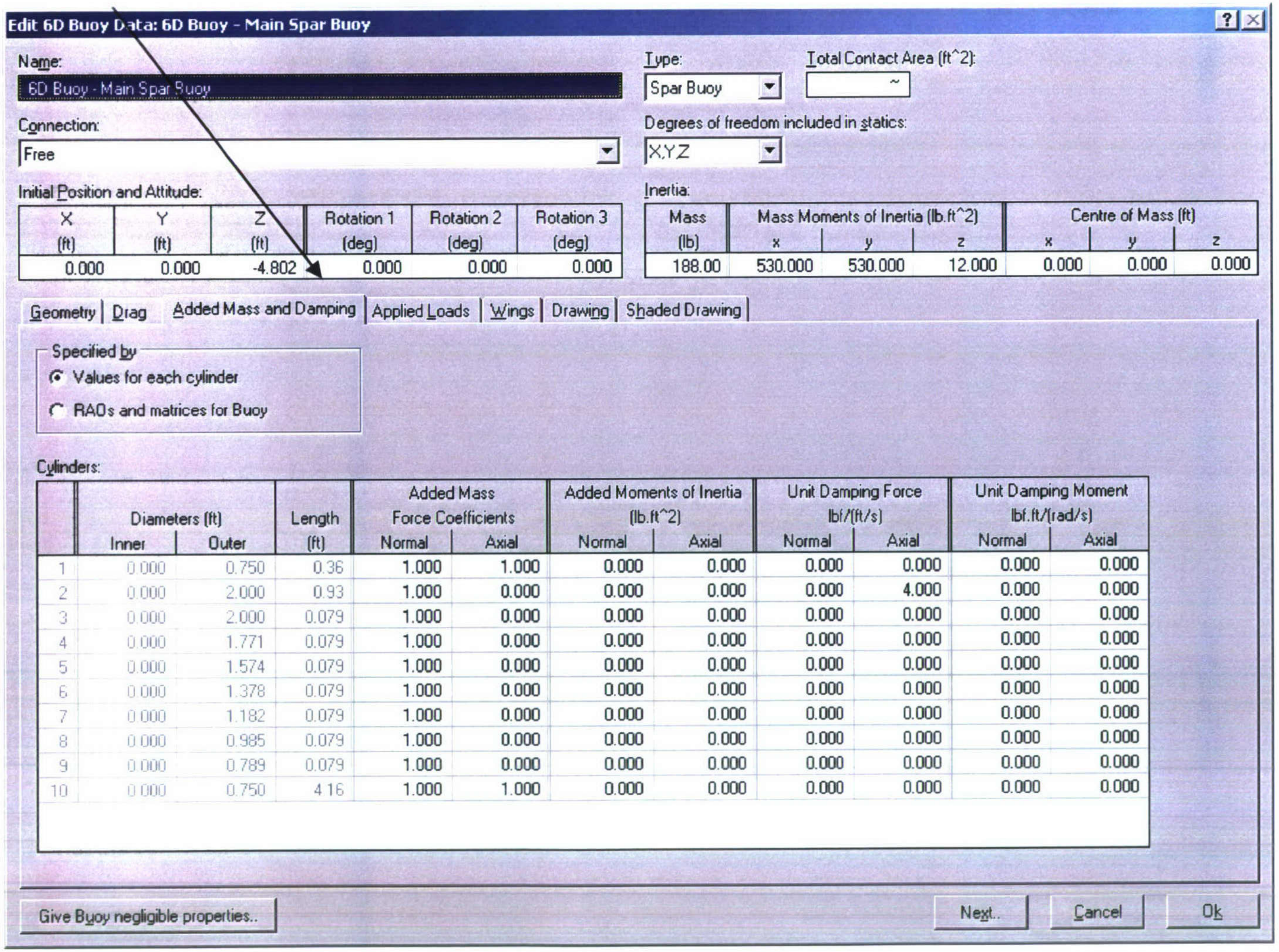

Added Mass depends on Shape. For sphere Ca=0.5, for cylinder, Ca=1.0

We are not considering frequency dependent added mass here

The default values are adjusted using results of pluck test data to help match the natural period as measured

The Drag values are adjusted as well to help match the decayed response from the pluck test in still water for both heave and pitch/roll.

Prepare Magnet Stack

We want to create another 6DOF buoy to represent the magnet stack/car assembly, so click 6D icon and click in workspace

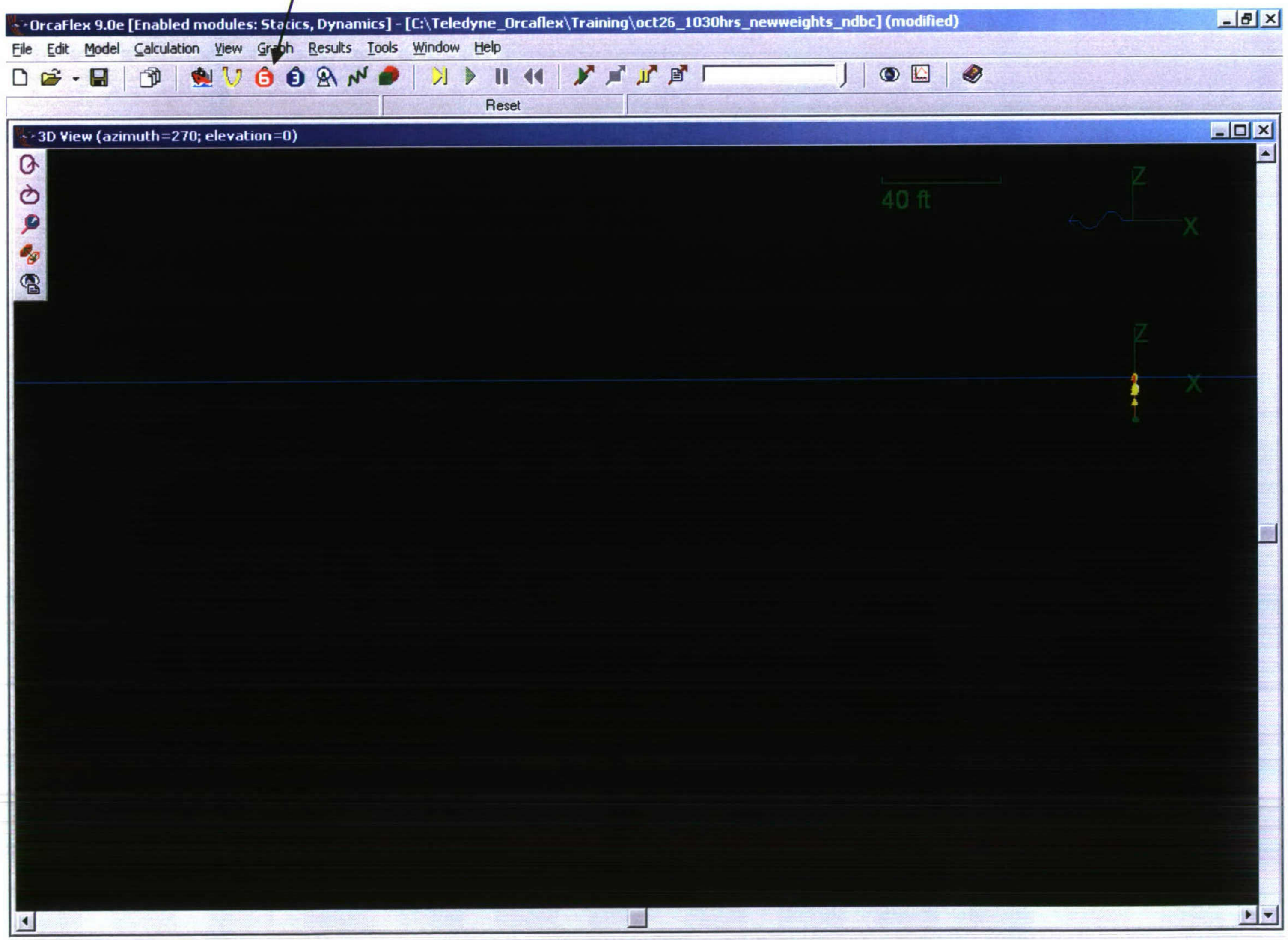

Prepare Magnet Stack (cont)

Set Magnet as arbitrary size. I chose 1 ft long and .1 ft diameter. The shape stiffeners have to have the same internal diameter is this outer diameter. Make the initial DOF to be XYZ for statics – sometimes ALL DOF can be selected but may have trouble reaching equilibrium in a static solution. Because the magnet stack is represented as a buoy, there will be buoyancy effects, so we make the body small but dense. The value of the mass should be same as actual for natural frequency effects. We want to turn off the drag and added mass effects since we do not want the magnet to have any fluid loading.

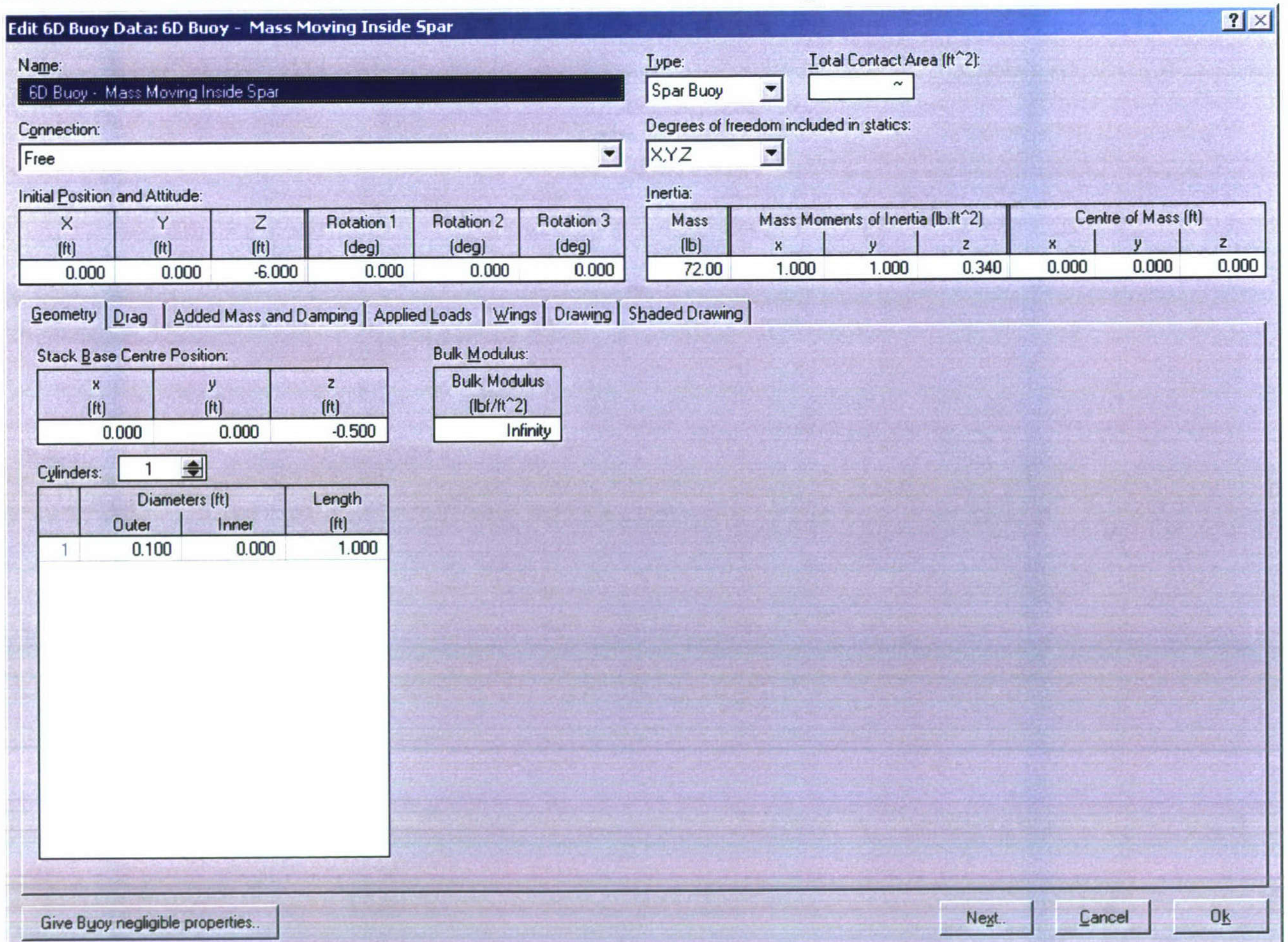

Set Magnet Bumper

The bumper shown in orange merely provides a stiffness restraint for the magnet stack and does not have mass or react to any hydrodynamic loads. Once it is built in the orcaflex model, the pen color is turned off so user cannot see it. The cylinder has an inside diameter the same as the magnet stack assembly in the model.

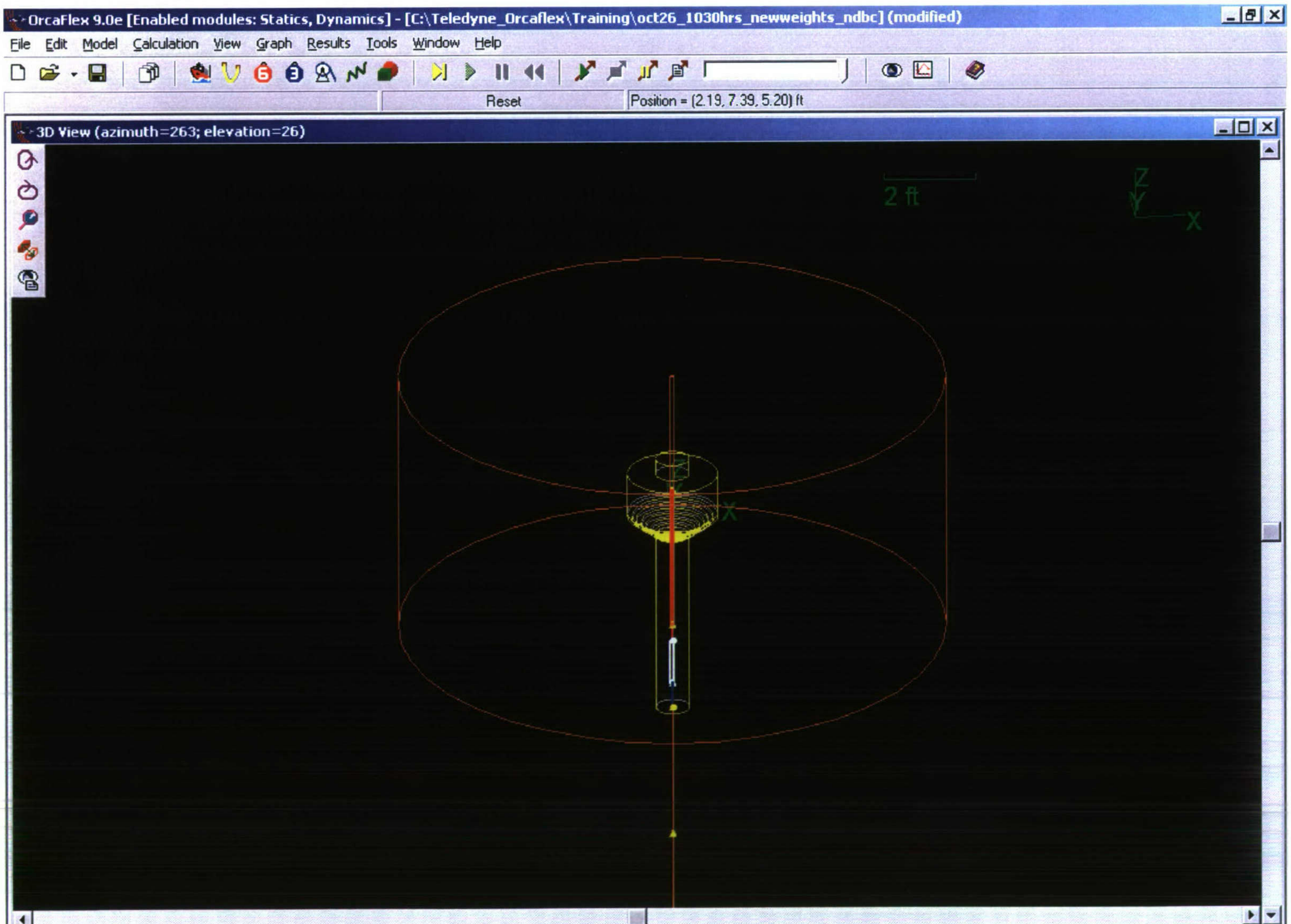

Set Magnet Bumper (cont)

These dialog boxes show settings for the magnet sliding restraint bumper to keep the magnet aligned inside the spar buoy as it slides up and down. If implicit method is selected for solution option, the damping is set to zero. The stiffness is set by trial and error to keep the magnet aligned as best as possible.

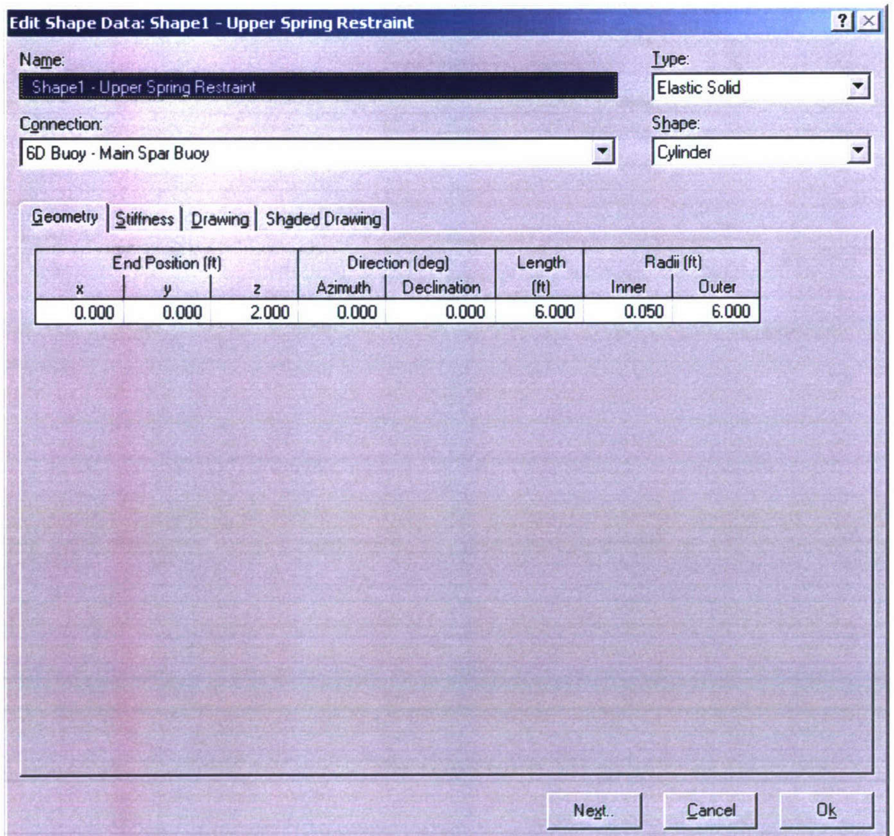

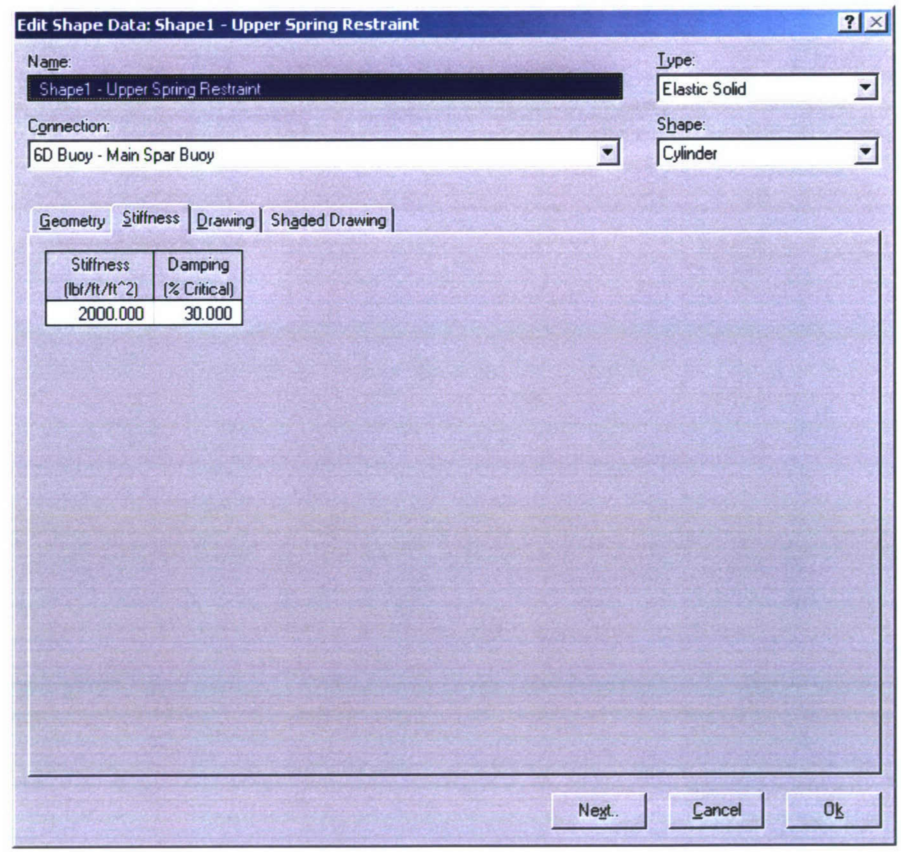

Prepare Line Types

Select Line Icon and click in workspace

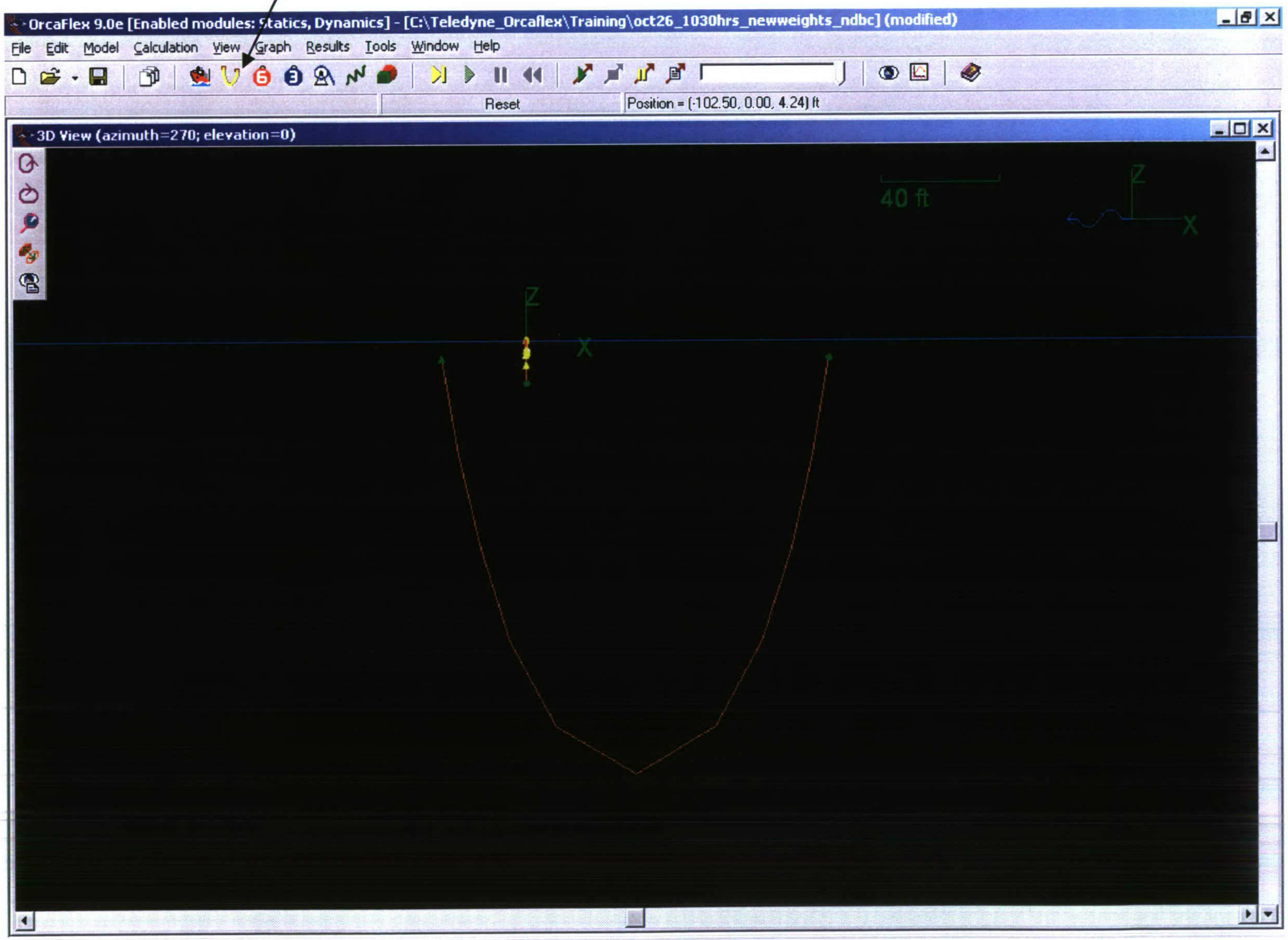

Prepare Line Types (cont)

- We need to prepare
  - An equivalent spring line
  - Release Line for pluck testing

Prepare Line Types (cont)

First, prepare the equivalent spring line. On this dialog box shown here, we need to give it a name, length and segment length. Then we will set the properties using the "Line Types" Button. The spring is connected to the main spar buoy and to the magnet stack as shown

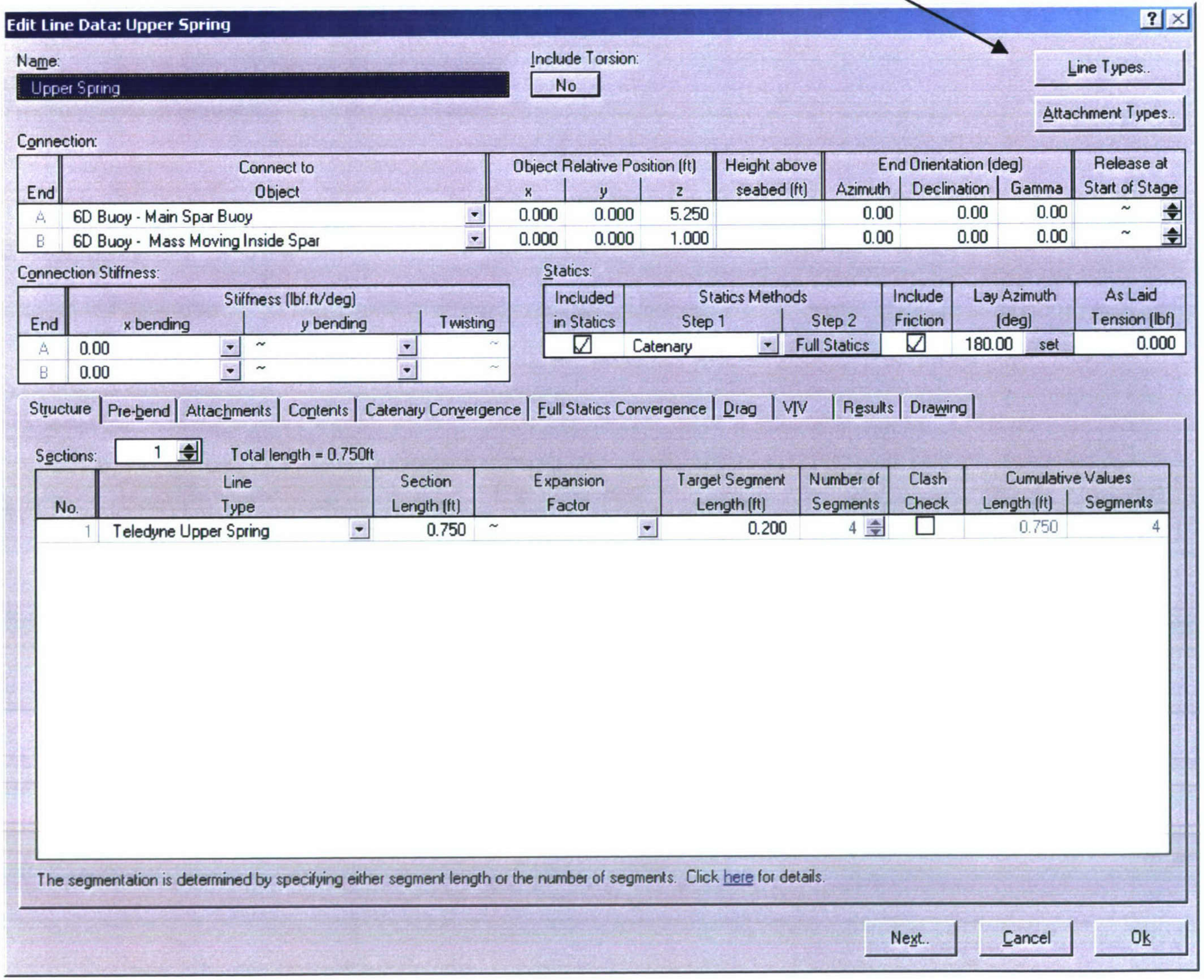

Prepare Line Types (cont)

For the Release Line, we will make it a moderate stretch line that is only used in statics to impose a displacement of the spar buoy and released under dynamics to check the oscillatory response of the buoy. This line is tied to the spar keel and the other end of the line is fixed in space. The line is released at Start of Stage Zero in Dynamics shown here.

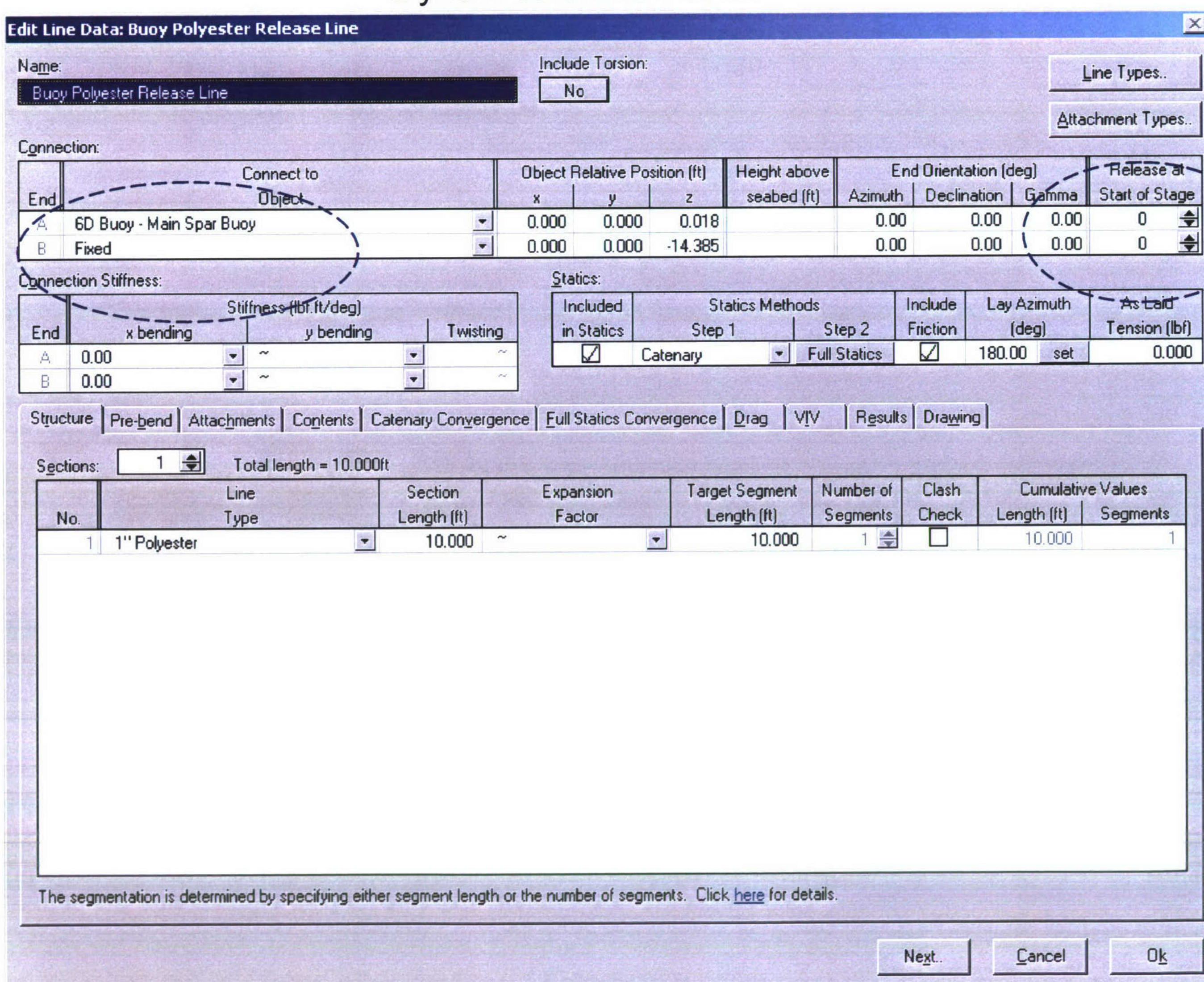

Prepare Line Types (cont)

Clicking on Tab, "Line Types", brings up dialog box for the line properties for each type of line. The improtant item here is the axial stiffness. None of our lines will use a bending or torsional stiffness. The drag coefficient is not important here until we use a line for a mooring.

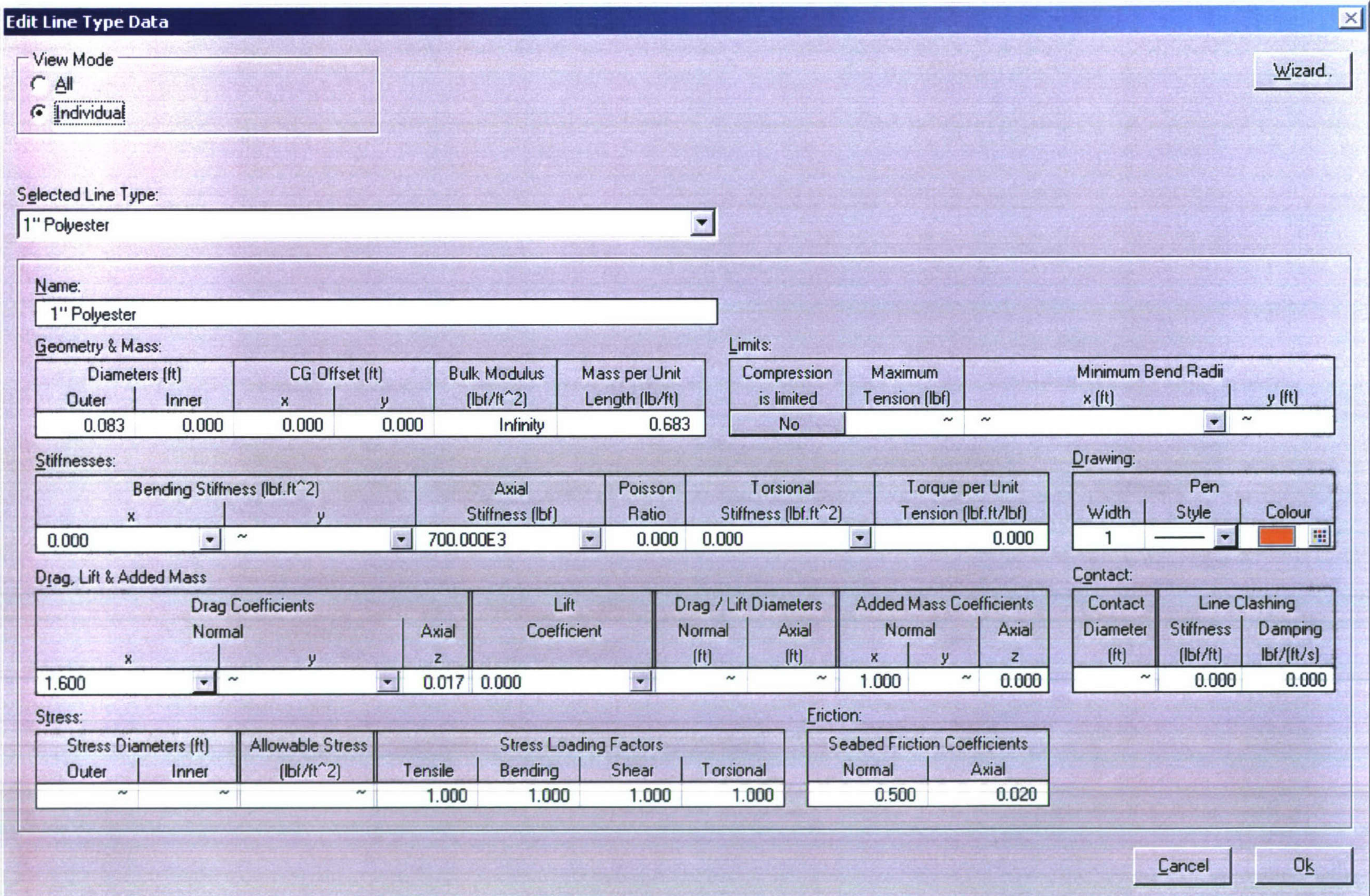

Prepare Link for EMF Damping

Click on Link Icon and then Click in Workspace

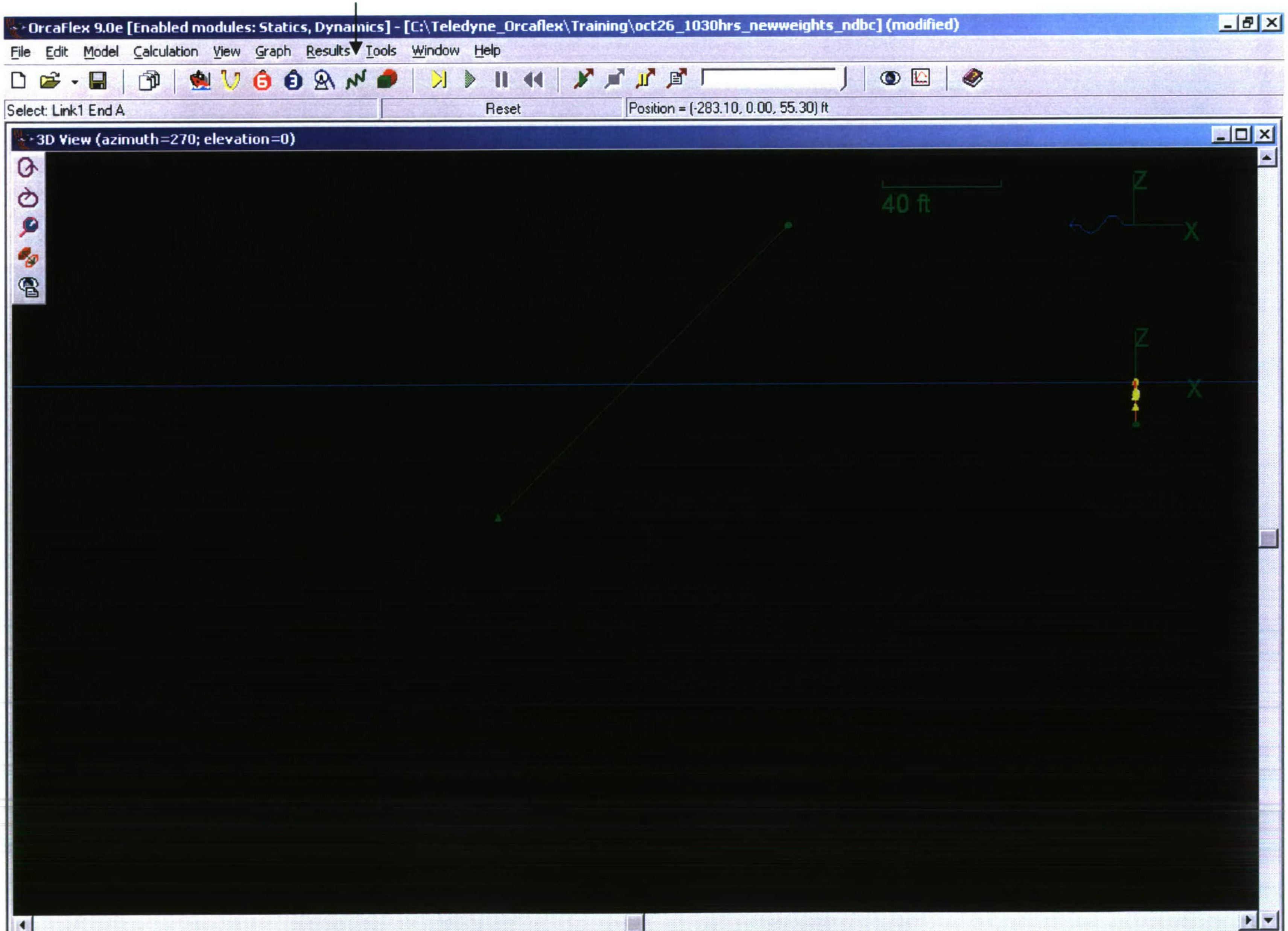

Prepare Link for EMF Damping (cont)

We want to connect the Link to the main spar buoy and to the magnet stack. The stiffness is set to zero, and the damping is adjusted based on values from the oscilloscope such that when we pluck the magnet stack, the decay is the same. The attachment points are similar to spring attachment points inside the spar. The unstretched length is arbitrary since we are only using damping not stiffness.

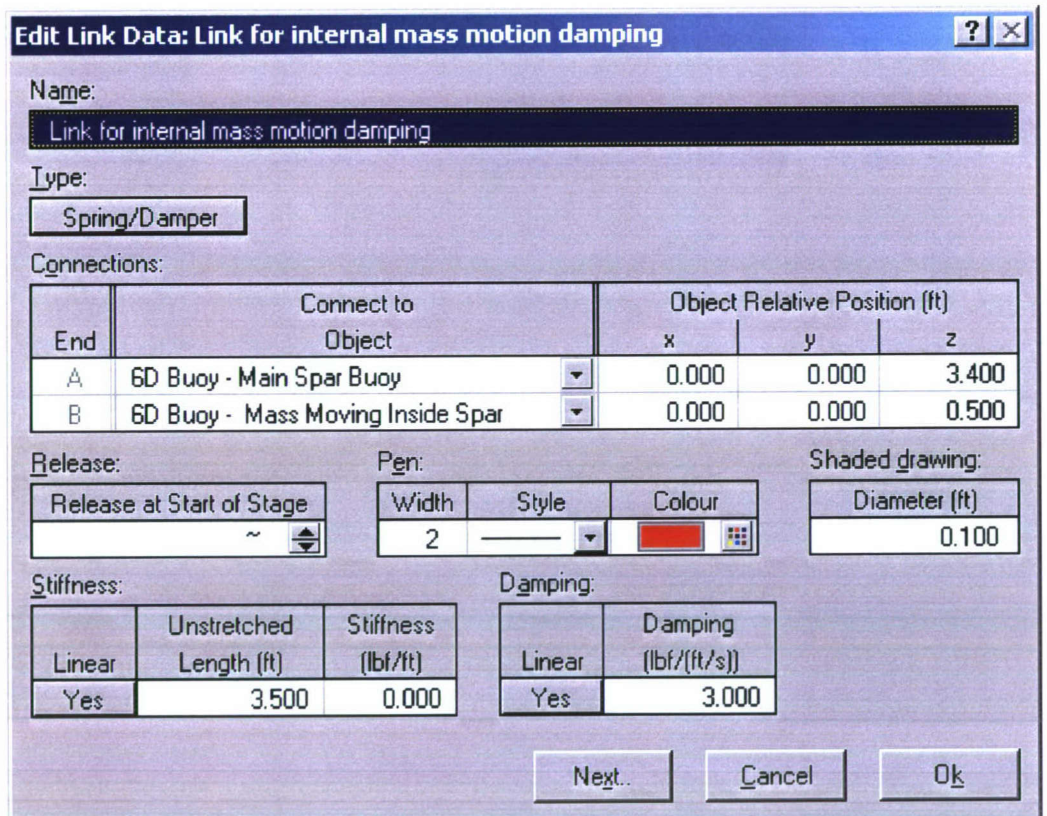

Set Equivalent Spring

These dialog boxes show the settings for an equivalent spring to represent all the springs. The attachment points inside the spar are shown on the left. The length of the spring and spring stiffness are shown in both left and right dialog boxes. We will verify it is correct in a pluck test to check the theoretical natural period with no damping; then with damping.

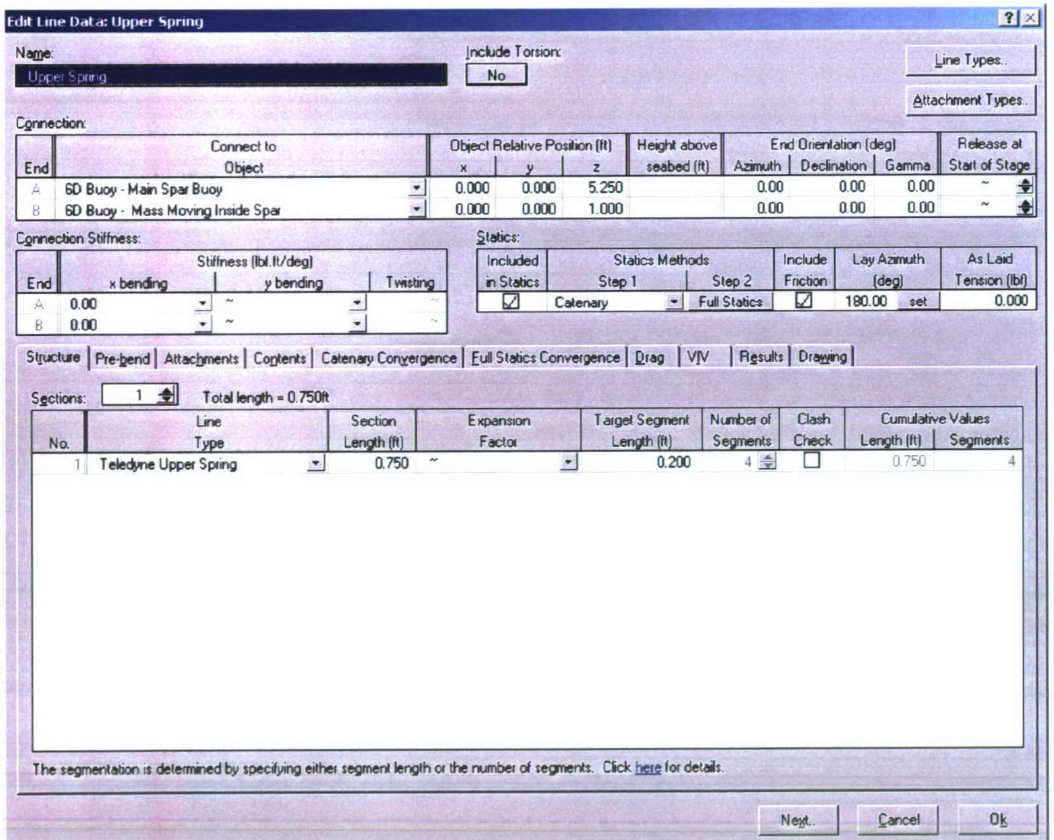

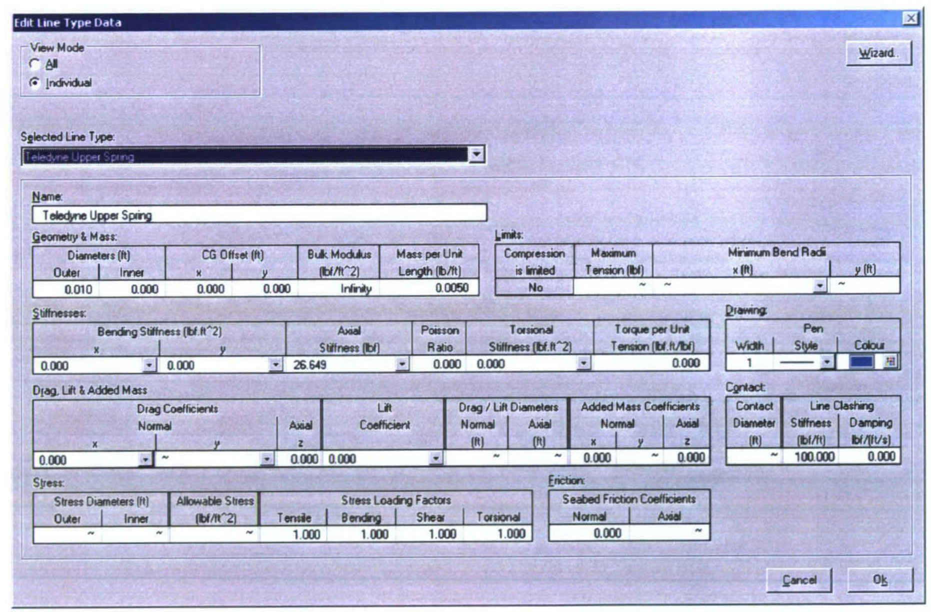

Prepare Winch Line for Magnet Velocity

We want to insert a "winch" line type with zero tension setting, attaching it to the magnet and to the spar such that we can get the time series of relative velocity of the magnet for computation of the power output. The stiffness is set to a small value. The winch line connection points are shown in the dialog box below.

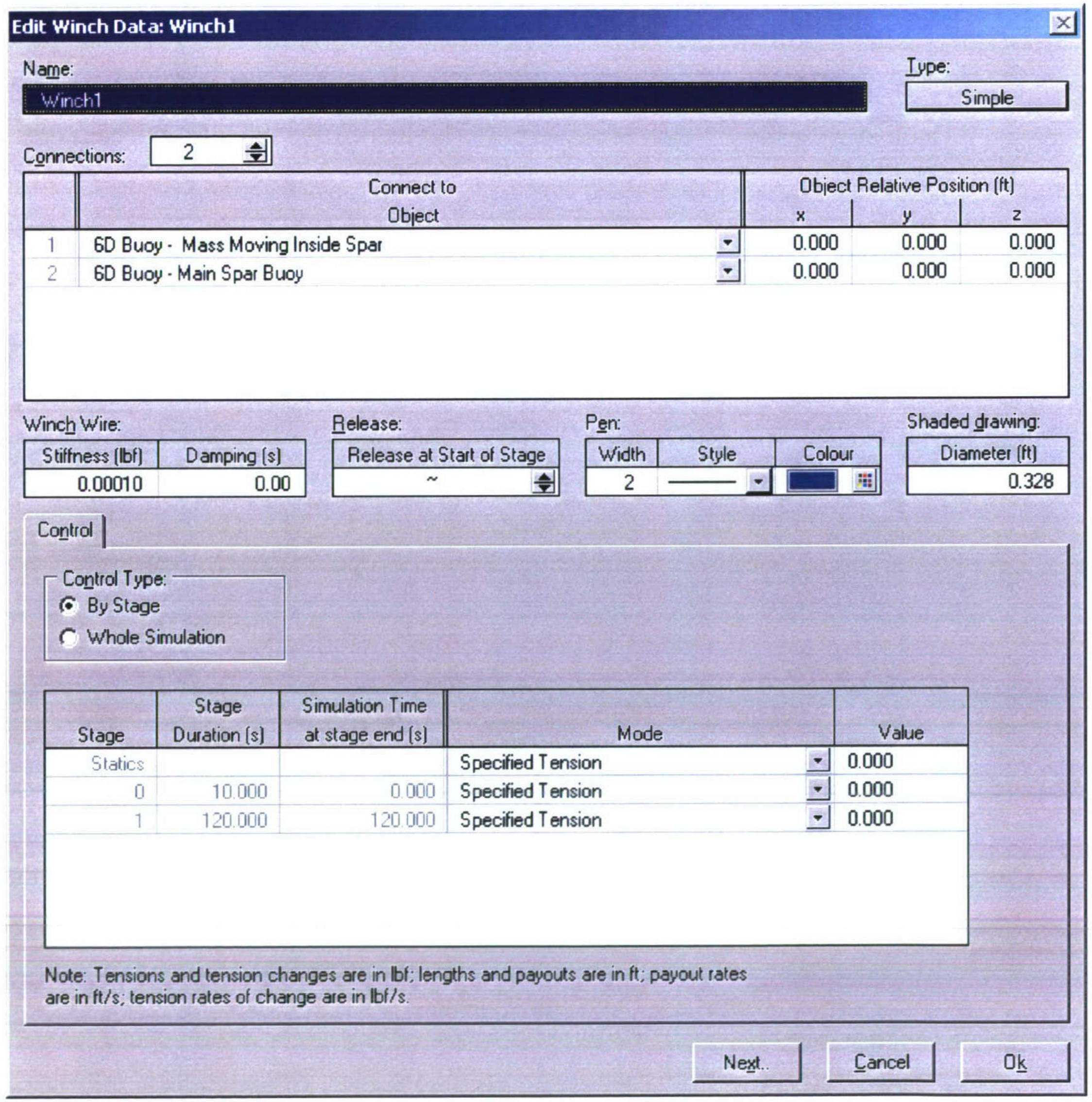

Prepare Release Line for Spar

The release line is a line to allow static solution of the 6D spar buoy and then release during dynamics. We will release the line in still water and check the draft for free floating condition. We will also use the release line for a pluck test to check the heave damped natural period with and without the magnet locked. Another release line is used internal to the spar to lock the magnet stack and/or free the magnet stack.

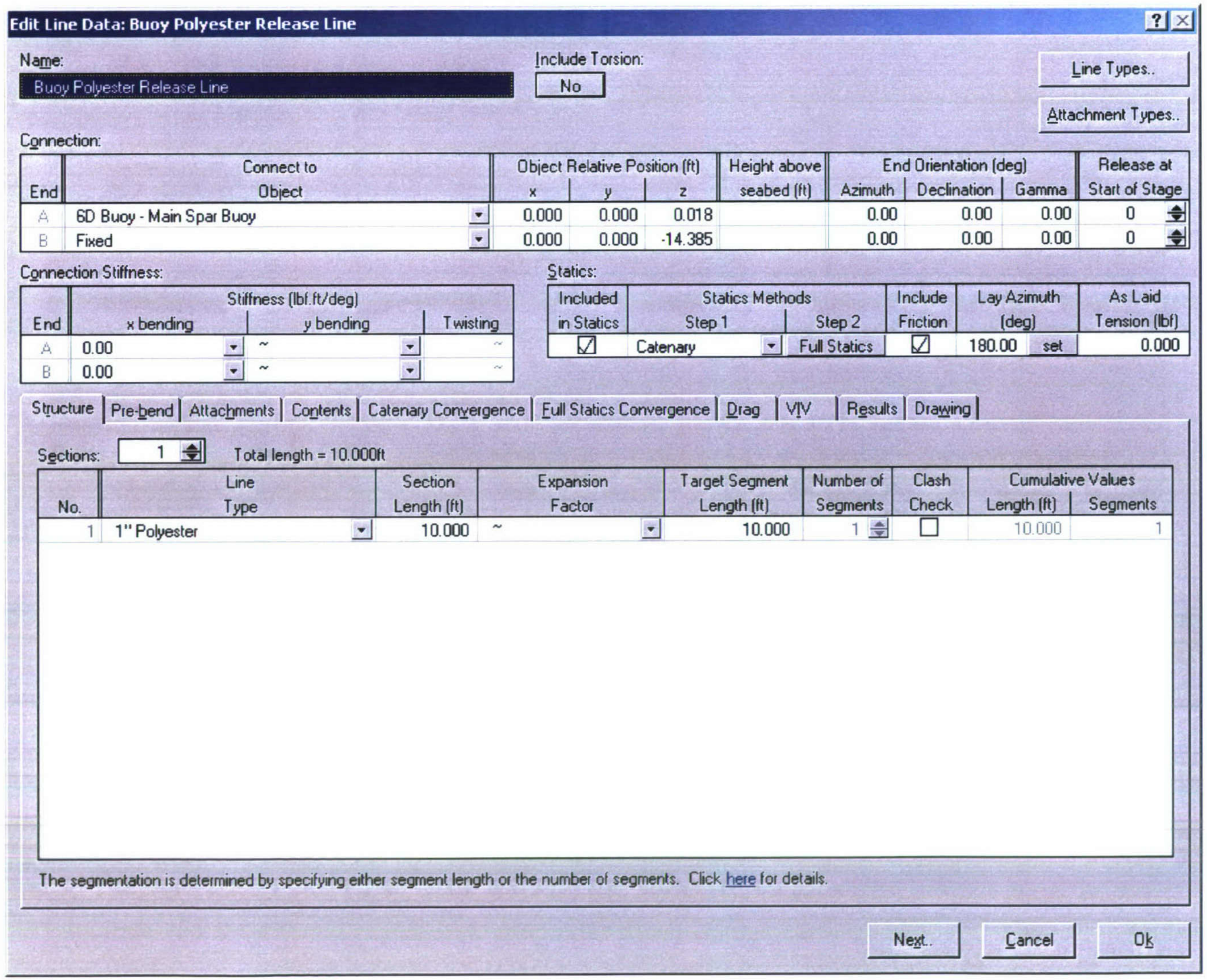

Prepare Release Link for Magnet Stack

The magnet release link is a link to allow plucking the magnet to check the natural period and also to lock the magnet for spar natural period tests. This link is released during dynamics when waves are applied as Shown in Release at Start of Stage 0

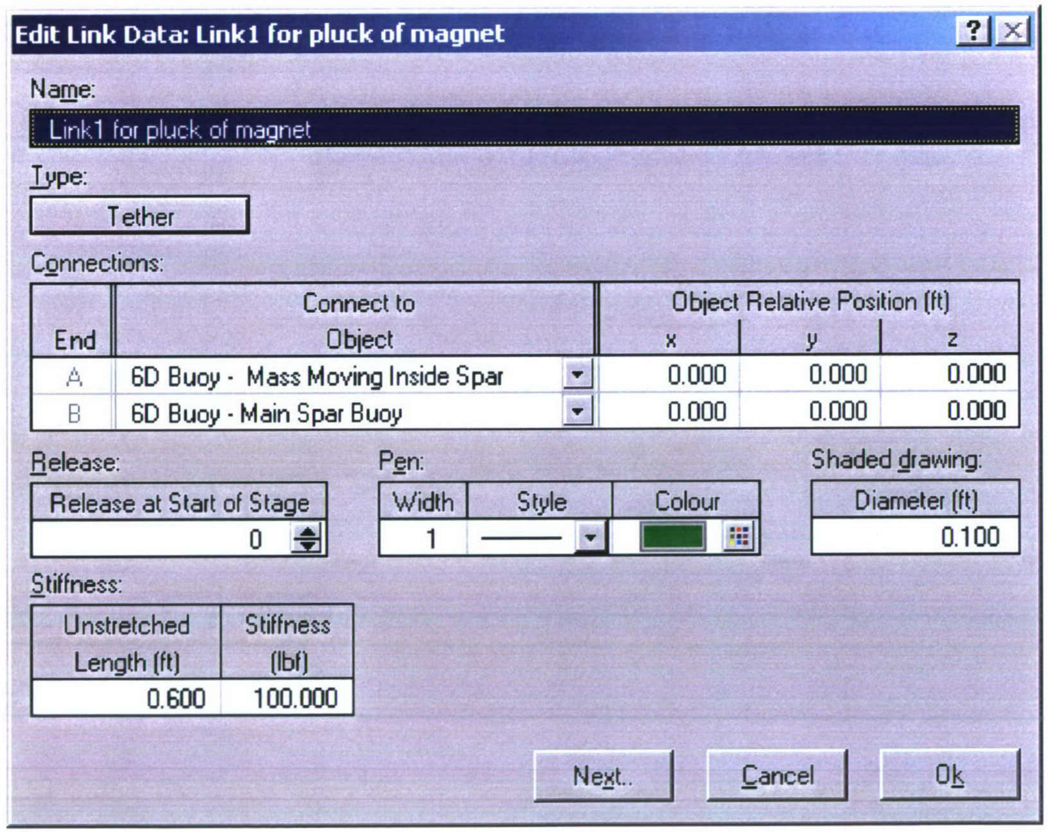

View of Fully Assembled Model

These views show the fully assembled model with the magnet stack bumpers and release lines.

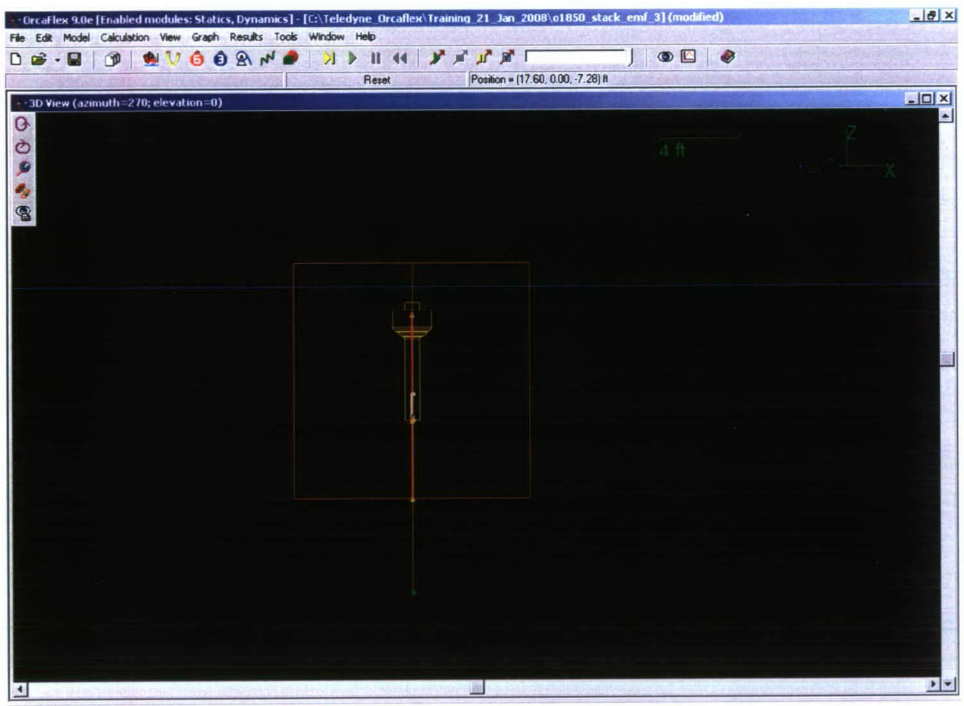

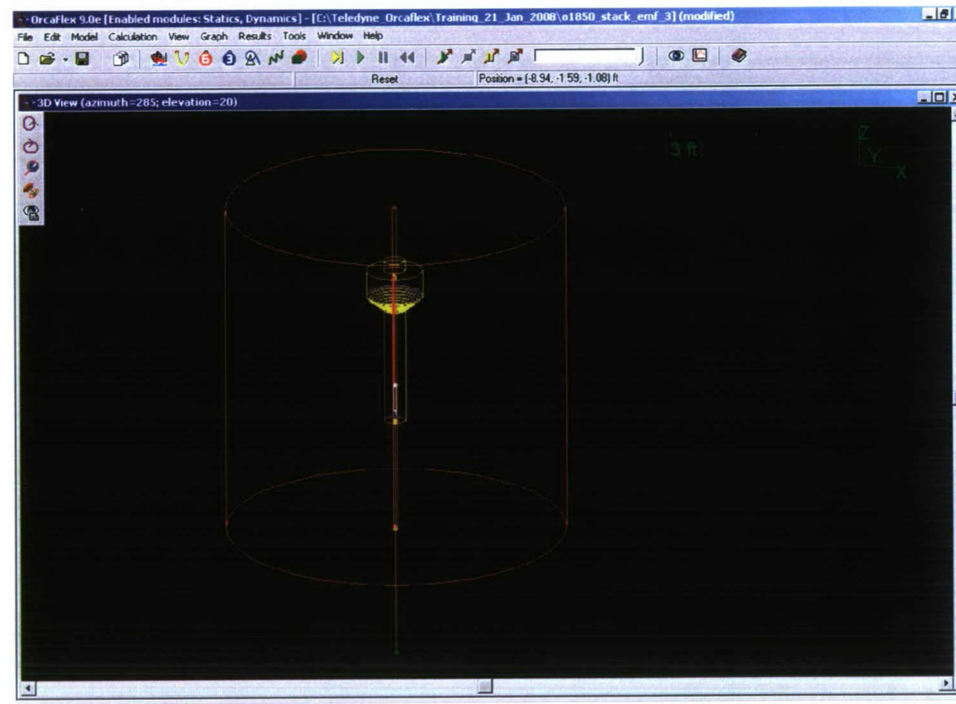

Check Free Floating Draft

It is good to confirm the Spar draft is correct, checking with hand calculations. So we will release the buoy in dynamics and let it settle to equilibrium.

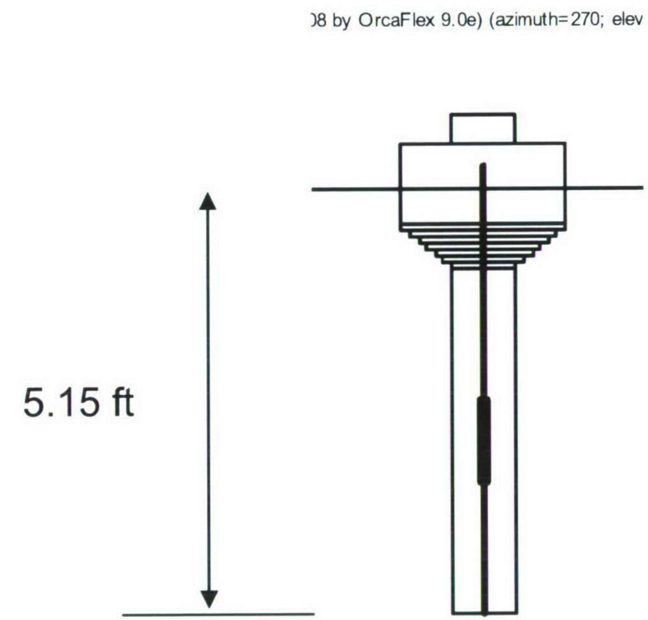

260 lbs = 64 lb/ft * (4.167 ft * pi/4*(.75 ft)^2 + .55 ft * 0.5 * pi/4 * (2ft)^2 + H * pi/4 * (2 ft)^2

H = .432 ft

So Draft = 4.167 ft + .55 ft + .432 ft = 5.15 ft

Check Magnet Stack Hangs at Correct Location

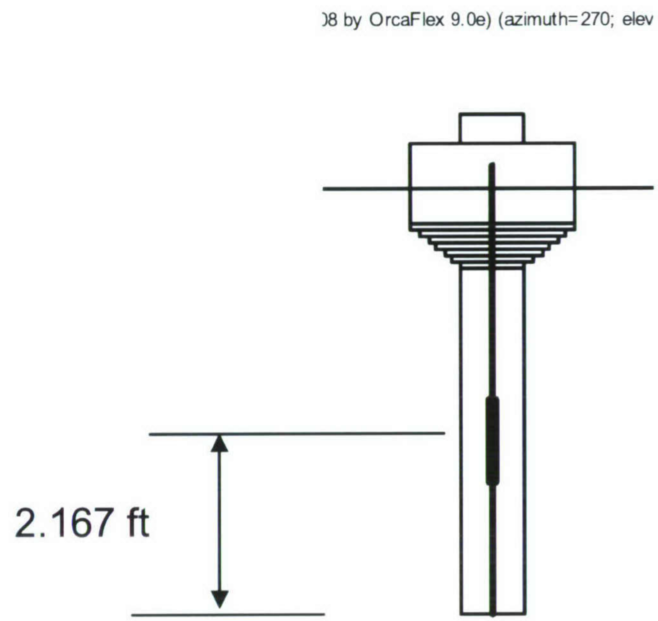

Adjust Spring Top Attachment Point to get Correct Height of Magnet from Base of Spar

EMF Decay Curves

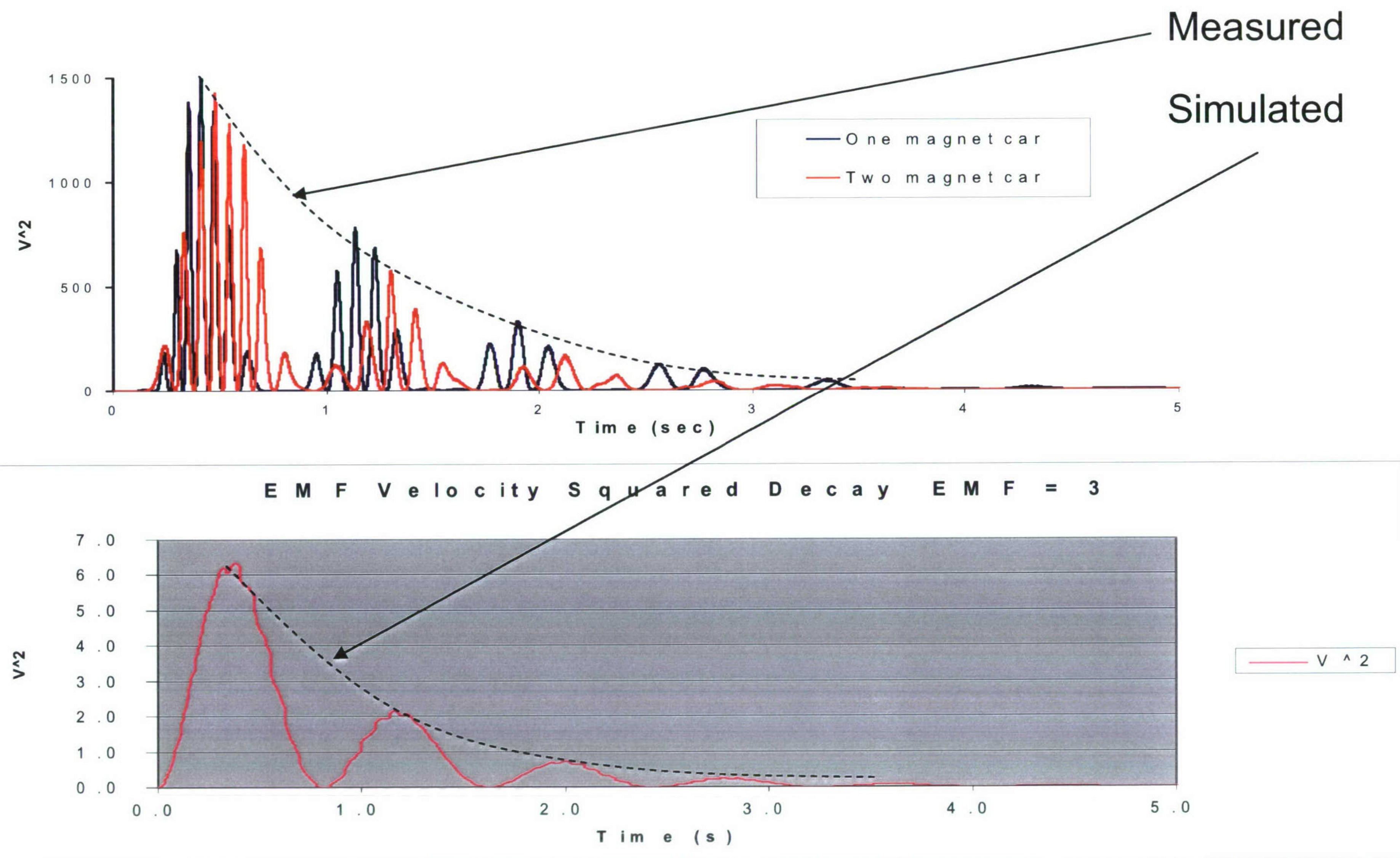

The Natural Period is set exact based on simple physics principles for the mass and spring stiffness

Default Buoy Drag Coefficients and Added Mass Values Will Initially be Used

See Appendix for References

The drag coefficients are set based on reference literature for buoy shape and expected flow regime (Re vs KC) and the added mass is similarly set based on literature.   These values are fine tuned if a field pluck test is performed on the actual buoy, the measured oscillations of the buoy in still water can be used to fine tune the model.

Check Magnet Stack Natural Period

We want to freeze the buoy and just release the magnet by pulling on it with a line and letting go

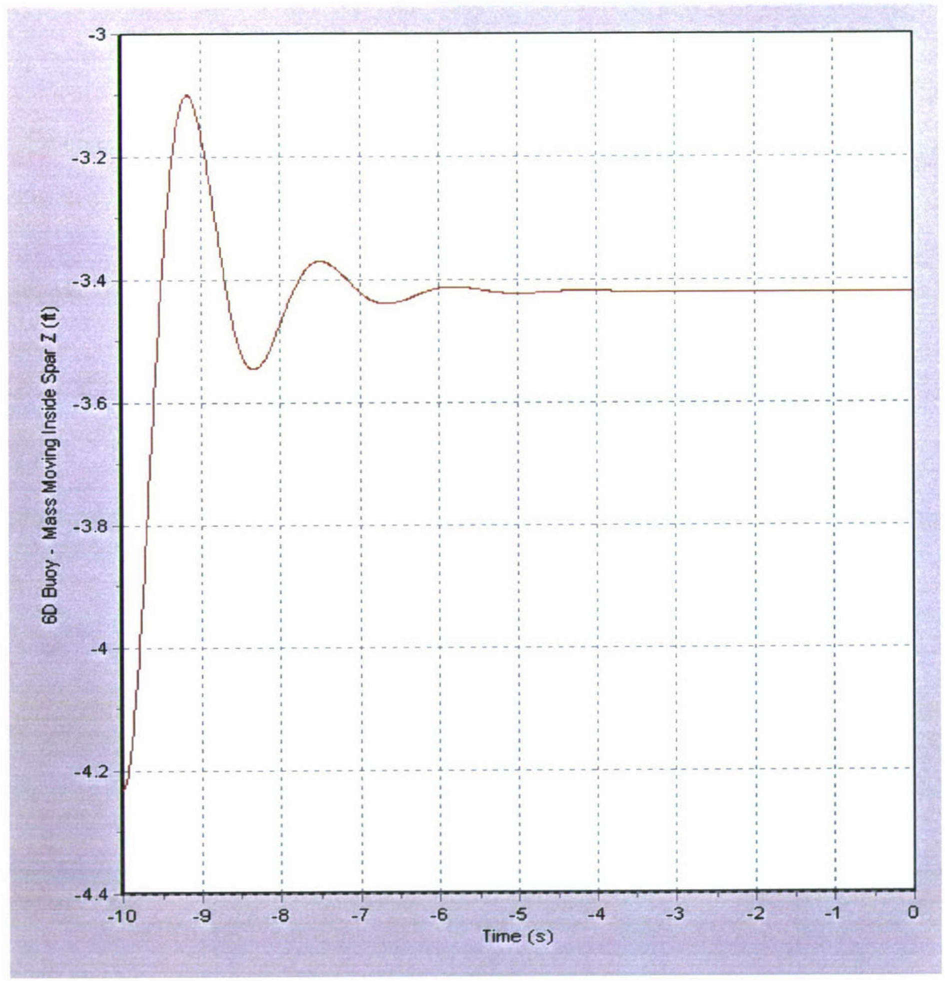

F = .625 Hz, T = 1.599 s

Check Spar Heave and Pitch Natural Periods

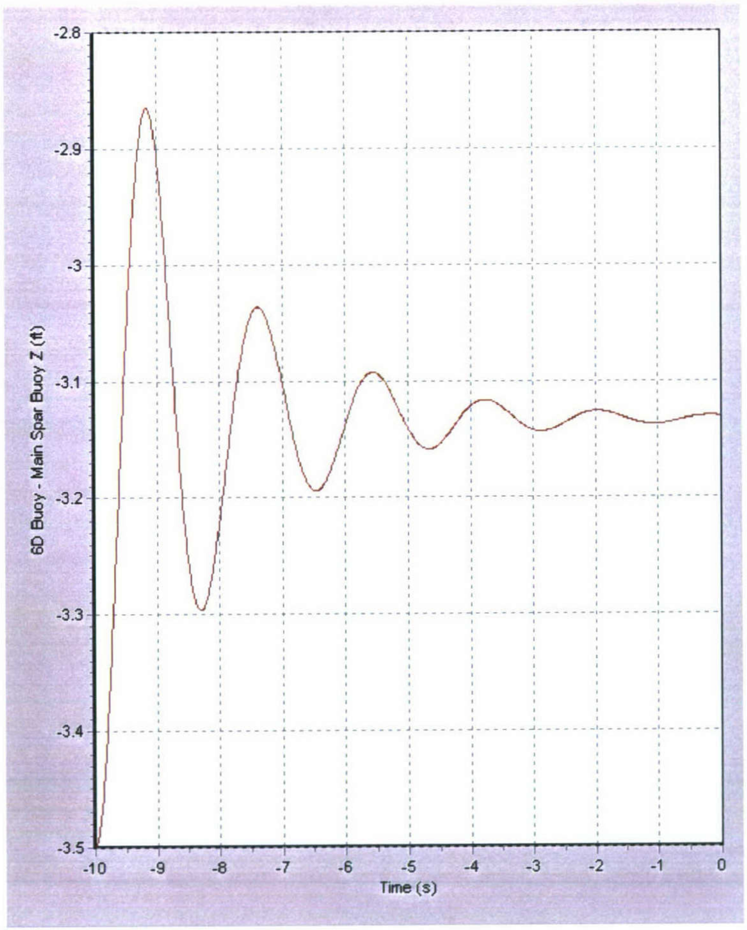

Heave , F = .557 Hz, T = 1.796 s

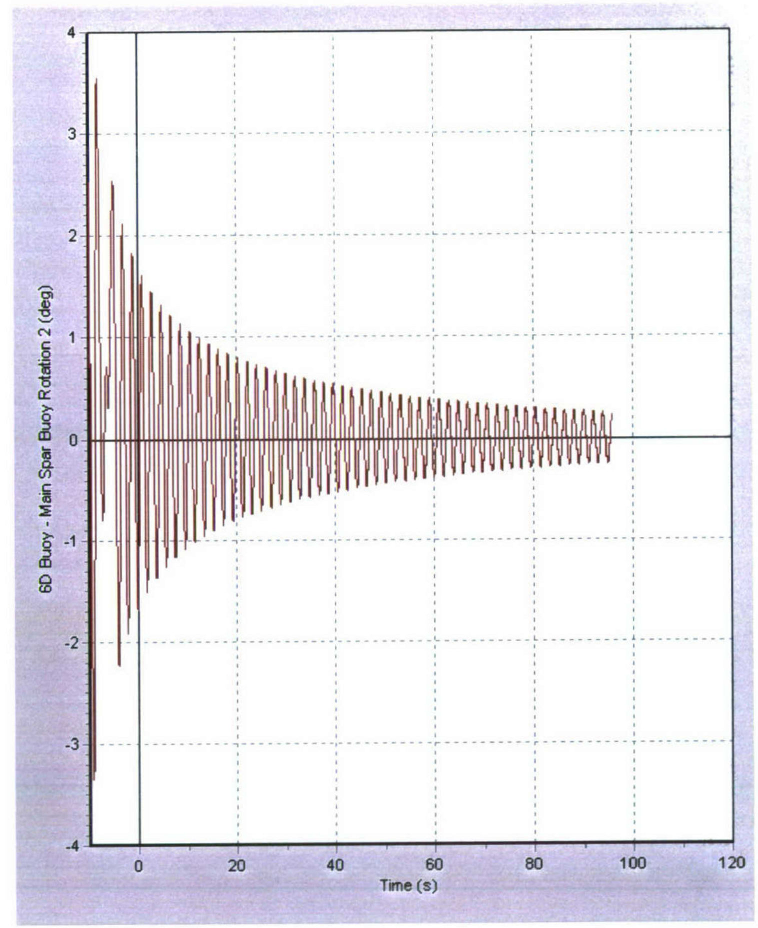

Pitch , F = .516 Hz, T = 1.939 s

Calculate Frequency Response Function

Get Peaks for FRF

Set Waves Keeping Wave Height constant and Change Wave Period to get Plot

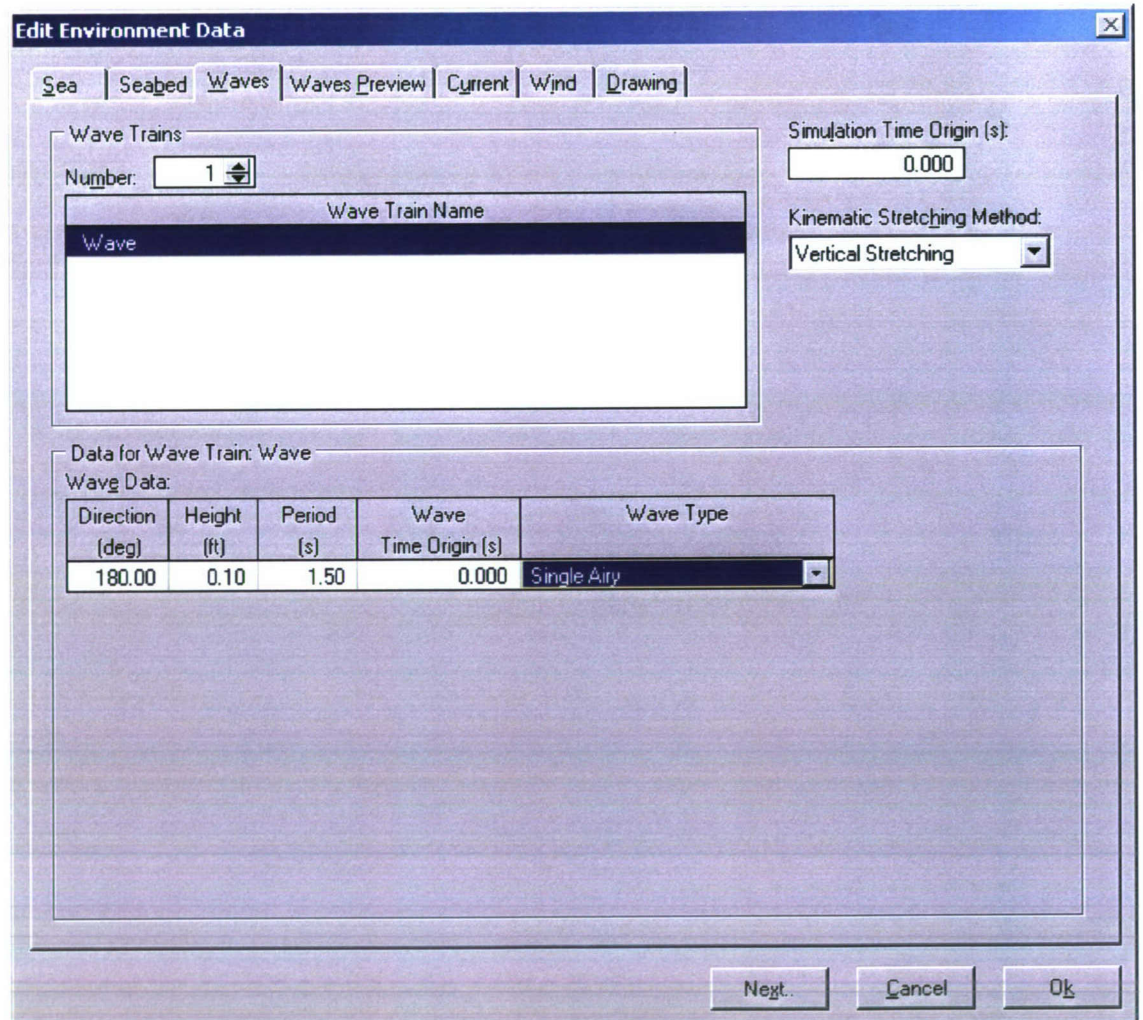

Frequency Response Function

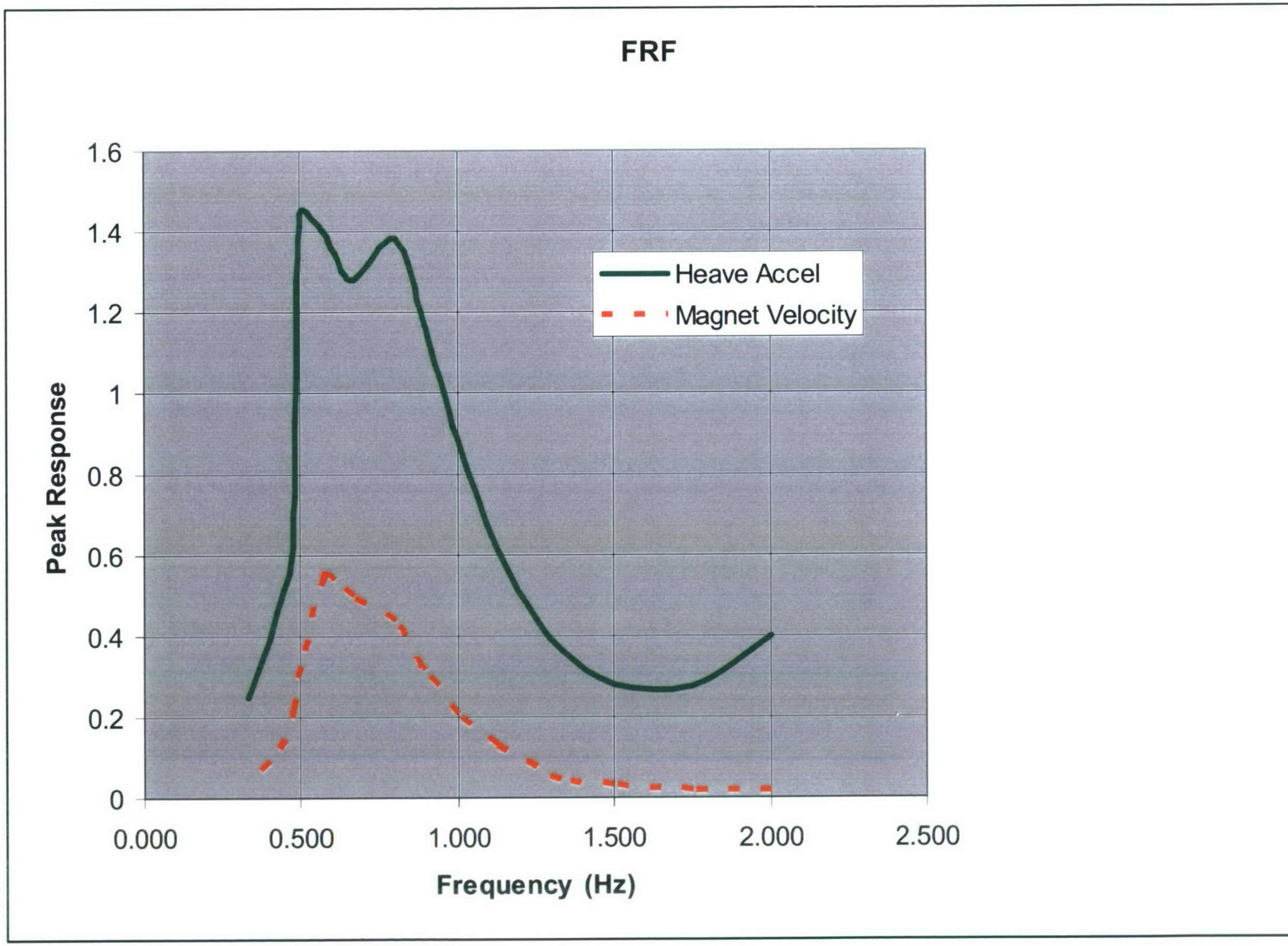

Time Domain Simulations with Waves

Ocean Wave Specification

Let's specify a linear single wave with height and period to coincide with the heave natural period to see if a resonant response occurs

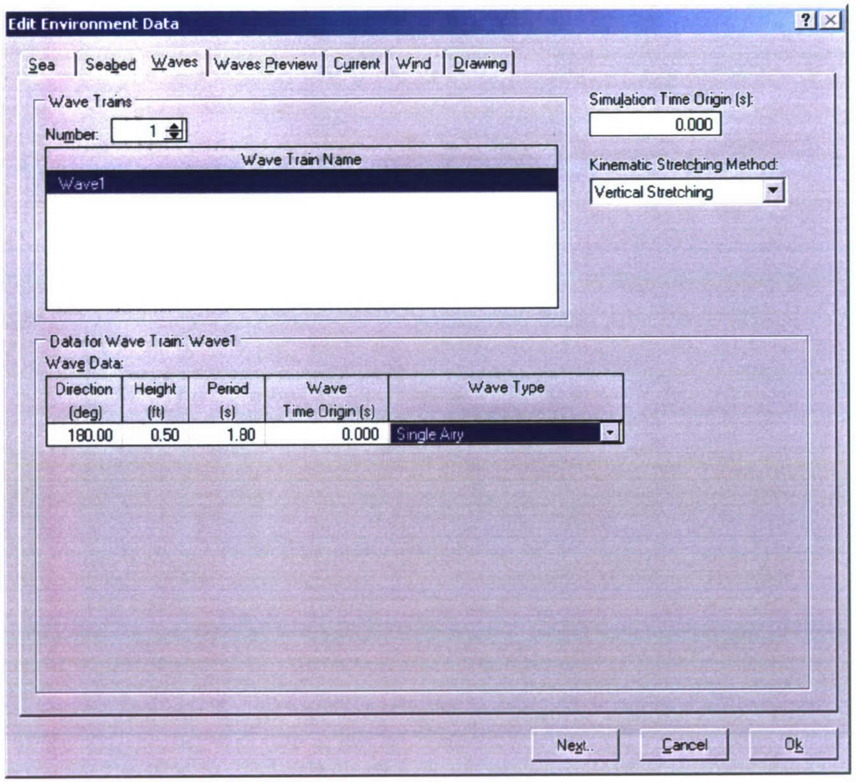

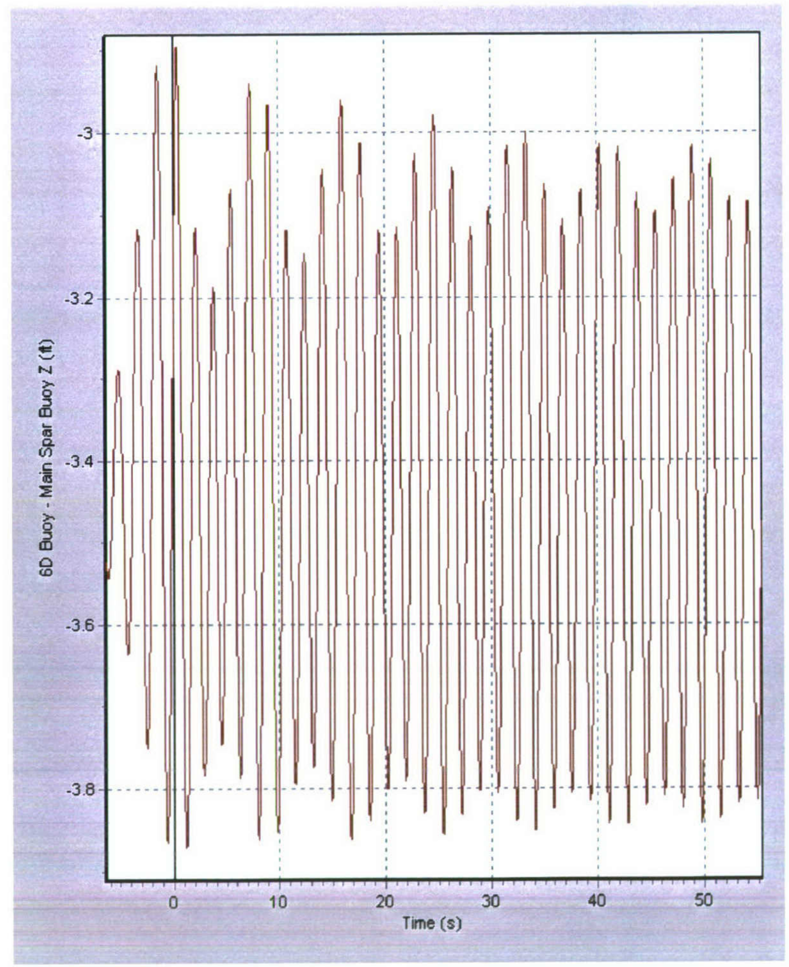

Specify an Ocean Spectrum

Here is a case where the ocean spectrum was measured and we cut/paste from MS Excel into here.

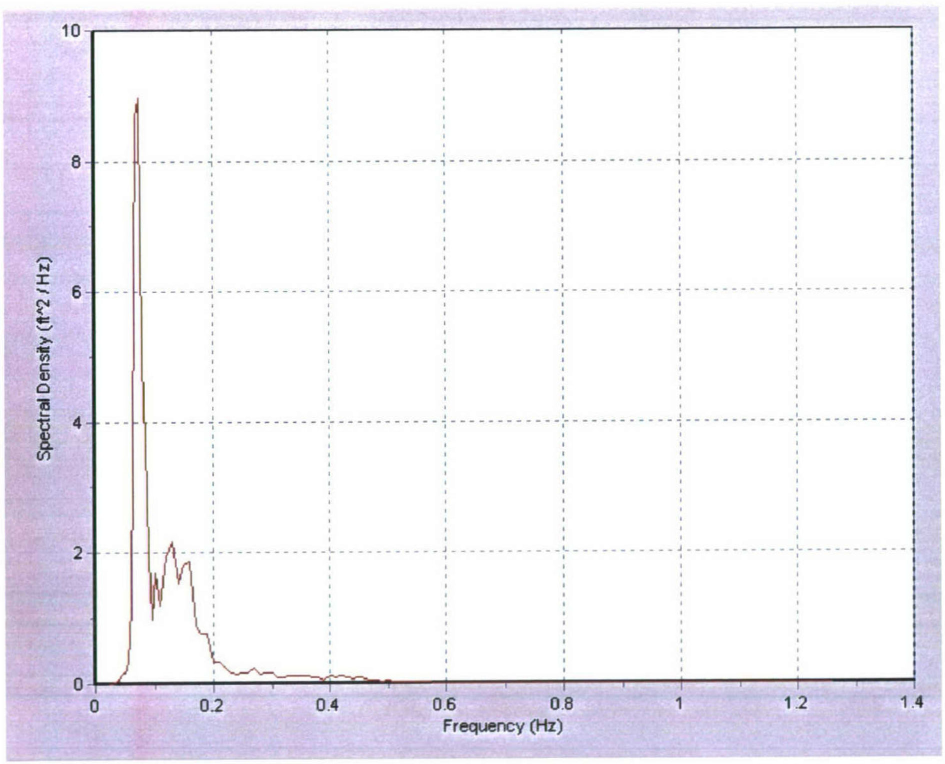

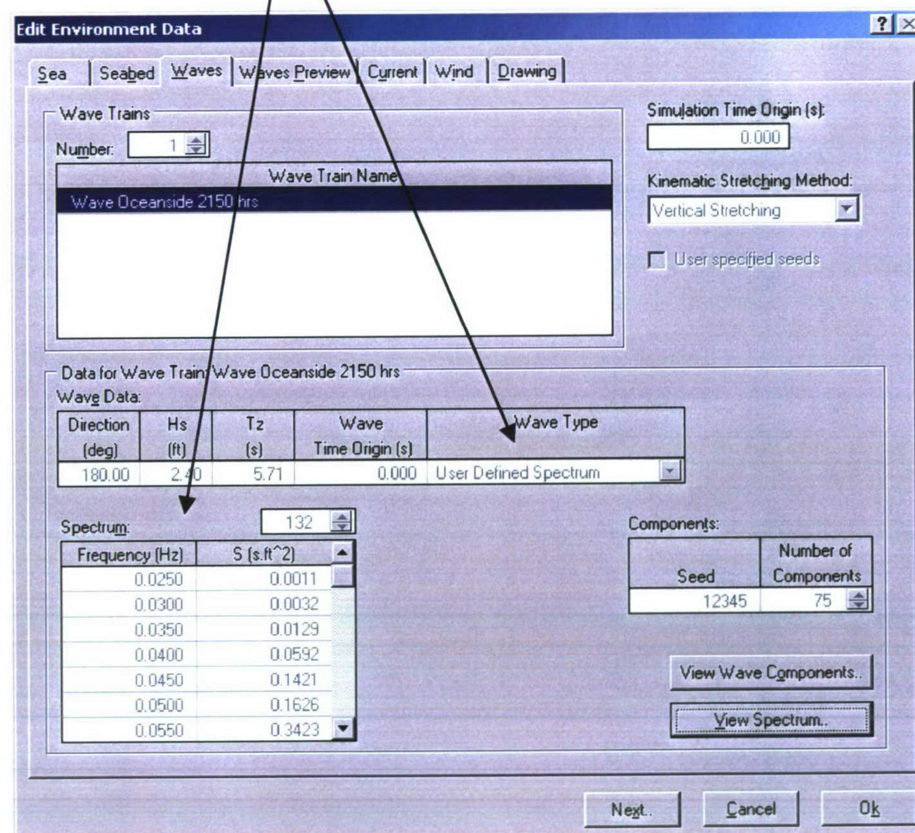

Output Time Series

Wave Profile

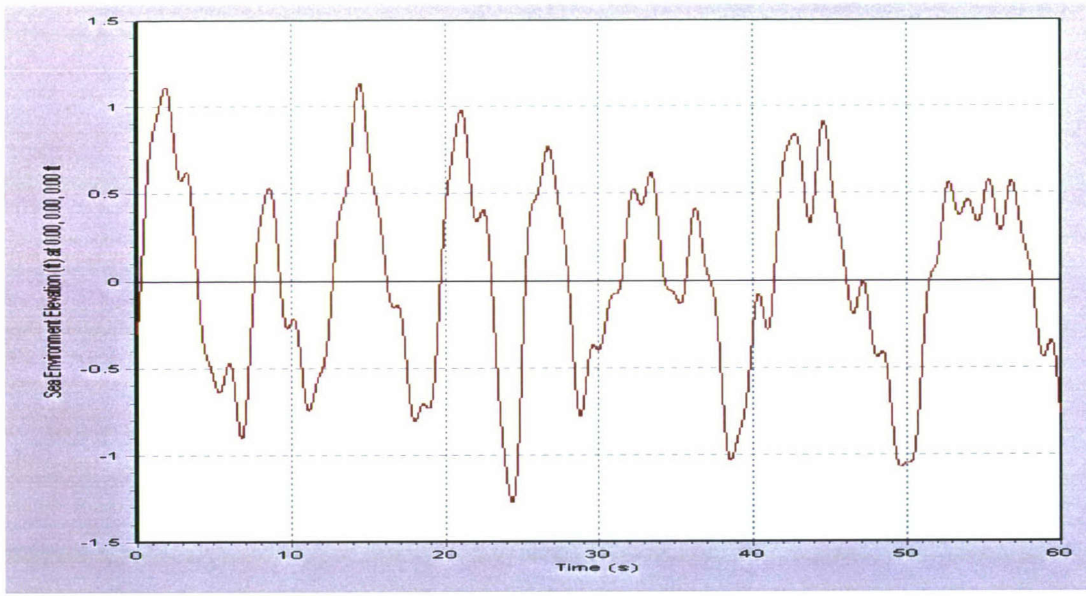

Magnet Stack Velocity used to Calculate Power

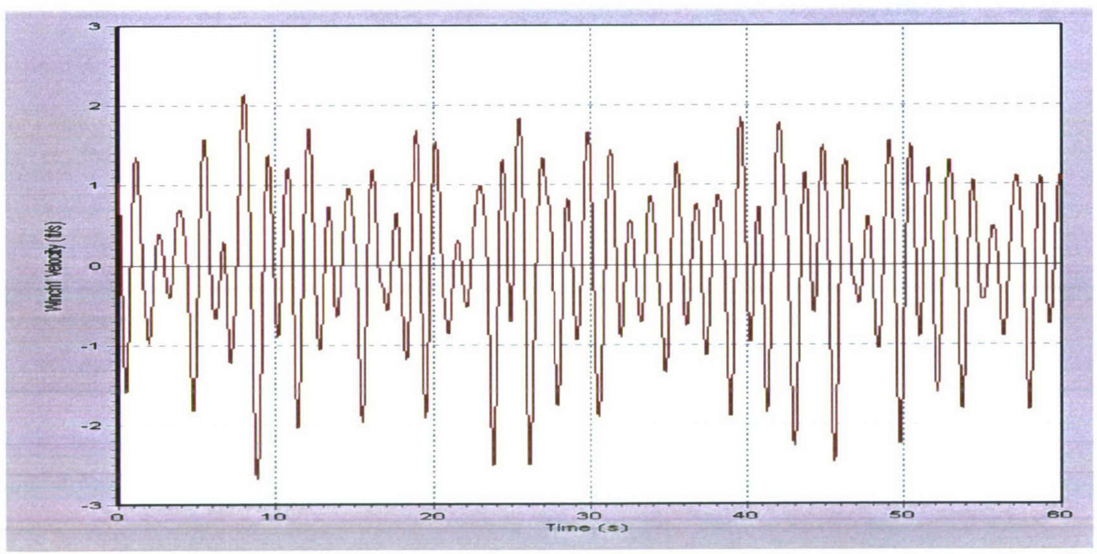

Matlab Script to Calculate Average Power

```
% diffv5.m


load m1430_damp7_half.txt;
t=m1430_damp7_half(:,1);
d=m1430_damp7_half(:,2);
damping_value = 7

plot(t,d)
xlabel('Time (s)')
ylabel('Relative Vel-Z (ft/s)')
%title('Wave')
%set(gca,'Xlim',[0 max(t)]);
set(gcf,'Color',[1 1 1]);

% get Power

%damping_value =1.2  % from orcaflex magnet damping value
P=damping_value*(d.*d).^2;
figure
plot(t,P)
xlabel('Time (s)')
ylabel('Power Output Watts')
%title('Wave')
%set(gca,'Xlim',[0 max(t)]);
set(gcf,'Color',[1 1 1]);

%Average power:
% 1.355 is to convert lb-ft/s to watts

AP1 = 1.355*sum(P)/max(size(t))
```

Questions ?

APPENDIX

Sea State Chart

WAVE AND SEA SCALE FOR FULLY ARISEN SEA

SEA STATE	SEA GENERAL: DESCRIPTION	WIND: (BEAUFORT) WIND FORCE	WIND: DESCRIPTION	WIND: RANGE (KNOTS)	WIND: WIND VELOCITY (KNOTS)	SEA: WAVE HEIGHT FEET: AVERAGE	SEA: WAVE HEIGHT FEET: SIGNIFICANT	SEA: WAVE HEIGHT FEET: AVERAGE 1/10 HIGHEST	SEA: SIGNIFICANT RANGE OF PERIODS (SECONDS)	SEA: T_{max} PERIOD OF MAXIMUM ENERGY OF SPECTRUM	SEA: $\bar{T}$ AVERAGE PERIOD	SEA: $\bar{\lambda}$ AVERAGE WAVE LENGTH	SEA: MINIMUM FETCH (NAUTICAL MILES)	SEA: MINIMUM DURATION (HOURS)
0	Sea like a mirror.	0	Calm	< 1	0	0	0	0	-	-	-	-	-	-
	Ripples with the appearance of scales are formed, but without foam crests.	1	Light airs	1-3	2	0.05	0.08	0.10	up to 1.2 sec	0.7	0.5	10 in.	5	18 min.
1	Small wavelets, short but pronounced; crests have a glassy appearance, but do not break.	2	Light Breeze	4-6	5	0.18	0.29	0.37	0.4-2.8	2.0	1.4	6.7 ft.	8	39 min.
2	Large wavelets, crests begin to break. Foam of glassy appearance. Perhaps scattered white horses.	3	Gentle Breeze	7-10	8.5	0.6	1.0	1.2	0.8-5.0	3.4	2.4	20	9.8	1.7 hrs.
					10	0.88	1.4	1.8	1.0-6.0	4	2.9	27	10	2.4
	Small waves, becoming larger; fairly frequent white horses.	4	Moderate Breeze	11-16	12	1.4	2.2	2.8	1.0-7.0	4.8	3.4	40	18	3.8
					13.5	1.8	2.9	3.7	1.4-7.6	5.4	3.9	52	24	4.8
3					14	2.0	3.3	4.2	1.5-7.8	5.6	4.0	59	28	5.2
					16	2.9	4.6	5.8	2.0-8.8	6.5	4.6	71	40	6.6
4	Moderate waves, taking a more pronounced long form; many white horses are formed. (Chance of some spray).	5	Fresh Breeze	17-21	18	3.8	6.1	7.8	2.5-10.0	7.2	5.1	90	55	8.3
					19	4.3	6.9	8.7	2.8-10.6	7.7	5.4	99	65	9.2
5					20	5.0	8.0	10	3.0-11.1	8.1	5.7	111	75	10
	Large waves begin to form; the white foam crests are more extensive everywhere. (Probably some spray).	6	Strong Breeze	22-27	22	6.4	10	13	3.4-12.2	8.9	6.3	134	100	12
					24	7.9	12	16	3.7-13.5	9.7	6.8	160	130	14
6					24.5	8.2	13	17	3.8-13.6	9.9	7.0	164	140	15
					26	9.6	15	20	4.0-14.5	10.5	7.4	188	180	17
	Sea heaps up and white foam from breaking waves begins to be blown in streaks along the direction of the wind. (Spindrift begins to be seen).	7	Moderate Gale	28-33	28	11	18	23	4.5-15.5	11.3	7.9	212	230	20
7					30	14	22	28	4.7-16.7	12.1	8.6	250	280	23
					30.5	14	23	29	4.8-17.0	12.4	8.7	258	290	24
					32	16	26	33	5.0-17.5	12.9	9.1	285	340	27
	Moderately high waves of greater length; edges of crests break into spindrift. The foam is blown in well marked streaks along the direction of the wind. Spray affects visibility.	8	Fresh Gale	34-40	34	19	30	38	5.5-18.5	13.6	9.7	322	420	30
					36	21	35	44	5.8-19.7	14.5	10.3	363	500	34
					37	23	37	46.7	6-20.5	14.9	10.5	376	530	37
					38	25	40	50	6.2-20.8	15.4	10.7	392	600	38
					40	28	45	58	6.5-21.7	16.1	11.4	444	710	42
8	High waves. Dense streaks of foam along the direction of the wind. Sea begins to roll. Visibility affected.	9	Strong Gale	41-47	42	31	50	64	7-23	17.0	12.0	492	830	47
					44	36	58	73	7-24.2	17.7	12.5	534	960	52
9					46	40	64	81	7-25	18.6	13.1	590	1110	57
	Very high waves with long overhanging crests. The resulting foam is in great patches and is blown in dense white streaks along the direction of the wind. On the whole the surface of the sea takes a white appearance. The rolling of the sea becomes heavy and shock-like. Visibility is affected.	10	Whole Gale	48-55	48	44	71	90	7.5-26	19.4	13.8	650	1250	63
					50	49	78	99	7.5-27	20.2	14.3	700	1420	69
					51.5	52	83	106	8-28.2	20.8	14.7	736	1560	73
					52	54	87	110	8-28.5	21.0	14.8	750	1610	75
					54	59	95	121	8-29.5	21.8	15.4	810	1800	81
	Exceptionally high waves. Sea completely covered with long white patches of foam lying in direction of wind. Everywhere edges of wave crests are blown into froth. Visibility affected.	11	Storm	56-63	56	64	103	130	8.5-31	22.6	16.3	910	2100	88
					59.5	73	116	148	10-32	24	17.0	985	2500	101
	Air filled with foam and spray. Sea white with [illegible]													

Ocean Wave Theory Chart

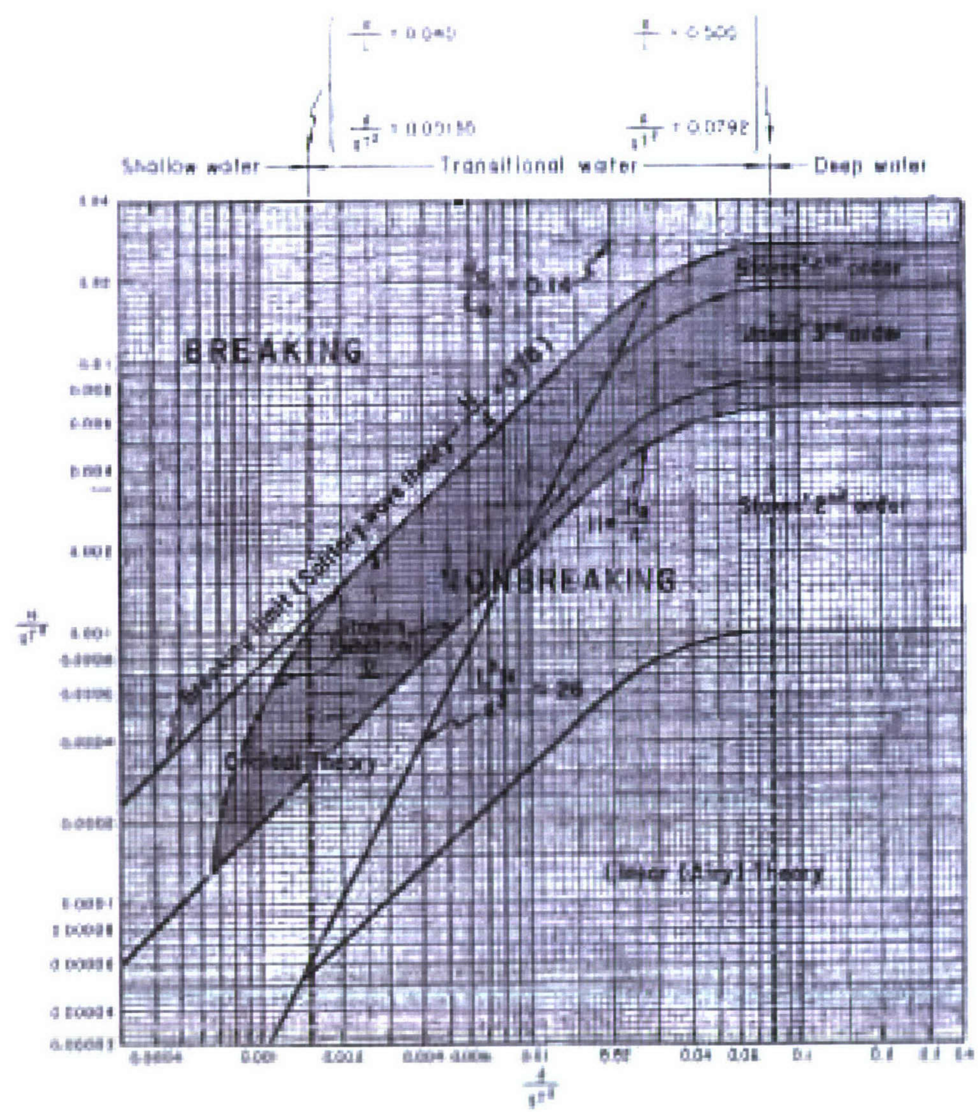

Drag Coefficient Chart

Body shape: Description	Body shape: Sketch	Reynolds number Rn	Dimension ratio L/D	Drag coefficient C_D
Circular flat-plate normal to stream	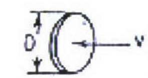	$>10^3$	...	1.12
Rectangular plate normal to stream	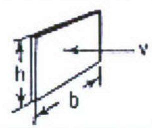	$>10^3$	$\frac{b}{h}=1$	1.16
			5	1.20
			10	1.50
			∞	1.90
Circular cylinder – axis parallel to stream	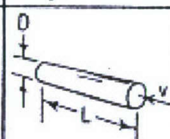	$>10^3$	$\frac{L}{D}=0$	1.12
			1	0.91
			2	0.85
			4	0.87
			7	0.99
Circular cylinder – axis perpendicular to stream	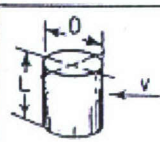	10^5	$\frac{L}{D}=1$	0.63
			2	0.68
			5	0.74
			10	0.82
			20	0.90
			40	0.98
			∞	1.20
		$>5\times10^5$	$\frac{L}{D}=5$	0.35
			∞	0.34

(a)

Body shape: Description	Body shape: Sketch	Reynolds number Rn	Dimension ratio L/D	Drag coefficient C_D
Sphere of diameter D	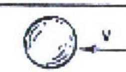	10^5	...	0.50
		3×10^5		0.20
Hemisphere concave to stream	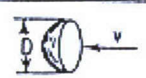	$>10^3$	...	1.33
Hemisphere convex to stream	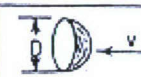	$>10^3$	...	0.34
Ellipsoid major axis perpendicular to flow	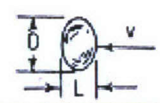	$<5\times10^5$	$\frac{L}{D}=0.75$	0.60
		$>5\times10^5$		0.21
Ellipsoid major axis parallel to flow	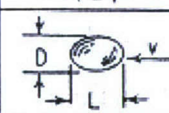	$>2\times10^5$	$\frac{L}{D}=1.8$	0.07
Model airship hull		$>2\times10^5$	...	0.05
Solid cone		...	...	0.34
Solid cone	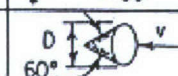	...	...	0.51

(b)

21 Drag Coefficient of 2D and 3D Body Shapes.

Drag Coefficient Chart

Circular Cylinders

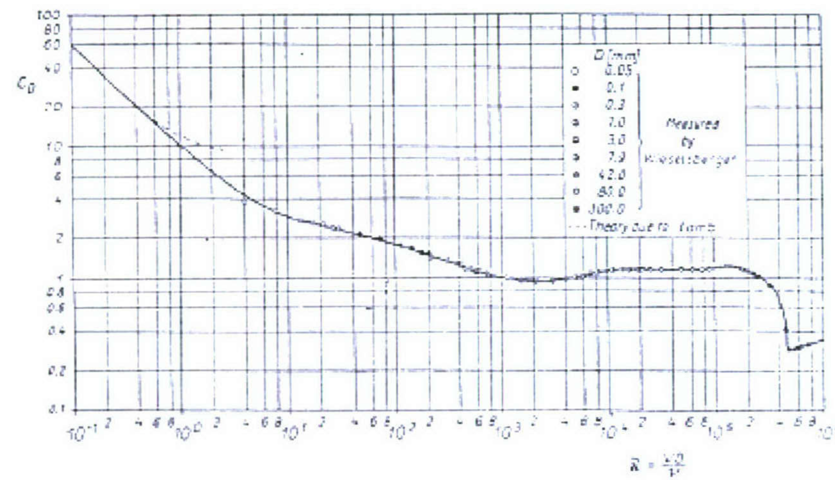

Fig. 1.4. Drag coefficient for circular cylinders as a function of the Reynolds number

Spheres

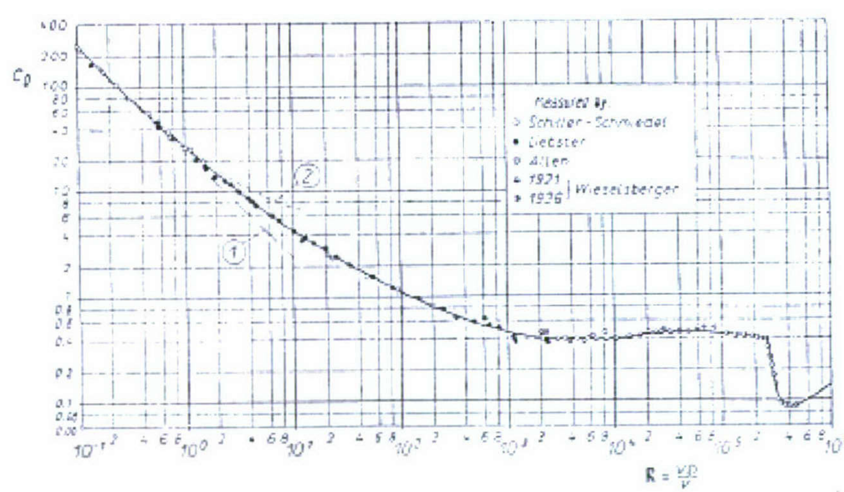

Fig. 1.5. Drag coefficient for spheres as a function of the Reynolds number
Curve (1): Stokes's theory, eqn. (6.10); curve (2): Oseen's theory, eqn. (6.13)

Drag Coefficient Chart (cont)

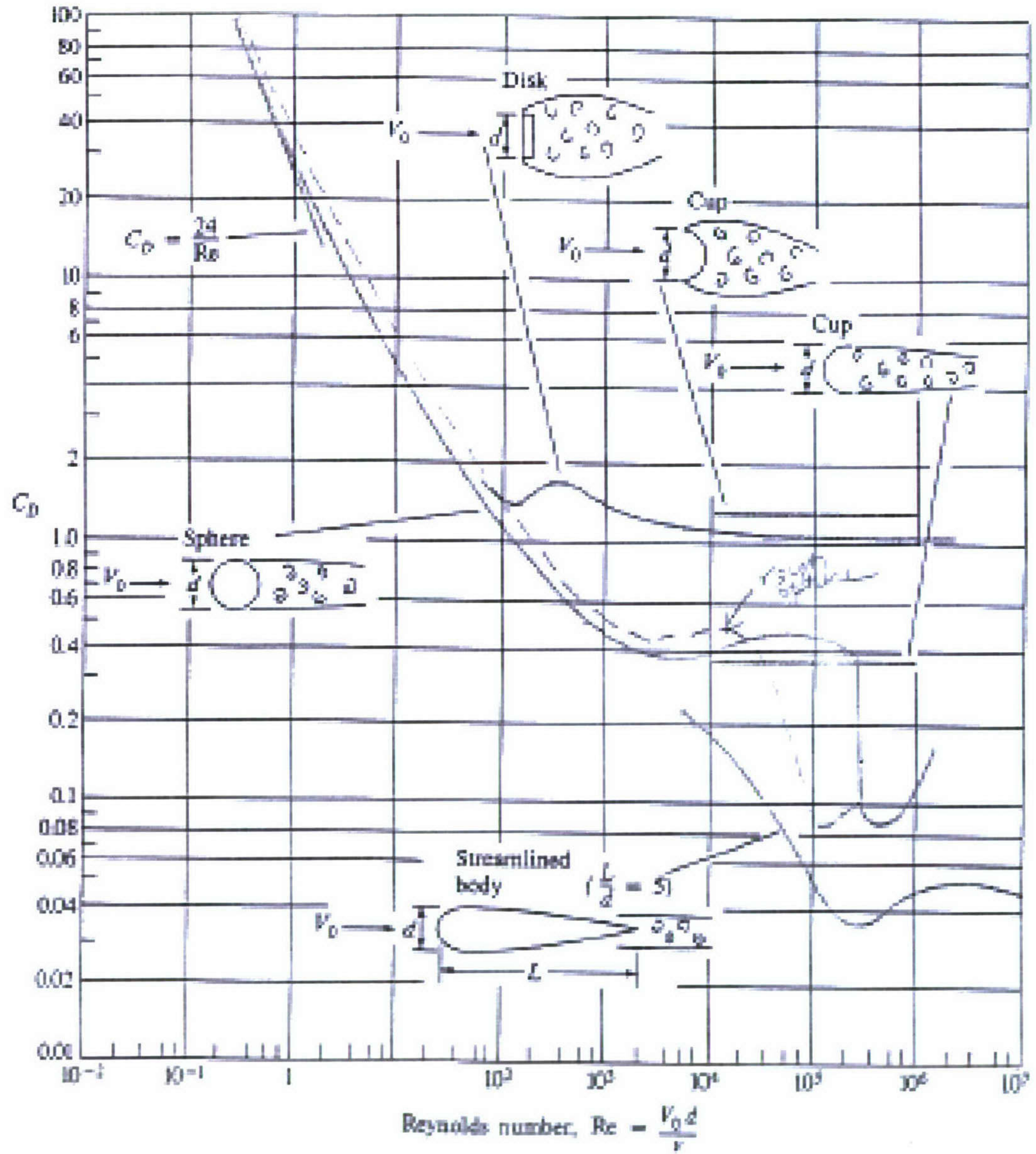

Drag Coefficient Chart (cont)

TABLE 11.1 APPROXIMATE C_D VALUES FOR VARIOUS BODIES

Type of Body		Length Ratio	Re	C_D
	Rectangular plate	$l/b = 1$	$>10^{[illegible]}$	1.18
		$l/b = 5$	$>10^{[illegible]}$	1.20
		$l/b = 10$	$>10^{[illegible]}$	1.30
		$l/b = 20$	$>10^{[illegible]}$	1.50
		$l/b = \infty$	$>10^{[illegible]}$	1.98
	Circular cylinder — axis // to flow	$l/d = 0$ (disk)	$>10^{[illegible]}$	1.17
		$l/d = 0.5$	$>10^{[illegible]}$	1.15
		$l/d = 1$	$>10^{[illegible]}$	0.90
		$l/d = 2$	$>10^{[illegible]}$	0.85
		$l/d = 4$	$>10^{[illegible]}$	0.87
		$l/d = 8$	$>10^{[illegible]}$	0.99
	Square rod	∞	$>10^4$	2.00
	Square rod	∞	$>10^{[illegible]}$	1.50
	Triangular cylinder	∞	$>10^{[illegible]}$	1.39
	Semicircular shell	∞	$>10^{[illegible]}$	1.20
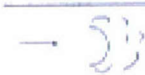	Semicircular shell	∞	$>10^{[illegible]}$	2.30
	Hemispherical shell		$>10^{[illegible]}$	0.39
	Hemispherical shell		$>10^{[illegible]}$	1.40
	Cube		$>10^{[illegible]}$	1.10
	Cube		$>10^{[illegible]}$	0.81
	Cone — 60° vertex		$>10^{[illegible]}$	0.49
	Parachute		$\approx 3 \times 10^{[illegible]}$	1.20

Drag Coefficient Chart (cont)

Normal Drag to Cable

Tangential Drag Along Cable

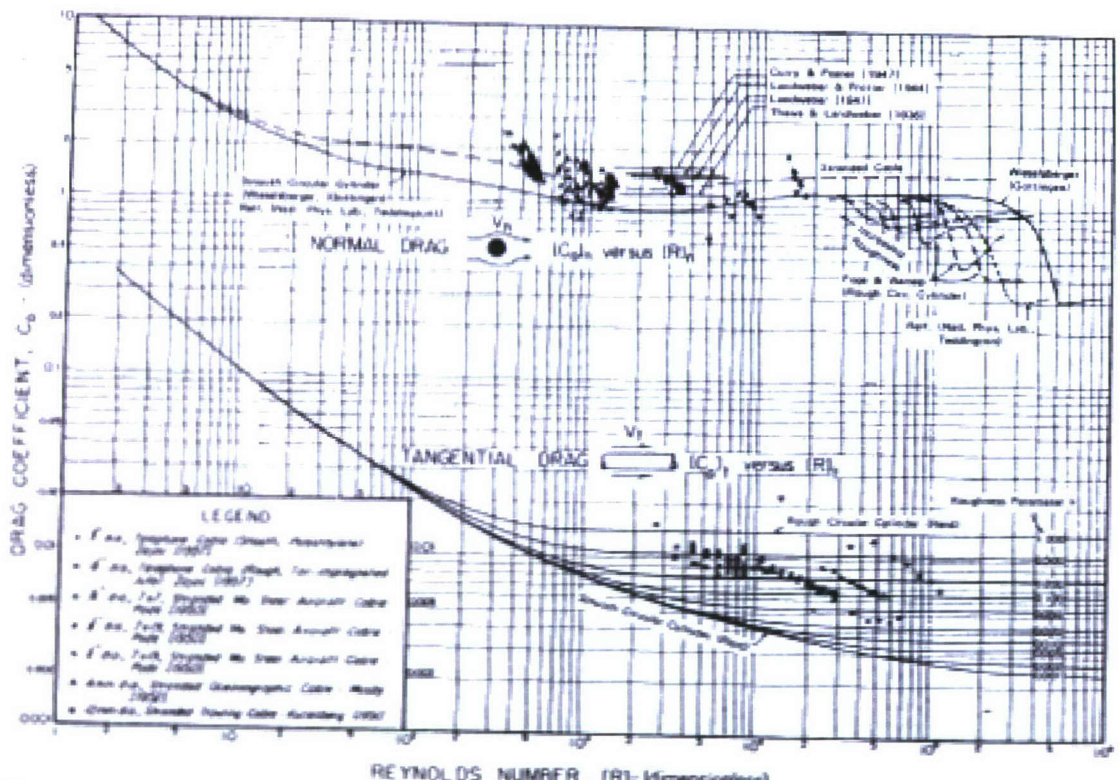

Figure 4.3. Drag coefficient versus Reynolds number for flow normal and tangential to smooth and rough circular cylinders (Wilson, 1960).

Added Mass Coefficient Chart

APPENDIX A

Table 2.3 Added Masses of Various Bodies

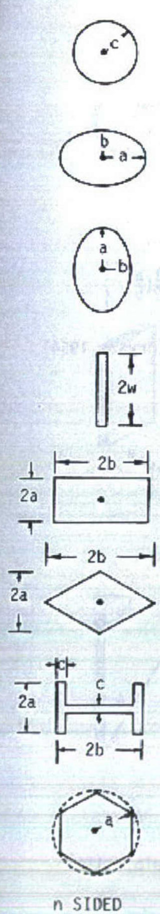

SHAPE	ADDED MASS PER UNIT LENGTH ⟷ MOTION				
CIRCLE	$\rho\pi c^2$				
ELLIPSE ⟷	$\rho\pi b^2$				
ELLIPSE ⟷	$\rho\pi a^2$				
PLATE ⟷	$\rho\pi w^2$				
	a/b		a/b		
RECTANGLE ⟷	∞	1.00 $\rho\pi a^2$	1	1.51 $\rho\pi a^2$	
	10	1.14 "	0.5	1.70 "	
	5	1.21 "	0.2	1.98 "	
	2	1.36 "	0.1	2.23 "	(Wendel 1950)
DIAMOND ⟷	2	0.85 "			
	1	0.76 "			
	0.5	0.67 "			
	0.2	0.61 "	(Wendel 1950)		
I-BEAM ⟷					
a/c = 2.6, b/c = 3.6		2.11 $\rho\pi a^2$	(Patton 1965)		
REGULAR POLYGON ⟷	n = 3	0.654 $\rho\pi a^2$			
	4	0.787 "			
	5	0.823 "			
	6	0.867 "			
OR ↕	∞	1.000 "	(Wendel 1950)		